

2007-2010  
**China National Report on Geodesy**

*For*  
*The XXV General Assembly of IUGG*  
*Melbourne, Australia, 27 June - 8 July 2011*

By Chinese National Committee for  
The International Union of Geodesy and Geophysics  
Beijing, China

**June, 2011**

**2007-2010**  
**China National Report on Geodesy**  
**by Chinese National Committee for IAG**

**CONTENTS**

---

1. Preface  
*CHENG Pengfei and DANG Yamin*
2. Modernization of China Geodetic Datum (2000-2010)  
*CHEN Junyong, ZHANG Peng, ZHANG Yanping and DANG Yamin*
3. The development of Compass/Beidou Satellite Navigation System  
TANG Jing, GE Xia, GAO Weiguang and YANG Yuanxi
4. Chinese Geodetic Coordinate System 2000  
*CHENG Pengfei, YANG Yuanxi, CHENG Yingyan, WEN Hanjiang, BEI Jinzhong and WANG Hua*
5. The Data Processing and Analysis of National GNSS CORS Network in China  
*DANG Yamin, ZHANG Peng, JIANG Zhihao and BEI Jinzhong*
6. Progress in the Research on Earth Gravity Field of China  
*NING Jinsheng, LI Jiancheng, CHAO Dingbo, JIN Taoyong and SHEN Wenbin*
7. Progress in Geoid Determination Research Areas in China  
*LI Jiancheng, CHAO Dingbo, SHEN Wenbin, ZHANG Shoujian, ZOU Xiancai, JIANG Weiping and YAO Yibin*
8. National Report on Absolute and Superconducting Gravimetry  
*SUN Heping, WANG Yong, XU Jianqiao, ZHANG Weimin and ZHOU Jiangcun*
9. Progress of Underwater Gravity-aided Inertial Navigation  
*WU Xiaoping and LI Shanshan*
10. Crustal Deformation Monitoring and Geodynamic Mechanism Study in China  
*XU Caijun and WEN Yangmao*
11. Progress of Geodetic Data Processing Theory and Method in China  
*ZHANG Liping and YANG Yuanxi*
12. Some Activities of Astro-Geodynamics in China during 2007-2010  
*HUANG Chengli, WANG Guangli, WANG Xiaoya, WU Bin and ZHOU Yonghong*
13. Geoid Determination in Coastal Region  
*ZHANG Chuanyin, GUO Chunxi and ZHANG Liming*

# **PREFACE**

The Chinese National Committee of IAG is pleased to present the 2003-2006quadrennial China National Report on Geodesy to the Chinese National Committee for IUGG.

During the last four years, significant advances have been made in the study of Geodesy in China. The presentation of the 2003-2006 China National Report on Geodesy is a reflection to these advances, and provides the record of Chinese contributions to geodesy. The report includes the following contents:

- (1) Crustal movement and astro-geodynamics research.
- (2) Gravity measurement and gravity field investigations in China.
- (3) Geocentric coordinate framework maintenance.
- (4) Ocean geodesy in China.
- (5) Advances made in data processing in China.

It is hoped that this National Report would be of help for Chinese scientists in exchanging the results and ideas in the research and application of geodesy with colleagues all over the world.

**Prof. CHENG Pengfei**  
Chairman of Chinese  
National Committee of IAG

**Prof. DANG Yamin**  
Secretary of Chinese  
National Committee of IAG

## Modernization of China Geodetic Datum (2000-2010)

*CHEN Junyong, ZHANG Peng, ZHANG Yanping and DANG Yamin*

State Bureau of Surveying and Mapping, Beijing 100830, China

From 1950s, CHINA government had defined and realized Beijing 1954 and Xian 1980 coordinate system, 1985 national height system and 1985 gravity Datum base on nationwide horizontal, vertical and gravity network. In the end of 1980s, Global Positioning System was introduced in CHINA that became main technique gradually replacing classic survey in construction of fundamental geodetic network.

Modernization of China Geodetic Datum process started from 2000 indeed. China government integrated domestic geodetic achievements and resources to define a new China geodetic coordinate system and related reference frame.

### I. GPS2000 Geodetic Control Network

Before 2000, three nationwide GPS networks in China existed which were constructed by SBSM (State Bureau of Surveying and Mapping), Military agency and CEA(China Earthquake Administration) etc. To unify national resources, SBSM joint military and CEA to integrate three networks and readjusted to one named GPS2000 network, which was going to be highest order in China. The following was brief information about those networks in following list.

	Network	Points	System	Precision	Agency	Period
1	National High Precision GPS A/B network	832	ITRF93 (1996.365)	$10^{-7}$	SBSM	1991-1995
2	Nationwide GPS I/II network	553	ITRF96 (1997.0)	$10^{-8}$	Military	1991-1997
3	China Crust Movement Observation Network	1222	ITRF96 (1998.680)	$10^{-8}$	CEA/SBSM/ Military/CAS	1998-2002

Besides three networks, several GPS networks for crust monitoring were included. The final GPS2000 network covers 2542 points. Counting on difference of observation period and movement of plate, the network solution involved scale and rotation factor for individual network to reduce reference frame influence. The final results of GPS2000 was under ITRF97 and epoch is 2000.0.

The accuracy of GPS2000 network in cartesian coordinate component was  $\pm 0.90\text{cm}$ ,  $\pm 1.57\text{cm}$ ,  $\pm 1.06\text{cm}$ , and was  $\pm 0.37\text{cm}$ ,  $\pm 0.77\text{cm}$ ,  $\pm 1.92\text{cm}$  in geodetic coordinate. The rms of points is  $\pm 2.13\text{cm}$ . After examination, the mutual difference in Cartesian coordinate component was

$\pm 0.37\text{cm}$ ,  $\pm 0.56\text{cm}$ ,  $\pm 0.53\text{cm}$ , and the mean error of mutual difference was  $\pm 0.86\text{cm}$ . According to above statics, The points accuracy of GPS2000 network in ITRF97(2000.0) should be  $\pm 3\text{cm}$  or better.

## II. Joint adjustment of GPS2000 and triangulate network

China triangulate network was built from 1950s to 1970s, which included triangulate points and traverse points 48433, Laplace points 458 and reference baseline 467. To redefine old triangulate network to geocenter reference frame is the final goal of joint adjustment. The preparations of adjustment were observations including coordinates, directions, baselines, astronomical azimuths, laser ranges, vertical deflections and GPS observations on triangulate points and so on.

Based on analysis, the final data covered 48919 triangulate points, 314962 directions, 2146 traverses and 1068 azimuths etc. All data were converted to WGS84 ellipsoid and made geodetic correction. The average accuracy of points in final results was  $\pm 0.08\text{m}$ , and the weakest point was  $\pm 1.45\text{m}$  in south of China. Through examination, the statistic of bias in  $|\Delta B|$  and  $|\Delta L|$  was 54% and 49% respectively in less than 0.05m range, 74% and 73% in less than 0.10m. The whole average mutual differences of  $|\Delta B|$  and  $|\Delta L|$  were 0.08m and 0.09m.

## III. China GNSS CORS

GNSS CORS (continuously operating reference station) played important role in China geodetic datum, although there are only 32 stations available at now. There are 6 stations adopted by IGS which they are Beijing, LaSa, Shanghai, Wulumuqi, Wuhan and XiAn. In 2010, the China crust movement observation network II will finish main task of 260 stations construction for national reference frame maintaining, deformation monitoring and meteorological service etc. The new GNSS CORS network will be important part of China geodetic datum. The GNSS CORS routine solution will be done each day and adjusted combined with IGS routine solutions. The current product contains stations coordinates and velocities.

China Local CORS network were developed remarkably by local government after 2000 for real time positioning using network RTK technique. The amount of these networks is more than 600 stations and they are operating respectively. China government started making policy and advising for construction and data management.

## IV. China Geodetic Coordinate System 2000(CGCS2000)

On 1, July 2008, China government announced new coordinate system named CGCS2000. The transition period is 8 years. CGCS2000 was consistent with ITRS in definition. The basic geodetic parameters are as following:

$$a=6378137\text{m}$$

$$f=1/298.257222101$$

$$GM=3.986004418\times 10^{14}\text{m}^3\text{s}^{-2}$$

$$\omega=7.292115\times 10^{-5}\text{rad s}^{-1}$$

$$J=1.08262983226\times 10^{-3}$$

The CGCS2000 reference frame was based on GPS2000 and the adjusted triangulate network. According to announcement, the old achievement will be transferred to CGCS2000 including control points and maps in transition period. The new surveying should be under CGCS2000.

#### **V. The infrastructure project of national geodetic datum modernization**

The project of China national geodetic datum Infrastructure modernization was approved in 2009 by China government and will be performed in 2011. The project goal is to promote and realize modernization of China geodetic datum through infrastructure and ability improvement in current stage. The main tasks are:

To construct 210 GNSS CORS to realize the amount of national GNSS CORS close to 500 in 2013 with 150km station spacing. Through data sharing, more local stations will be added to national GNSS CORS which is approaching to 1000 in 2015. The new 4500 geodetic control points will be set up for easier using of engineering project, mapping etc.

To construct 3rd nationwide 1st order leveling network. The total length of leveling will be close to 12.2km. The GPS/Leveling points were designed along the routes which will serve for China geoid improvement.

To densify China gravity fundamental network.

#### **VI. Summary**

The modernization of geodetic datum in China has been gone through 10 years. At now, the main achievements are China geodetic coordinate system (CGCS2000) and its reference frame. The GNSS CORS will be main part of China geodetic infrastructure and be key technique to maintain CGCS2000. China geodetic coordinate system has finished transformation to geocenter system which is more accuracy, more ease of use. The GNSS CORS, GPS2000 and adjustment triangulate network will be current CGCS2000 reference frame.

# The Development of COMPASS/BeiDou Navigation Satellite System

*TANG Jing, GE Xia, GAO Weiguang, YANG Yuanxi*

Xi'an Research Institute of Surveying and Mapping, Xi'an 710054, China

## I. General Description of COMPASS Navigation Satellite System

China was determined to build an independent satellite navigation system in 1980s'. The COMPASS navigation demonstration system, also called COMPASS Phase I (CPI) was completed in 2003, since then it has been used in many areas. Now the COMPASS navigation satellite system is under construction.

The COMPASS Navigation Satellite System consists of five geostationary satellites and 30 non-geostationary satellites. The geostationary satellites are located at 58.75° E, 80° E, 110.5° E, 140° E and 160° E. The non-geostationary satellites include the medium-Earth orbit (MEO) and inclined geosynchronous orbit (IGSO) satellites. The inclined geosynchronous orbit intersect node is 118° E.

The basic polices of the system are openness, independency, compatibility and gradualness.

According to the timetable, the COMPASS navigation satellite system CPII (COMPASS Phase II) will cover China and the nearby area by around 2011, but the full deployment of the system, CPIII (COMPASS Phase III), will be completed between 2015 and 2020. At present, the system is being developed as planned.

The COMPASS navigation satellite system uses CGCS 2000 as its coordinate system with the accuracy of several centimeters which is consistent to ITRS (Yang 2009, Yang et al. 2009). The Compass time is named as BDT. It can be traced to UTC, and synchronized with UTC within 100ns. The epoch time of BDT is UTC 00d 2006. Interoperability of BDT with GPS time (GPST) and Galileo time (GST) was considered in the design of Compass time system. The offset between BDT and GPST/ GST will be measured and broadcasted.

## II. System Deployment

Up to now 9 satellites have been launched. The Table 1 and Table 2 have shown the details of the launched satellites of COMPASS navigation demonstration system and COMPASS navigation satellite system.

Table 1: The launched satellites of COMPASS navigation demonstration system

No.	Time of Launch	Location	Type of Satellite
1	October 31 2000	140° E	GEO
2	December 21 2000	80° E	GEO
3	May 25 2003	110.5° E	GEO

Table 2: The COMPASS Navigation Satellite System

No.	Time of Launch	Type of Satellite
1	February 2007	IGSO
2	April 2007	MEO
3	April 2009	GEO
4	January 2010	GEO
5	June 2010	GEO
6	August 2010	IGSO

There will be two more launches late this year.

### III. Signal Characteristics

COMPASS will transmit three signals in CPII and two of them are for open service.

Table 3: COMPASS Signals in CPII

Component	Carrier Frequency (MHz)	Chip Rate (Mcps)	Modulation Type	Service Type
B1	1561.098	2.046	QPSK	Open
		2.046		Authorized
B2	1207.14	2.046	QPSK	Open
		10.23		Authorized
B3	1268.52	10.23	QPSK	Authorized

COMPASS will transmit six signals in CPIII. B1 and B1-C signals are centred on 1575.42MHz, B2 signal is centred on 1191.795MHz with two side lobes, the lower side lobe, B2a, is centred on a frequency of 1176.45MHz, the upper side lobe, B2b, is centred on 1207.14MHz. The two side lobes can be used alone or in combination. B3 and B3A signals are centred on 1268.52MHz. B1-C, B2a and B2b signals are used for open service. B1, B3 and B3-A signals are used for authorized service.

Table 4: COMPASS signals in CPIII

Component	Carrier Frequency (MHz)	Chip Rate (Mcps)	Data/Symbol Rate (bps/sps)	Modulation Type	Service Type
B1-C <sub>D</sub>	1575.42	1.023	50/100	MBOC(6,1,1/11)	Open
B1-C <sub>P</sub>			No		
B1	1575.42	2.046	50/100	BOC(14,2)	Authorized
			No		
B2a <sub>D</sub>	1191.795	10.23	25/50	AltBOC(15,10)	Open
B2a <sub>P</sub>			No		
B2b <sub>D</sub>			50/100		
B2b <sub>P</sub>			No		
B3	1268.52	10.23	500	QPSK-R(10)	Authorized
B3-A <sub>D</sub>		2.5575	50/100	BOC(15,2.5)	Authorized
B3-A <sub>P</sub>			No		

#### **IV. Applications of COMPASS Navigation Satellite System**

The Compass system provides regional navigation by RDSS and extended regional continuous navigation services by RDSS+RNSS (Tan 2009, Yang 2009a, b). The COMPASS system can provide positioning, timing and short-message communication services to users in China and nearby areas. Besides, a GPS augmentation function is included. The system has been widely used in many areas including surveying, communication, fishery, mineral prospecting, forest fire prevention, and national security etc. The system played a significant role in rescue and relief efforts during the ice-snow disaster that took place in southern China and in the Wenchuan and Yushu earthquakes in the recent three years.

#### **V. Services Provided by COMPASS Navigation Satellite System**

The COMPASS Navigation Satellite System can provide two types of service at the global level: open service and authorized service (Yang 2009). By open service, it provides free positioning, velocity and timing services. By authorized service, it provides safer and better positioning, velocity and timing services, as well as system integrity information, for authorized users. Also in China and nearby areas the System can provide two more authorized services, including a wide-area differential service (with a positioning accuracy of 1 m) and a short-message communication service (Tan 2009).

#### **References**

- [1] Yang Y. 2010, Review on Progress, Contribution and Challenges of Beidou Satellite Navigation System, *Acta Geodaetica et Cartographica Sinica*, 39(1): 1-6.
- [2] Yang Q. 2009, China Satellite Navigation Project Center. COMPASS/Beidou Navigation Satellite System Development. The 4th Meeting of International Committee on GNSS (ICG), Sep. 13-18, 2009, Saint Petersburg, Russia.
- [3] Tan Shu-sen. 2009, Theory and Application of Comprehensive RDSS Position and Report. *Acta Geodaetica et Cartographica Sinica*, 2009, 38(1): 1-5.
- [4] Yang Y. 2009, COMPASS Innovative Application. The 4th Meeting of International Committee on GNSS, Sep. 13th-18th, 2009, Saint Petersburg Russia.
- [5] Yang Y. 2009, Development and Applications of Compass/Beidou Satellite Navigation System, *IGNSS 2009*, December 1-3, Gold Coast, Australia.
- [6] Yang Y. Chinese geodetic coordinate system 2000, *Chinese Science Bulletin*, 2009, 54: 2714—2721.
- [7] Yang Y, Tang Y, Chen C, Wang M, Zhang P, Wang X, Song L, Zhang Z. 2009, Integrated Adjustment of Chinese 2000' GPS Control Network, *Survey Review*, 41(313): 226-237.

## Chinese Geodetic Coordinate System 2000

CHENG pengfei<sup>1</sup>, YANG Yuanxi<sup>2</sup>, CHENG Yingyan<sup>1</sup>, WEN Hanjiang<sup>1</sup>,  
MI Jingzhong<sup>1</sup> and WANG Hua<sup>1</sup>

<sup>1</sup> Chinese Academy of Surveying and Mapping, Beijing, P.R.China

<sup>2</sup> Xi'an Institute of Surveying and Mapping, Xi'an 710054, China

Establishment of the terrestrial reference system (TRS) includes the definition of a coordinate system and implementation of the terrestrial reference frame. The definition of the TRS includes the origin, orientation of the coordinate axes and the scale. A reference coordinate system (RCS) consists of a set of reference stations with high accurate coordinates and velocities to represent and realize the reference system. Such kind of reference stations of is called terrestrial reference frame (TRF).

### I. History of the Chinese geodetic coordinate system

In the geodetic history, China has used various reference systems in different periods due to some reasons, such as Beijing coordinate system 1954 (BS-54), modified Beijing coordinate system 1954 (new BS-54), Xi'an coordinate system 1980 (XS-80), geocentric coordinate system I (DX-I) and geocentric coordinate system II(DX-II), as well as the world geodetic system 1984(WGS-84). These RCSs is of importance in national economic construction, aeronautic and astronautic as well as nautical navigation. However, there exist a lot of problems in applying different RCSs. Firstly, some trouble occurs in geospatial information due to the confused RCSs. Secondly, the widely used old and new BS-54 as well as the XS-80 belongs to local coordinate systems referred to the center of the locally located and oriented reference ellipsoid. These local reference systems are not so accurate to meet the needs of the economic development, national defence, aeronautic development and nautical navigation. Thirdly, the ever used geocentric reference systems, DX-I and DX-II, are in fact expressed by only 3 and 7 transformation parameters respectively with respect to the new BS-54, without any actual reference frames. Furthermore, the precision of the transformation parameters is not accurate enough to satisfy the requirements of scientific research[1,2]. Therefore an idea of establishing and using a new geocentric coordinate system in China has been proposed[2-4].

#### 1. Beijing reference system 1954

The BS-54 was established through three baseline networks of Huma, Jilalin and Dongning in northeast China connected to the geodetic control network of the former Soviet Union. Thus, BS-54 was the extension of Pulkovo coordinate system of the former Soviet Union.

After BS-54 being established, we obtained the adjusted coordinates of about 50,000 control points in China by an adjustment. There exist some problems in the BS-54: (1) The reference ellipsoid is different from the modern reference ellipsoid, with the semi-major axis being 108 m longer than that of the present ellipsoid and the reciprocal of the flattening being 0.04 larger. (2) The location and orientation of the ellipsoid is biased, especially the ellipsoid has systematic slope from west to east relative to the geoid in China. (3) The origin of the coordinate is not in Beijing but in Pulkovo of the former Soviet Union, thus the name "Beijing reference system" is not true. (4) The ellipsoids used by geometric geodesy and physical geodesy are inconsistent. (5) The accuracies of the coordinates are poor, with the relative precision being about  $5 \times 10^{-6}$ . (6) Since the regional part adjustment method was employed, there exist the systematic errors in the coordinates, and the corresponding geodetic network was twist and deformed. As a result, there exists fractures between the different neighbor networks. (7) The two-dimensional coordinate with poor accuracy does not match accurate satellite measurements.

## 2. Xi'an reference system 1980

The XS-80 was also an ellipsoidal centering system and realized by the integrated adjustment of the nationwide astronomical geodetic networks. The shape and orientation of the reference ellipsoid fit the geoid in China. The origin of the coordinate system is located in Jingyang County in Shaanxi Province. After the establishment of the XS-80, the integrated adjustment was carried out. The poor influences caused by the regional adjustments and unsuitable network control order by order have greatly been reduced, thus the accuracy of the adjusted coordinates is improved. After the integrated adjustment, the coordinates of nearly 50 thousand stations were obtained and the fundamental reference frame of the XS-80 was established. However, a free net adjustment method was employed, in which the origin of the network and the astronomical azimuth as well as the high accurate baselines were fixed, which resulted in twist and deformation of the adjusted astronomical geodetic network, since the systematic errors of the astronomical azimuths and the starting baselines were brought into the results of the adjusted network.

Some problems also exist in the XS-80: (1) This coordinate system can only provide two-dimensional services. (2) The employed reference ellipsoid is the one proposed by the International Association of Geodesy (IAG) in 1975, in which the major axis was 3 m longer than that of the ellipsoid proposed by the IERS (2003). This may cause the length error about  $5 \times 10^{-7}$ . (3) The orientation of the minor axis directs to the pole origin of JYD1968, which does not coincide with that of the present reference ellipsoid. (4) The China sea area which is about 1/3 of the whole national land has not been considered in the location and orientation of the reference ellipsoid.

## 3. Modified Beijing coordinate system 1954

Even though a progress has been made by the XS-80, the essential modification has not yet taken place. In the meantime, considering the continuous use of the magnanimous topographic maps with basic scales referring to the BS-54, the coordinates in the system of the XS-80 have been transformed into the BS-54, which is called new BS-54. The new BS-54 employed the same reference ellipsoid as that of the old BS-54, but the precision of the coordinates is nearly the same as that referred to the XS-80.

## 4. DX-I and DX-II reference systems

In order to meet the scientific and technological urgent needs of astronautics, two kinds of geocentric coordinate systems, DX-I and DX-II, were set up in the 1980s. In fact, the two geocentric coordinate systems have only two sets of coordinate transformation parameters. The reference coordinate system DX-I has only 3 translational parameters without rotation and scale parameters, which means that the center position of the reference ellipsoid of BS-54 deviates from the geo-center, and the differences between the axes of the BS-54 and the geo-centric coordinate system are neglected, and the shapes of the reference ellipsoids are not the same. In addition, the original data are limited and inaccurate, and the data processing method is not optimal, thus the precision of the transformation parameters of DX-I is only about 15 m. In the 1980s, China set up a satellite geodetic network with 37 stations by using Doppler measurements. Another satellite dynamic network with 7 stations was established in 1982. A combined adjustment was carried out in 1985, by which the geocentric coordinates of the adjusted stations distributed over the whole country were obtained. In the meantime, an integrated adjustment of the nationwide astronomical geodetic network was carried out, by which the geodetic coordinates of nearly 50 thousand stations were determined. Then, the new corresponding coordinate transformation parameters were calculated, and DX-II was established. The DX-II consists of 7 transformation parameters including 3 translational parameters, 3 rotation parameters and 1 scale parameter with precision about 5 m for each coordinate component.

## II. China geodetic coordinate system 2000

### 1. The definition of CGCS2000

China started to use earth centered Coordinate System on July 1 in 2008. The Bulletin along with conversion guideline between CGCS2000 and the existing national geodetic coordinate systems was published by the State Bureau of Surveying and Mapping (SBSM), in which the technical

parameters of CGCS2000 was published and the transition period is regulated 8 to 10 years. During this period, all existing geographic information systems should be gradually converted to CGCS2000.

The definition is: The origin of the CGCS2000 coincides with the center of mass of the Earth which is defined for the whole Earth, including oceans and atmosphere, the orientation is initially given by the BIH orientation at 1984.0. The constants used in the reference ellipsoid of the CGCS2000 are:  $a$ , semi major axis of the ellipsoid,  $f$ , flattening,  $G$ , gravitational constant and  $\omega$ , rotation velocity of the Earth, in which  $a$ ,  $f$  and  $\omega$  are the same as those of the geodetic reference ellipsoid 1980 (GRS1980),  $G$ , however, coincides with that of the reference ellipsoid used by WGS-84[4]. It should be pointed out that the real time positioning by GPS usually refers to WGS-84 which differs from the CGCS2000 in the flattening  $f$ , and this will result in 1 mm error in the equator. Thus we consider that the real time GPS positioning results also belong to the CGCS2000.

## *2. The realization of the CGCS2000*

The realization of the CGCS2000 is divided into three levels. Level 1: The permanent GPS tracking network. It is a fundamental frame of the CGCS2000 with the accuracies of few millimeters in position and 1 mm/a in velocity. Level 2: 2000' national geodetic GPS control network. It is the extended reference frame of the CGCS2000 with more than 2500 stations with three-dimensional coordinate accuracy about 3 cm [9–11]. It consists of an integrated adjustment of the whole nationwide GPS networks, including the first and second order nation-wide GPS networks [12], the A order and B order national GPS networks[13], the monitoring GPS network and the Crustal Movement Observational Network of China (CMONOC) [14]. Level 3: The national astronomical geodetic network. It is a densification of the reference frame of the CGCS2000 with nearly 50 thousand stations. It consists of the combined adjustment of the astronomical geodetic network and the 2000' national GPS network. The average precision of the two-dimensional position is about 0.11 m[15], three-dimensional position is about 0.3 m and the height precision is about 0.5 m [16].

## **III. Main strategies in establishing the reference frame of the CGCS2000**

In China the measurements required for the realization of CGCS2000 started as early as in 1992. Since then several GPS densifications have been made in order to achieve improved accuracy.

The CGCS2000 realization is carried out in following two steps: 1) GPS data of the domestic GPS stations and IGS stations adjustment within the framework of the ITRF, this constitutes a geocentric coordinate system skeleton, called GPS2000; 2) Readjustment of astro-geodetic network with GPS2000. Because GPS2000 network distribution is too sparse according to whole China territory, and at present astro-geodetic control network is still the most practical and the most fundamental way to serve the users. In order to make astronomical geodetic network continue to play a role in economical construction. Terrestrial Network need to get the geocentric coordinates through adjustment with GPS2000 network, to make tens of thousands of astro-geodetic points align to geocentric coordinate system.

### *1. China permanent GPS network*

China CORS networks were established in different periods and based on different periods of ITRFs. The first permanent GPS tracking station was established in Wuhan by the SBSM and the U.S. Geodetic Survey, for the global terrestrial reference frame definition and GPS satellite orbit determination. during the 1993-1996 period, permanent GPS tracking station Lhasa, Urumqi, Beijing, Shanghai, Xi'an, Changchun were established in China by the SBSM, Chinese Academy of Sciences and other units through international cooperation projects, the main purpose of the construction is for the international GPS dynamic services. In which Lhasa, Wuhan, Urumqi and Shanghai have become the core stations of ITRF. Through nearly a decade of continuous observation, China CORS network made due contributions to the definition of the ITRF frame.

IERS establish the precise transformation relationship between ITRFs through various technologies and means, based on this relationship, CORS established in different periods in our country can be unified into one framework. In order to keep the CGCS2000 consistent with ITRS,

some international GPS service (IGS) stations were selected as control points to process the permanent GPS network. Those IGS stations must meet the following requirements: ① The IGS stations should be distributed over the whole Earth as evenly as possible, ② the IGS stations should have high accurate coordinates and velocity referring to ITRF97, ③ these stations should have high quality measurements during the observation period of the CMONOC. In this way, 47 IGS stations have been selected as control points to process the daily solution for the permanent GPS network in a loosely constrained adjustment method. By using the resolved velocity we can reduce the measurements to the particular epoch, and obtain an integrated solution free from any datum. Then the coordinates with respect to each epoch are transformed into those referenced to ITRF97, by the 7 transformation parameters (3 translational, 3 rotation and 1 scale parameters) provided by the IERS. These domestic permanent GPS stations constitute the skeleton of GPS2000 network, The accuracy of the evaluated coordinates is about 3 mm, speed accuracy is  $\pm 1\text{mm/a}$ .

## 2. China 2000' national GPS geodetic network

The 2000' national GPS network is integrated from several nationwide GPS networks, covering the whole mainland and parts of the islands in China. The measurements of the 2000' national GPS network sustained for 12 years, starting from 1988 through 2000. There are about 2,600 three-dimensional geodetic control points. The sub-networks contain various locally systematic errors, random errors and even outliers, due to the different observation time, different surveyor teams, receivers, geo-graphic environments, climate and observation schemes as well as different network designs and so on. Further-more, the accuracy is not distributed uniformly. In order to obtain high accurate uniform coordinates of the reference frame, some technical strategies were executed as follows.

(1) Datum unification. In order to weaken the accuracy losses in the integrated adjustment of the 2000' national GPS network, ITRF97 was chosen as a reference frame. The coordinates of the IGS stations selected in the whole Earth were kept fixed, and the GPS measurements at each epoch were reduced into the same reference datum and the same reference epoch[9].

(2) Systematic error compensation for the sub-networks. In order to weaken the systematic errors of the GPS sub-networks, including the datum errors, systematic measurement and receiver errors, orbit and ephemerid errors, as well as the crust deformation errors and so on, a scale parameter  $m$  and 3 rotational parameters ( $\omega_x, \omega_y, \omega_z$ ) were introduced into the observation equations of the baseline vectors of each sub-network with respect to the coordinates of the IGS stations and the permanent GPS tracking stations in China. Thus a parameter adjustment model with additional systematic error parameters was applied. In this way, the datum for each sub-network was unified, and the influences of the systematic errors and the crustal deformation errors in each sub-network were weakened[9,10,17].

(3) Outlier's effect control. The error detecting procedure was performed before the integrated adjustment of the 2000' national GPS network. If the standard residual is larger than 3, the corresponding synchronous measurement set should be considered as outlying one, and be temporarily canceled, so that the reliable parameter estimates can be provided for the successive iterative robust estimation procedure. The well developed bifactor robust estimation principle for correlated observations was applied, which not only controls the effects of the outliers, but also keeps the equivalent weight matrix symmetric and the correlations un-changed[18-20]. This scheme is equivalent to the robust estimation procedure based on the variance dilation

model[21], but the calculation procedure is simpler.

(4) Stochastic model error compensation for the sub-networks. The precision of the sub-networks is usually overestimated, some stochastic model errors may exist. The variance component estimation was therefore applied in the data processing for the sub-networks and the integrated adjustment procedure to control the influences of the stochastic model errors on the unified estimated coordinates of the integrated GPS network. Furthermore, the robust variance component estimation was developed and applied in order to resist the outlier's effects on the estimates of the model parameters and variance components[22].

The establishment of the 2000' national GPS network has unified the geodetic reference

coordinate frame in China, by which the accuracy of the reference frame has been improved, and the average positional accuracy is about 3 cm.

### 3. National astronomic geodetic network

The national astronomic geodetic network, measured for more than 70 years by the Chinese geodetic surveyors with relatively high precision and high density, is very valuable. In order to densify the CGCS2000 reference frame, a combined adjustment project of the national astronomic geodetic network and the 2000' GPS network had been performed since 1991 and completed by military in 2003 and SBSM in 2004 separately. Nearly 50 thousand stations with more than 326 thousand measurements were analyzed among which 48,919 points were finally chosen including 336 co-located points between NAGN and GPS2000. The measurements including 314,976 directions, 2,146 EDM distances, 1,064 astro-azimuths, 72 zero-order traverses and 1,022 baselines were processed during the adjustment. Some technical strategies have been designed and applied.

(1) The datum of the adjustment for the astronomic geodetic network. In order to unify the different coordinate systems for the two kind networks into the CGCS2000 by the adjustment, the coordinates of the 2000' GPS network were constrained with  $1\sigma$  in the combined adjustment. In theory, if the coordinates are constrained with their whole variance covariance matrix, the combined adjustment is equivalent to the integrated adjustment of the measurements of the two kinds of networks. Here only the variances of the coordinates of the GPS network were considered in the combined adjustment, thus it kept the datum of the 2000' GPS network nearly unchanged. [23].

(2) Factors considered. Firstly, the plate movement was neglected because the classical terrestrial measurements were relative ones and the distances were within 10 km, thus the crustal deformation errors did not need to be corrected under the control of the GPS network. Secondly, the influences on the astronomical measurements due to the change from the fourth fundamental Catalogue (FK4) to the fifth fundamental Catalogue (FK5) is quite small, so also not be considered in combined adjustment. Only the correction from the earth pole (JYD 1968.0 for NAGN) to CIO(IRP) was considered. Analysis shown that the conversion of deflections of the vertical from Xi'an80 ellipsoid into ITRF2000 is needed, because the origin and orientation differs a lot between the two systems. The influences due to vertical deflection and height anomaly were considered [25-27].

(3)The model improvement. One scale parameter and one azimuth parameter were introduced to compensate the systematic error between terrestrial network and 2000' GPS network. The variance component estimation was applied to adjust the variances and weights of various kinds of measurements. Quality control was used to check the all kinds observation of terrestrial network and in analysis of collocated points of NAGN and GPS2000 networks. By a series of strategies the quality of the combined adjustment results was greatly improved.

(4) Normal equation calculation. Because more than 150 thousand parameters were needed to be solved, the Helmert partitioning method was applied to dividing the nationwide geodetic network into 16 sub-networks in longitude, so resulting the unknown parameters of inner parameters and connected ones. Each of the sub-networks included about 3000 stations. The connections between the blocks were only through lines, so the different sub-networks were processed separately and later combined with the weight matrix of the parameter vector of the GPS stations [27,30]. In order to save memory and enhance computation efficiency due to the sparse matrix of the normal equation of the combined adjustment, One-dimensional compression and storage was used to store and solve the normal matrix [27].

(5)Accuracy of unknowns estimated. Because no matrix inversion is performed in solving the unknowns, the variance and covariance of all parameters could not be obtained as byproducts. Coordinate accuracy can be estimated at some specified points or at all points with Cholesky factorization instead of inverting a huge matrix.

By the external checks, the coordinate RMS is better than 0.3 m after the combined adjustment. The relative standard deviation of the new combined adjustment results is one third of those of the adjustment results finished in 1980. It indicates that the new adjustment project has improved the

accuracy of the nationwide geodetic control network significantly.

#### **IV. Application and Promotion of CGCS2000**

Replacing a national coordinate frame with a new one is a major undertaking that takes decades to complete. Started on 1 July in 2008 when SBSM set up a working group "Geocentric coordinate system promotion project" with the task, the work are responsible for existing products conversion used for national mapping purposes and the task of maintaining the national reference frames, and to prepare a proposal on how to carry out the transformation from the reference frame used at the time to the new one based on its experimental and studying. The working group consisted of specialists from a wide range of institutions within the field of surveying and mapping and is responsible by the Chinese Academy of Surveying and Mapping. The working group accordingly published two official recommendations titled 'Technical Guide for Conversion of existing mapping results to China Geodetic Coordinate System 2000' and 'The implementation program of China Geodetic Coordinate System 2000'.

The surveying and mapping administrator of each province, municipal and autonomous incorporated the recommendations made by the working group into its strategy for public surveying for later use.

The study shows topographic maps in former reference coordinate system transformed to CGCS2000 are required to make the necessary corrections. Such as the map changes from BS-54 to CGCS2000, within the scope of latitude 56N ~ 16N and longitude 72E ~ 135E, is -29 ~ -62m in X direction, -56 ~ +84m in Y direction. From XS-80 to CGCS2000 -9 ~ +43m in X direction, 76 to +119m in Y direction[31].

After joint efforts of Chinese Academy of Surveying and Mapping, China Geodetic Data Processing Center of SBSM, National Geomatics Center of China. In 2008 and 2009, the working group mainly focus on conversion of a large number of mapping products and database products to CGCS2000, The coordinate conversion scheme of various types of products was made based on the analysis of current geodetic points, spatial databases and maps, including technical guidelines of national basic scale maps of 1:50,000 and 1:10,000, mapping products and database conversion of 1:50,000, and independent coordinate system transformation and specific implementation plan to guide the relevant provinces, autonomous regions to complete mapping product conversion. Readjustment of astronomical geodetic networks of order three and order four in CGCS2000 was completed, up to now, 150,000 coincidence coordinates nationwide in both reference coordinate system and CGCS2000 have been gotten. Average accuracy of the products obtained from control point of order one and order two astronomical point is about  $\pm 0.11\text{m}$ , the position accuracy of order three and order four terrestrial networks accuracy is: 85.6 percent of the points is better than 0.1 m, 96 percent of the points is better than 0.2 m. About half of new 1:50,000 topographic maps based on CGCS2000 have been produced to meet the various practical applications. Now the products were supplied to all applications relevant to it.

The first version of the coordinate conversion software "Supercoord 1.0", was distributed to all provinces and cities in October 2009. Coordinate conversion regulation for 1:10,000 basic geographic information database of the provinces was made, 1:50,000 and 1:10,000 scale topographic map shift transformation from XS-80 to CGCS2000 was calculated, about 25,801 National Grid coordinate corrected to CGCS2000, the average accuracy of x direction is 0.565m, maximum is 3.070m, average accuracy of y direction is 0.554m, maximum is 2.695m, the average location precision is 0.869m, maximum is 3.254m. Fully meet the conversion accuracy of 1:50,000 map series. 413,288 high-precision coordinate of 1:10,000 scale national maps have corrected to CGCS2000. in which, interior accuracy of 95 percent of points satisfy the conversion accuracy and is better than 0.05m, an average location precision is about  $\pm 0.014\text{m}$  with well continuity, complete meet conversion accuracy of 1:10,000 or larger scale maps. Technical manual for 1:10,000 DLG, DEM, DOM, DRG, geographical name and other database conversion were made based on 1:10,000 geographic information database in three regions of Guanzhong, South Shaanxi and North Shaanxi in Shaanxi province to guide the local conversion. The software of 1:50,000 scale and below GIS database conversion was developed, 1:250,000 basic geographic information data conversion was made. The user guideline was made based on typical characteristics of local independent coordinate system and its associated control points to instruct

building relation of independent coordinate system and CGCS2000.

## V. Main problems existing in the CGCS2000

(1) The CGCS2000 meets the urgent needs of the economic development and national defense construction, but the reference frame stations are sparse, especially in the west part of China, where the control stations are not only sparse but also inaccurate. It does not meet the development requirements in that area.

(2) The coverage of the frame of the CGCS2000 needs to be extended. There are not control stations in the most part of the ocean area as well as the islands and reefs, which does not meet the requirements of navigation safety, the ocean exploitation and the national defense construction.

(3) The accuracy of the CGCS2000 is still poor compared with the advanced coordinate systems in the world, which cannot provide the deformation information in three-dimensional positions. Furthermore, it cannot meet the requirements of natural disaster reduction and precautions against natural calamities as well as geodynamic

researches.

(4) It is very difficult to make the position reduction in epochs. The CGCS2000 employs ITRF97, which is not convenient to the widely used GPS positioning at present, since the daily GPS positioning uses ITRF2005 at the present epoch. If we want to convert the coordinates of the stations from the epoch 2000.0 into those at the epoch 2005, the velocity information with high resolution is needed. Then the known stations with the coordinates of the CGCS2000 could be transformed into the coordinates at the present epoch. However, the CGCS2000 cannot provide the required information at the present stage. Therefore the reference frame of the CGCS 2000, especially the epoch, still needs to be renewed in time.

## VI. CGCS2000 frame maintenance

The coordinate system frame can be improvement and upgrading through observing and data processing in order to obtain the new coordinates and velocity field.

The maintenance of the current CGCS2000 mainly depends on continuous GPS reference stations, so the next step of project will focus on tasks related CGCS2000 maintenance. Include: geodetic datum modernization, velocity field refinement and plate motion model building, integrated Data Processing, analysis and services of modern spatial data, and promote CGCS2000 applications in all other fields.

### 1. Plate Movement Model Building

With the higher and higher the precision of geodetic results required by the application, the more and more attention to time-varying position was paid. The accuracy of geocentric position determined has reached the order of several centimeters. In this precision, factors not considered previously should be considered, such as geodynamics, geological and geophysical processes (such as crustal motion, geological disasters, ocean tide loading effect, atmospheric loading effect, snow and soil moisture effects, local point stability, etc.). All of these can make the surface position shift with time. CGCS2000 can be more accurately preserved if the characters of time-varying CGCS2000 frame can be well understood through analysis of the earth time-varying causes. one important factor to scientifically build up ground reference coordinate frame is to choose or to build up the correct plate movement and crustal deformation model in our region, although the high precision geological plate model has been recommended by the international community, the efforts on analyzing the motion features in our region and studying the plate motion model suit for our country have been made some progress. At presents, years of continuous GPS data will be joined in our data analysis and then will further refine our geological plate motion model.

### 2. The Continuous Operation GNSS Stations Densification

The efforts on dynamic framework maintenance are required to increase the number of the GPS continuous operation stations in China and distribution density. Adequate and uniform distribution of CORS stations is the key element of modern geodetic coordinate frame and the main technical

support for high accuracy applications, is also guarantee of the three-dimensional geocentric framework accuracy and quasi-present position (dynamic). Only CGCS2000 and its framework with real-time communication and coordination linked with international standard Coordinate can maintain a dynamic framework. China will increase GNSS CORS stations to 150 in nearly 5 years.

## Reference

- [1] Gu D S, Zhang L, Cheng P F, et al. Objectives of the geodetic in China (in Chinese). Bull Surv Map, 2003, 1-5
- [2] Wei Z Q, Duan W X, Yang Y X. On the updating of national geodetic coordinate system. In: Collection on the Adjustment of Terrestrial and Space Geodetic Network (4) (in Chinese). Beijing: PLA Publishing House, 1999. 85-91
- [3] Chen J Y. Consideration of improving and updating Chinese geodetic coordinate system. In: Collection of Geodesy (in Chinese).
- [4] Beijing: Press of Surveying and Mapping, 1999 4 Wei Z Q. National geodetic coordinate system to next generation(in Chinese). Geomat Inf Sci Wuhan Univ, 2003, 28: 138-143
- [5] Chen J Y. Necessity and feasibility for a geocentric 3D coordinate system employed in China (in Chinese). Acta Geod Cartogr Sin, 2003, 32: 283-288
- [6] Chen J Y. Modernization of geodetic datum in the neighboring countries (in Chinese). Bull Surv Map, 2003, 1-3
- [7] Adam J, Augath W, Boucher C, et al. The European Reference System coming to age, International Association of Geodesy Symposia, Vol. 121. In: Schwarz ed. Geodesy Beyond 2000—— The Challenges of the First Decade. Berlin Heidelberg: Springer, 2000. 47-54
- [8] Bai O, Zhu X H. Progress and prospect of modern geodetic coordinate system. In: Collection of Science and Technology Information Communication of Surveying and Mapping (in Chinese). Chengdu: Chengdu Map Press, 2007. 494-497
- [9] Yang Y X, Tang Y Z, Chen C L, et al. National 2000' GPS control network of China. Prog Nat Sci, 2007, 17: 983-987
- [10] Tang Y Z, Yang Y X, Song X Y. Adjustment method and result of national 2000 GPS control network (in Chinese). J Geod Geodyn, 2003, 23: 77-82
- [11] Yang Y X. Main progress of geodetic coordination system in China (in Chinese). Bull Surv Map, 2005, 6-9
- [12] Duan W X, Wang G, Yuan X, et al. Data procession and analysis of the second order nationwide GPS network. In: Collection of Combined Adjustment of Terrestrial and Space Geodetic Network (in Chinese). Xi'an: Xi'an Mapping Press, 1999. 137-148
- [13] Li Y L, Liu J N, Ge M R, et al. Data processing and result accuracy analysis of China national A-order GPS network (in Chinese). Acta Geod Cartogr Sin, 1996, 25: 81-86
- [14] Wang M, Shen Z K, Niu Z J, et al. Contemporary crustal deformation of the Chinese continent and tectonic block model (in Chinese).Sci China Ser D-Earth Sci, 2003, 46(Supp): 25-41
- [15] Cheng Y Y, Cheng P F, Gui D S, Mi J Zh, Data processing method of Astro-geodetic Network and GPS2000 network combined adjustment, Geomatics and Information Science of Wuhan University, 2007(2),148-151
- [16] Yang Y X, Zha M, Song L J, et al. Combined adjustment project of national astronomical

- geodetic networks and 2000' national GPS control network. *Prog Nat Sci*, 2005, 15: 435-441
- [17] Shi C, Liu J N, Yao Y B. The systematical error analysis of high precision GPS network adjustment (in Chinese). *Geomat Inf Sci Wuhan Univ*, 2002, 27(2): 148-152
- [18] Yang Y X. Robust estimation for dependent observations. *Manuscripta Geod*, 1994, 19: 10-17
- [19] Yang Y X, Song L J, Xu T H. Robust estimator for correlated observations based on bifactor equivalent weights. *J Geod*, 2002, 76: 353-358
- [20] Yang Y X, Song L J, Xu T H. Robust parameter estimation for correlated geodetic observations. *Acta Geod Cartogr Sin*, 2002, 18-24
- [21] Liu J N, Yao Y B, Shi C. Theory research on robustified least squares estimator based on equivalent variance-covariance. *Sci Surv Map*, 2000, 25(3):1-5
- [22] Yang Y X, Xu T H, Song L J. Robust estimation of variance components with application in Global Positioning System network adjustment. *J Surv Eng*, 2005, 131: 107-112
- [23] Yang Y X. The general schemes for the nationwide astronomical geodetic network and space geodetic network. In: *Collection on the Adjustment of Terrestrial and Space Geodetic Network (4)* (in Chinese). Beijing: PLA Publishing House, 2003. 66-71
- [24] Zhang H Y, Tang G L, Zhang X B, et al. On the re-computation of the astronomical observation. In: *Collection on the Adjustment of Terrestrial and Space Geodetic Network (4)* (in Chinese). Beijing: PLA Publishing House, 2003. 211-220
- [25] Sun F H, Chen C W, Kong W B, et al. The research and establishment of Chinese 1'×1' vertical deflection models in coastal and sea. In: *Collection on the Adjustment of Terrestrial and Space Geodetic Network (4)* (in Chinese). Beijing: PLA Publishing House, 2003.197-202
- [26] Zhang C D, Wu X P, Sun F H, et al. The establishment of Chinese 1'×1' geoid and vertical deflection models. In: *Collection on the Adjustment of Terrestrial and Space Geodetic Network (4)* (in Chinese). Beijing: PLA Publishing House, 2003. 155-158
- [27] Cheng P F, Cheng Y Y, Mi J Zh. Combined Adjustment of National Astro-Geodetic Network and National GPS2000 Geodetic Network. *Observing our Changing Earth, International Association of Geodesy Symposia 133*, Springer-Verlag Berlin Heidelberg 2009. 89-96
- [28] Ou J K. Quasi-accurate detection of gross errors (QUAD) (in Chinese). *Acta Geod Cartogr Sin*, 1999, 28: 15-20
- [29] Song L J, Yang Y X. On outlier detecting and deleting (in Chinese). *Bull Surv Map*, 1999, 5-6
- [30] Song L J, Ouyang G C. Fast method of solving partitioned adjustment for super large scale geodetic network (in Chinese). *Acta Geod Cartogr Sin*, 2003, 32: 204-207
- [31] Cheng P F, Cheng Y Y, Wen H J, Huang J, Wang H, Huang G M. *Practical Manual on CGCS2000*. Press of Surveying and Mapping. 2008,10

# The Data Processing and Analysis of National GNSS CORS Network in China

*DANG Yamin<sup>1</sup>, ZHANG Peng<sup>2</sup>, JIANG Zhihao<sup>2</sup>, BEI Jinzhong<sup>1</sup>*

1 Chinese Academic of Surveying and Mapping, Beijing, 100830, China

2 National Geomatics Center of China, Beijing 100044, China

**Abstract:** The China national GNSS CORS network aims to integrate all GNSS CORS infrastructure in China in order to generate a consistent high quality national level GNSS CORS network. The GNSS data processing strategy, as well as the strategy for obtaining the coordinate and velocity field under the CGCS2000 (China Geodetic Coordinate System 2000, that is, Chinese geocentric 3D coordinate system) was introduced. The Euler pole of plate displacements in mainland China was determined at 64.77°N, 94.093°E with the rate of 0.2997(°)/Ma regarding to the regional No-Net-Rotation (NNR) under the reference frame of CGCS2000. The crustal movement velocity model in China has also been established by using the Finite Element Interpolation method, this model turns out to be used to monitor the stability and integrity of geodetic datum in China.

**Key words:** CGCS2000, GNSS CORS, velocity field model

## I. The CGCS2000 and GNSS CORS Infrastructure in China

China Geodetic Coordinate System 2000 (CGCS2000) and its related coordinate reference frame formally came into effect since July 1st, 2008. CGCS2000 is a ITRF97 based reference frame, the epoch of the reference frame is set at January 1st, 2000. The CGCS2000 reference frame consists of two parts: Chinese CORS network and national high precision geodetic network. The realization of CGCS2000 augments the reliability, accuracy and consistence of Chinese regional coordinate reference frame.

Since the end of the 20th century, there have been many regional and national GNSS CORS networks were established in China, these different CORS networks have their exclusive purposes. In general, the CORS network system consists of five parts: continuous operational GNSS observation stations, GNSS data processing center, data transmission system, data broadcasting system and users' application system. The first national GNSS CORS network was established by SBSM (State Bureau of Surveying and Mapping) in China in 1993, and the datum network of "China Crustal Movement Observation Network" was formally put into effect in 1998. There are about 31 national GNSS CORS stations continuously operated from then on. Besides, there are many repetition national high precision GPS networks were established as well, the network consists of a basic network and regional networks. The basic network of which have 56 GPS stations and be measured each year, there have been 6 repetition measurements up to now. The regional network including 1000 GPS stations, observed every two years and four days for each station, 4 times of observations have accomplished. The distribution of Chinese CORS network

and national GPS network are as shown in Fig.1.

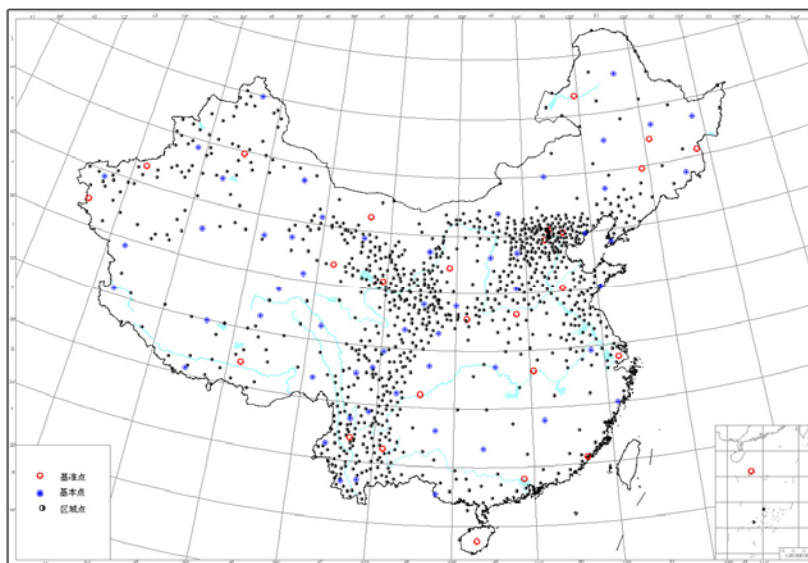


**Fig. 1 Chinese CORS network and national GPS network**

## II. The Strategy of Data Processing of China National GNSS CORS Network

Four steps data processing strategy was applied for processing Chinese CORS network and national high precision GPS network data. Firstly, obtain the coordinates of Chinese CORS station and national GPS network as well as the daily relaxation solution of satellite orbit using GAMIT software. Secondly, combine the above domestic solution with global IGS station relaxation solution using GLOBK software, get a daily relaxation solution including both domestic and global station. Thirdly, use GLOBK to carry on adjustment of the combined solution, estimate the coordinates and velocities of domestic CORS station. Finally, perform unified adjustment of domestic CORS station and national GPS network by using GLOBK software, adopt similar transformation method and use the coordinate results of Chinese CORS network under CGCS2000, to bring national GPS network result into CGCS2000 coordinate frame, solve the coordinate and velocity of GPS network.

The continuous observation results of Chinese CORS station in recent 10 years and the repeat observed data of national GPS network from 1999 to 2007 were processed, eliminate the poor data according to positioning repeatability inspection result. The result shows that the relative precision of coordinate of CORS station is less than 2mm in horizontal, and less than 5mm in vertical direction. The relative precision of CORS velocity field is less than 1mm in horizontal and less than 2mm in vertical, the baseline precision of CORS networks is  $10^{-9}$ . The relative precision of national GPS networks is less than 3mm in horizontal direction and less than 10mm in vertical, the baseline precision of the whole networks reach  $3 \times 10^{-9}$ . By combined adjustment of CORS station and national GPS station, the measured coordinate and velocity field with high precision, wild coverage (the whole mainland) and many observation points (1081 points) were obtained. The results all above have reached high precision, guarantee the maintenance of stability, dynamic and precision of CGCS2000, and also laid a foundation for the establishment of velocity field model of china continental region crustal movement.

## III. The Crustal Movement Model in China

In consideration of the current distribution condition of national GPS networks, the Finite Element Interpolation method was employed to establish the model of crustal movement velocity field in mainland China.

### 1. Establishment of the displacement datum of Chinese continental plate

On the basis of selecting stable and reliable CORS station with repeatability experience method by using accurate coordinate and velocity obtained from data processing, adopt the following two strategies to establish the displacement datum of Chinese mainland plate under the condition of non-net rotate.

#### (1) Model of Euler vectors

For the determination of displacement datum of Chinese continental plate, the plate was consider as rigid body; estimate the euler pole direction and rotation rate of the whole continental movement. Then since the movement is mainly reflected by the horizontal velocity of station, the euler vectors of Chinese continental plate can be solved as follow by using horizontal component of the CORS station:

$$\begin{bmatrix} v_e \\ v_n \end{bmatrix} = r \begin{bmatrix} -\sin \varphi \cos \lambda & -\sin \varphi \sin \lambda & \cos \varphi \\ \sin \lambda & -\cos \lambda & 0 \end{bmatrix} \begin{bmatrix} \omega_x \\ \omega_y \\ \omega_z \end{bmatrix} \quad (1)$$

Where  $v_e$ 、 $v_n$  is velocity in east direction and north direction of any point on the plate, R is the earth radius,  $\omega_x$ 、 $\omega_y$ 、 $\omega_z$  is the euler vectors of the plate,  $\varphi$  is latitude of geographic coordinate,  $\lambda$  is longitude of geographic coordinate.

If amount of point position coordinate and velocity are known, then the euler vectors  $\omega_x$ 、 $\omega_y$ 、 $\omega_z$  can be solved by formula (1).

The expression of spherical euler vectors ( $\Omega$   $\lambda$   $\varphi$ ) is as follows, where  $\lambda$  is euler pole longitude,  $\varphi$  is euler pole latitude:

$$\begin{aligned} \Omega &= \sqrt{\omega_x^2 + \omega_y^2 + \omega_z^2}; \\ \lambda &= \tan^{-1} \frac{\omega_y}{\omega_x}; \\ \varphi &= \tan^{-1} \frac{\omega_z}{\sqrt{\omega_x^2 + \omega_y^2}}; \end{aligned} \quad (2)$$

The error of ( $\Omega$   $\lambda$   $\varphi$ ) can be solved by error propagation rate:

$$\begin{aligned}
\sigma_{\Omega} &= \sqrt{\omega_x^2 \sigma_{\omega_x}^2 + \omega_y^2 \sigma_{\omega_y}^2 + \omega_z^2 \sigma_{\omega_z}^2} / \Omega \\
\sigma_{\lambda} &= \sqrt{\omega_x^2 \sigma_{\omega_x}^2 + \omega_y^2 \sigma_{\omega_y}^2} / (\omega_x^2 + \omega_y^2) \\
\sigma_{\phi} &= \sqrt{(\omega_x^2 + \omega_y^2) \sigma_{\omega_z}^2 + \frac{\omega_z^2}{\omega_x^2 + \omega_y^2} (\omega_x^2 \sigma_{\omega_x}^2 + \omega_y^2 \sigma_{\omega_y}^2)} / \Omega^2
\end{aligned} \tag{3}$$

In formula (3),  $v_e$ 、 $v_n$  is velocity in east direction and north direction of any point on the plate,  $r$  is the earth radius,  $\omega_x$ 、 $\omega_y$ 、 $\omega_z$  is the euler vectors of the plate.

## (2) Coordinate similar transformation method

The coordinate of Chinese CORS station was obtained at any epoch since the long term observation and accurate coordinate and velocity under CGCS2000 frame. The CORS station coordinate at 2000.0 epoch and 2008.0 epoch for similar transformation were chosen, to acquire the transformation parameters of these two group of coordinates. Then such parameters to perform frame transformation of GPS networks reference free solution was used, and then obtain the position coordinate and velocity under CGCS2000. The acquired velocity excluding the generally movement trend of the mainland plate, so it can be regarded as the velocity under the datum of Chinese continental plate.

### 2. The horizontal crustal movement velocity field in mainland China

The horizontal crustal movement velocity field was obtained by using the coordinate and velocity of national GPS networks under the CGCS2000, the result is shown as Fig 2.

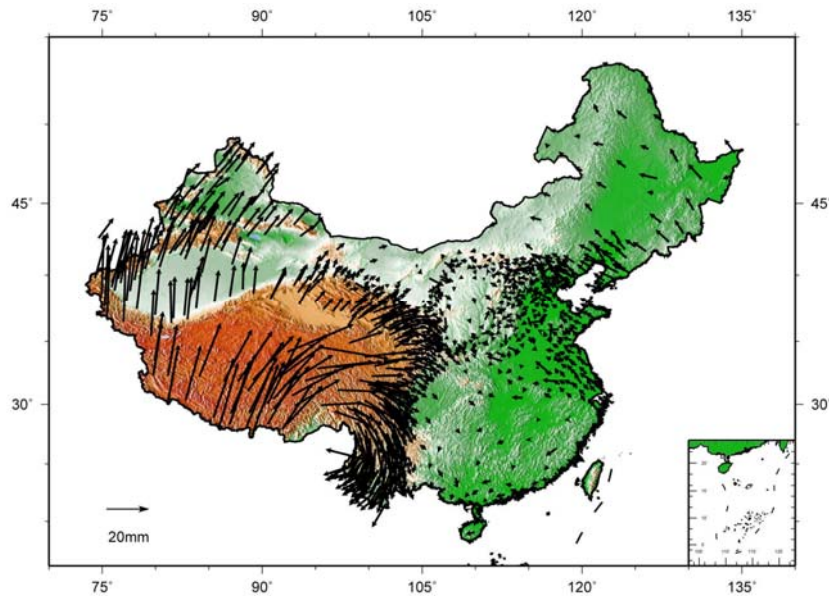


**Fig. 2 The horizontal crustal movement velocity field under CGCS2000**

### 3. The model of crustal movement velocity field in mainland China

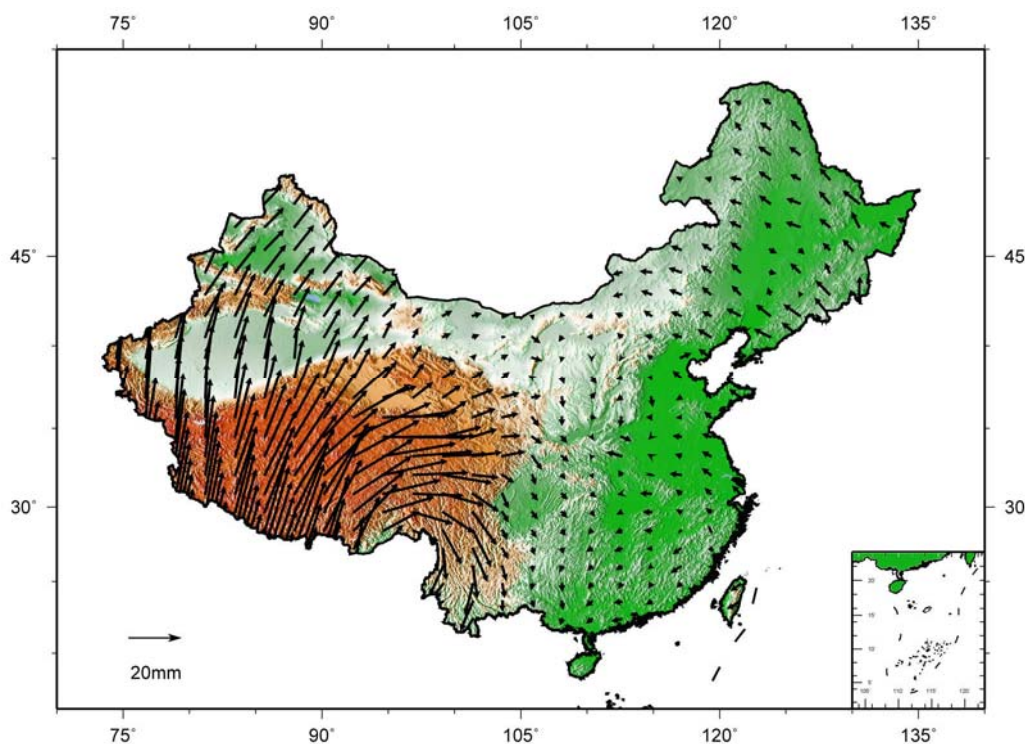
The model of Chinese crustal movement velocity field is established by using Finite Element Interpolation method.

Fig. 3 shows the  $2^{\circ} \times 2^{\circ}$  model of crustal movement velocity field under Chinese continental region background field. The length of arrow represents movement velocity, the direction of arrow represents movement direction and the solid line is fault. The whole figure reflects the model of Chinese crustal movement velocity, directly and clearly describe the main trend of relative change of the velocity between the west and east, south and north China. Such model can provide useful prior information for the research of block movement national wide, as well as high precision velocity correction information of the observe stations for national GPS networks data processing.

The model of velocity field describes the following features of Chinese crustal movement:

- The general trend of velocity field vector is decreases gradually from south to north, west to east.
- Represents the change of movement direction

The differentiation of movement direction in E and W is obvious around east longitude  $90^{\circ}$ . The structural deformation in west region has a feature of gradually shift from north to ne-trending, from ne-trending to nearly east-westward then to southeast in the eastern region and eastward components are larger. In the east of Tetisi-Himalayan tectonic area, the movement direction rotate nearly  $180^{\circ}$  clockwise, and in Sichuan-Yunnan area it shows a trend of SE-SSE-SSW, composing a distributed left lateral shear belt.



**Fig. 3 The model of crustal movement velocity field in mainland China**

#### IV. Conclusions

The continuously observations of national GNSS CORS network and the repetition measurements of national GPS network were employed for determining the crustal movement velocity field in mainland China. Firstly obtain accurate station coordinate and velocity result through data processing under CGCS2000, secondly studies the method for establishing the displacement datum of Chinese mainland plate under the condition of non-net rotate, and finally establish the

model of Chinese velocity field by using Finite Element Interpolation method on the basis of study and analysis of relevant research result domestic and international.

The displacement datum of Chinese mainland plate was established under the condition of non-net rotate by using Euler vectors and similar transformation method respectively.

The calculated model of crustal movement velocity field in mainland China can provides high precision velocity correction information. Meanwhile, the research results can also provide scientific and basic data of high temporal and spatial resolution for the study on the features of Chinese crustal movement under CGCS2000 coordinate reference frame.

## References

- [1] BEI Jin-zhong, JIANG Zhi-hao, ZHANG Peng, DANG Ya-min. On Framework Sites Selection for Unite -Processing of IGS CORS and Domestic CORS [J], Geomatics and Information Science of Wuhan University, 2007,(8): 704~706.
- [2] LIU Jing-nan, SHI Chuang, YAO Yi-bin,TAO Ben-zao. Hardy Function Interpolation and Its Applications to the Establishment of Crustal Movement Speed Field. [J]. Geomatics and Information Science of Wuhan University, 2001,(12): 500 -508.
- [3] Yang Shao-min, You Xin-zhao, Du Rui-lin. Contemporary Horizontal Tectonic Deformation Fields in China Inversed From GPS Observations[J]. Journal of Geodesy And Geodynamics, 2002,22(1),16~30.
- [4] Barber, C. B., D.P. Dobkin, and H.T. Huhdanpaa, The Quickhull Algorithm for Convex Hulls, Vol. 22, No. 4, Dec. 1996, p. 469-483.
- [5] JIANG Zhihao,ZHANG Peng,LI Yulin,BI Jinzhong.Analysis of Crustal Movement in Northern Qinghai-Tibet Plateau Based on Multiple GPS Data in Xinjiang. Geomatics and Information Science of Wuhan University. 2003, 8:417~421.
- [6] ZHANG Peng, JIANG Zhihao, BI Jinzhong,DANG Yamin.Data Processing and Time Series Analysis for GPS Fiducial Stations in China. Geomatics and Information Science of Wuhan University. 2007,(03):251~254.

## Progress in the Research on Earth Gravity Field of China

NING Jinsheng<sup>1,2</sup>, LI Jiancheng<sup>1,2</sup>, CHAO Dingbo<sup>1,2</sup>, JIN Taoyong<sup>1,2</sup>, SHEN Wenbin<sup>1,2</sup>

1 School of Geodesy and Geomatics, Wuhan University, Wuhan 430079, China

2 The Key Laboratory of Geospace Environment and Geodesy, Ministry of Education,

Wuhan University, Wuhan 430079, China

### I. Preface

After the completion of the expected five-year observation program of CHAMP and GRACE satellite gravity exploration missions, using the satellite gravity measurements, several research institutions each released a new generation of satellite gravity model sequence in the past few years. The research on model accuracy analysis, testing, evaluation and application in a wide range were carried out as well, which contribute to the development of basic theory and new method. The data processing methods and technologies in satellite altimetry have matured, and the applied research is still very active. In order to meet the implementation of GOCE mission, the practical preparations for high-resolution Earth gravity field recovery using GOCE data are still on the way. Based on the three satellite gravity missions, the most active part in the today's research area of Earth gravity field continues to achieve new progress. The release of ultra-high gravity field model EGM2008 was a landmark progress in the developing of high accuracy Earth gravity field model over the past few years. Large-scale test of model accuracy and reliability were jointly conducted by different nations. The results showed that the accuracy of EGM2008 geoid is close to 10 cm level on average, and the long-wave accuracy of which has been reached or exceeded centimeter level. It has provided an unprecedented high-resolution and high-precision reference gravity field for the region or country where gravity measurements sparsely distribute to refine the local geoid. Therefore, the conversion of GPS geodetic height to orthometric height or normal height with centimeter-level accuracy can be achieved. This latest development has been received widely attention of the academic and geodetic surveying and mapping industry. With the new development mentioned above, geodesy research group in China has endeavored to absorb the new progresses and technologies, conducted re-innovative research and exploration in many areas of Earth gravity field, including the refinement of SST and SGG data processing and the exploration of new method for constructing the corresponding satellite gravity models; analysis of related error sources and new technologies for noise reduction filtering; the new theory, new methods for refining regional geoid model with the support of the new generation of gravity field model and the new ideas, new strategy for the determination of global geoid with centimeter-level accuracy; the basic theories such as over-determined geodetic boundary value problem, GPS/gravity boundary value problem, gravity field element observations, the harmonic continuation problem of gravitational potential field and isostatic gravity effect; the new algorithms such as wavelet analysis and new application of least squares collocation method. Meanwhile, using satellite altimetry and GRACE time-variable gravity data, the research on ocean

dynamic environment, global or regional water storage changes, crust-core super rotation effect of time-varying gravity and other relevant applied problem in Earth science have been widely conducted. Considering that the fine structure of Earth's gravity field is very helpful for relevant Earth science, especially for global change problem, China has launched the preliminary research program of the independent development of satellite gravity measurement system, including domestic demands, key technology capacity investigation, the system mode selection, the design of the core payload performance, system function simulation and feasibility study. A series of preliminary research results has been made. Following the above-mentioned aspects on the relevant research will be introduced.

## II. Research on satellite gravity surveying

### *1. The theory, method and model of recovering the Earth gravity field using SST observations*

The high precision observation equations of the GRACE satellite-to-satellite tracking observations include light-of-sight-distance  $\rho$ , light-of-sight-velocity  $\dot{\rho}$  and light-of-sight-acceleration  $\ddot{\rho}$  were established. The transition relationship between reference frame CTS and CIS was strictly considered and the variation equation of SST state vector and its numerical solution were derived. Based on the observation equation of  $\dot{\rho}$ , the basic observation of GRACE twins-satellite, using 30 days' GRACE measurements (June ~ August in 2004), an Earth gravity field model up to degree/order 100 named DQM2006S2 was determined by Xi'an Research Institute of Surveying and Mapping. Take GGM02C geopotential model and the height anomalies of 846 GPS/leveling point in China as the reference value, DQM2006S2 is compared with EGM96, EIGEN-CHAMP03S and GGM01S. The comparison of potential coefficients and height anomalies showed that the precision of DQM2006S2 is better than that of the former two models and worse than that of the last one. A possible reason may be that the data used in GGM01S is 4 times of that used in DQM2006S2 (Xiao Yun, Xia Zheren, et. al., 2007; Luo Jia, Ning Jinsheng, et. al., 2008).

Several improvements on algorithm in establishing the observation equation of single satellite disturbing potential and double satellite disturbing potential difference based on the method of conservation of energy were achieved (Xu Tianhe and Ju Xiangming, 2007; Xu Tianhe and Gan Yuehong, 2008; Wang ZhengTao, Li JianCheng, et. al., 2008; Zheng Wei, Hsu Houze, et. al., 2009a; Xu Tianhe, He Kaifei, et. al., 2009; You Wei, Fan Dongming, et. al., 2010), including:

(1) The rigorous formula for computing the kinetic energy difference of double satellite using KBR light-of-sight-velocity  $\dot{\rho}$  was derived, which has improved the existing approximate formula;

(2) The unitary method which takes the scale factor, bias, drift and integration constant of the ACC measurements as the unknown parameters was investigated, which avoids the negative effect on the potential coefficient solution brought by calibrating ACC using a prior gravity model or the approximation of integration constant;

(3) The refinement processing method of SST measurements was studied, which includes the track splicing method that used to process on-board GPS tracking data track of 3 minutes overlap is

tested; 31 minutes' low precision data of the beginning and the end of orbit are removed, respectively; gross error detection of GPS and KBR data has been done by the T test criterion; KBR data which has been interrupted less than or equal 5 epochs is interpolated using Lagrange polynomial;

(4)The least squares method based on variance component estimation for solving potential coefficients was studied. Numerical example indicates that the least squares adjustment with equal weights used in SST observations of different time and space scale and different types is a kind of biased estimation which degrades the solution;

(5)The time-wise method and space-wise method in solving potential coefficients with the method of conservation of energy and high-low SST orbit measurements were studied. The advantages and defects of each method were analyzed. The continuation error and girding error of space-wise method were emphasized. And numerical results showed that time-wise method is slightly better than space-wise method in overall.

Based on the improvements mentioned above, several SST gravity models were obtained, including:

(1)XISM-CHAMP01 (degree/order 50) and XISM-CHAMP1S (degree/order 60) were computed by Xi'an Research Institute of Surveying and Mapping. XISM-CHAMP01 was determined by least squares method based on variance component estimation using 100 days' CHAMP data, the precision of which is better than that of EGM96 and EIGEN1S, and comparable with EIGEN2. XISM-CHAMP1S was determined by unitary method using 300 days' CHAMP data, the precision of which is better than that of EGM96, EIGEN1S and EIGEN2, and comparable with EIGEN-CHAMP03S;

(2)JGG-GRACE (degree/order 120) is computed by Institute of Geodesy and Geophysics, Chinese Academy of Sciences using half year's GRACE data, the precision of which is slightly better than that of EIGEM-GRACE02S at long wavelength;

(3)SWJTU-GRACE01 (degree/order 89) is computed by Southwest Jiao Tong University, which was computed by unitary method using 102 days' GRACE data. The model precision is better than EGM96, EIGEN2 and EIGEN-CHAMP03S, and comparable with GGM02S at long wavelength.

Except for the research jobs of calculating satellite gravity field models based on the method of conservation of energy, the research on gravity field determination using low orbit onboard GPS high-low SST data was conducted by Chinese scientists as well (Guo Jinyun, Hwang Cheinway, et. al., 2007; Zhao Qile, Guo Jing, et. al., 2009), including:

(1)Determination of the gravity model using satellite acceleration data proposed by P. Ditmar (2003) is investigated and improved. A new method using onboard GPS phase data to directly compute the mean acceleration of satellite was introduced, which is free of ambiguity parameter determination and can avoid the systematic bias between different epochs effectively. Using 101 days' CHAMP and GRACE onboard GPS phase data, a gravity field model up to degree and order 70 was computed, the precision of which is better than that of the model determined with orbit data;

(2)The gravity field determination method based on satellite dynamics principle using combined onboard GPS data and ground IGS station observations was studied, in which Cowell II

numerical orbit integration method and Bayes least squares parameter estimation were used. A geopotential model up to degree and order 70 using 7 days' CHAMP onboard GPS data and 43 IGS station measurements was computed, the validity of which was confirmed.

## *2. Research on the Gravity Field Inversion with SGG measurements*

Over the past four years, Chinese researchers made a further study on calculating a new generation of high-degree gravity model with gravity gradient data which measured by the forthcoming GOCE (Gravity field and steady state Ocean Circulation Explorer) mission, involving data processing, simulation analysis and solution method of GOCE gravity field (Wu Xing, Zhang Chuanding, et. al., 2008; Xu Xinyu, Li Jiancheng, et. al., 2009; Wu Xing, Zhang Chuanding, et. al., 2009a; Wu Xing, Zhang Chuanding, et. al., 2009b; Luo Zhicai, Zhong Bo, et. al., 2009; Luo Zhicai, Wu Yunlong, et. al., 2009), which include:

(1) Formulae which used to calculate the complex-valued components of the gravity gradient disturbance at single point, grid points and grid mean values with the Earth's gravitational field were derived. New method was proposed for the computation of the generalized spherical harmonics as well as their fixed integrals. Then, grid mean observations of the components of gravity gradient at the satellite orbit of global coverage were calculated using EGM96. The results were testified using the Laplace Equation by adding the three diagonal components together, which showed the method was efficient. A method of fast simulation of GOCE satellite gravity gradient observations along the orbit with high-degree gravity field model was proposed. Firstly, we set a number of geocentric interval spherical surfaces at the height of GOCE orbit and calculate the model gravity gradient of each spherical surface with FFT algorithm. Secondly, we select orbital parameters to simulate the GOCE orbit and interpolate the gradient of point on each spherical surface according to the satellite's position on spherical coordinates ( $\varphi, \lambda$ ). Lastly, the gradient of satellite orbit is interpolated along the radial direction. The numerical analysis results based on the comparison between the interpolated values and the ones from the direct evaluation with the spherical series expansion show that this method is effectiveness and efficiency.

(2) The GOCE satellite orbit is simulated using the method of orbit integration. The maximum perturbation accelerations and their percentage contribution in the sum of all accelerations are estimated. And the effects of gravity gradient measurements due to conservative force, such as the lunar and solar perturbations, solid earth tides, ocean tides, atmospheric tides and pole tides, are computed and analyzed on the basis of simulated orbit. The results show that all the perturbation accelerations should be taken into account except the atmospheric tides, when the measurement accuracy of non-conservative force is  $1.0 \times 10^{-9}$  m/s<sup>2</sup>. If the target accuracy of GOCE orbit determination is 3cm, you can ignore the polar tides and atmosphere tides when the orbit arc length is shorter than 2.0h arc, but all types of perturbation should be taken into account when orbit prediction is longer than 12h arc. Based on the study, it is discussed that the problem of GOCE satellite gravity gradient data preprocessing, including conditioning regimen, the calculation process, various types of time-variable gravity field information correction, gross error detection and external calibration methods, intended to achieve the scientific goals of GOCE mission: 70km spatial resolution, 1mGal gravity anomalies and 1~2cm geoid accuracy of the global static gravity field determination.

(3) A generalized torus spherical harmonic analysis method for the recovery of an Earth gravity

field model using gravity observations that up to the second order components of the disturbing gravity gradient tensor is studied. The relationship between harmonic analysis and Fourier analysis of torus is established according to mapping from a sphere, when the sphere is rotated by  $180^\circ$  to a torus and the B-spline interpolation technique is used. As a result, self-consistent harmonic analysis of the Earth's gravity field with high accuracy and efficiency is implemented, which eliminates errors caused by the choice of inexact smoothing and de-smoothing factor in conventional harmonic analysis. And the torus harmonic analysis method is expanded to a generalized one. Numerical results indicate that the recovery of an Earth gravity field model with higher accuracy can be attained using the generalized torus harmonic analysis method than the spherical harmonic analysis method. The method of point-mass model construction was researched. The basic equations for the solution of global point mass from the complex combination of global gravity gradients were established using the differential operation relationship between the computation point and the spherical moving point within a spherical polar coordinate system. With the latitudinal and longitudinal partition arrangement of satellite gravity gradients and point-mass model, a method was set up for the decomposition of large linear equations using blocked cyclic matrix based on the characteristics of Toeplitz matrix and fast Fourier transform algorithm, which has solved the stability problem in the solution of medium and large linear equations for global point-mass model.

### *3.The error analysis, calibration, and the accuracy assessment and validation*

Error analysis associate with accuracy assessment is referred to the research on construction of satellite gravitational field model by observed or simulated data. The follow statements present the research on general theory and analysis of specific error source in this field (Zhou JiangCun and Sun HePing, 2007; Xu Xinyu, Li Jiancheng, et. al., 2008; Wang Zhengtao, Jin Xiangsheng, et. al., 2009; Zheng Wei, Hsu Houze, et. al., 2009b; 2009c; Zhang Xingfu and Shen Yunzhong, 2009). The main research work contains:

(1)On the basis of energy conservation principle, the accuracy of Earth's gravitational field complete up to degree and order 120 recovered from GRACE measurements are evaluated by the prior Earth's gravitational field model method (PEM) and least-squares covariance method (LSM), respectively. Based on the GRACE orbital parameters and accuracy indexes of key payloads published by JPL, the accuracy of geopotential coefficients are  $5.192 \times 10^{-10}$  and  $6.633 \times 10^{-10}$  by PEM and LSM, respectively. And the accuracy of each degree is in good agreement with that measured by Earth's gravitational field model EIGEN-GRACE02S.

(2)Based on the theory of dynamic equation in satellite orbit determination and geopotential coefficient calculation, the accuracy demands of the initial satellite state vector in the technology of satellite orbit numerical integration is investigated by GPS orbits measured by CHAMP satellite, through the computation examples of orbit numerical integration. Also the effects on the orbit integration from satellite force model parameters are analyzed, which refers to the stability of orbit determination. The results show that the initial satellite state vectors as well as force model parameters have great influence on the fluctuation of satellite orbit shapes, which is highly sensitivity to initial orbit vector errors especially.

(3)The problem of the ocean tide effect on recovery of satellite gravity field is discussed. The ocean tide loading effect on satellite gravity up to harmonic degree 60 is estimated by FES02 and

TPX06 ocean tide models. And the effect of ocean tide error on satellite gravity is computed, when the difference of the two ocean tide models is considered as the error estimation. The comparison between the numerical results and the standard deviation of gravity recovered from GRACE shows that, the effect of ocean tide on satellite gravity is more serious than the recovering accuracy from GRACE below degree 40. Additionally, the effect of the local ocean tide in the vicinity of China on GRACE measurements is also investigated using tidal data of the East and South China seas and FES02 model. The result shows that this effect is comparable with that of the current global ocean tide model error, which indicates the uncertainty of the ocean tide model.

(4)The determination of calibration parameters of GRACE accelerometer using reference gravity field model and energy conservation method is investigated. The selected models include EGM96, TEG4, EIGEN-CHAMP03S, GRIM5-C1 and EIGEN-GL04S1, which the first four models are used to calibrate and the fifth is used to check calibration results. The results using one month GRACE acceleration measurements show that the calibration parameters calculated by the first four models are in the same order of magnitude, whose effect on disturbing potential is almost  $0.5 \text{ (m}^2/\text{s}^2)$ . This indicates that the calibration parameters have little sensitivity to the reference models. But there is still influence actually, so the higher accuracy model is expected to be selected in the computation.

(5)The accuracy of Earth's gravitational field influenced by the adjusted accuracy of the center of mass between GRACE satellite and accelerometer is carried out using the energy conservation method. The results show that cumulative geoid height error is 17.6cm, 18.1cm, 19.0cm and 27.3cm with the adjusted accuracy of center of mass designed as 0m,  $5 \times 10^{-5}\text{m}$ ,  $10 \times 10^{-5}\text{m}$  and  $50 \times 10^{-5}\text{m}$  at degree 120, respectively. And when the adjusted accuracy of center of mass designed as  $(5 \sim 10) \times 10^{-5}\text{m}$ , it can be matched with the accuracy indexes of GRACE key payloads.

### III. Research on the development of satellite gravity measurement system in China

At the turn of the century, the scientists of geodesy and aerospace in China propose to develop the national satellite gravity measurement system, and launch a series of pre-research project, which include research on the needs of the Earth's gravitational field by related disciplines, selection of satellite gravity measurement model, demonstration on the overall technical design and scientific objectives, design of the technical indicators of payload and analysis of the key techniques, error analysis of the satellite gravity measurement system and virtual simulation, et, al. While in the tracking research on the satellite gravity missions include CHAMP, GRACE and GOCE in recent years, a new round research on the plan for the development of satellite gravity measurement system in China is carried on with the rich experience and results of the international satellite gravity measurements (Zou Zhengbo, Luo Zhicai, et. al., 2007; Ning Jinsheng, Zhong Bo, et. al., 2008; Zhong Bo, Luo Zhicai, et. al., 2008a; Zhong Bo, Luo Zhicai, et. al., 2008b; Zheng Wei, Hsu HouZe, et. al., 2009d; 2009e; Zheng Wei, Hsu Houze, et. al., 2010a; Zheng Wei, Hsu Houze, et. al., 2010b). The results include:

(1)The satellite gravity gradiometer (SGG) system is an alternative model of the future satellite gravity measurement system in China. On the basis of the satellite orbit perturbation theory, the effects of gravity field on the accuracy are analyzed with the time-wise least square method, due to the choice of SGG parameters, such as satellite's altitude, inclination of satellite, time span of sampling, accuracy of radiometry, and sampling rates. These jobs provide a good reference of the

optimized mission design.

(2)The spectral relationship between range-rate error and gravity potential error for SST-LL is established based on energy conservation theory. The performances of satellite separation, altitude of orbit, and precision of range-rate in recovering the Earth's gravitational field are analyzed using the related indicators of GRACE. Comparing to the models of GGM02S and EIGEM-GRACE02S, it proves the feasibility of this method and provides a reference design of the future SST-LL system in China.

(3)The major technical indicators of SST-HL is simulated, analyzed and verified. The error analysis models of onboard accelerometer and GPS receiver in recovering the Earth's gravitational field for SST-hl are established based on analytical theory. Take the relative technology of CHAMP for example, the performance of the altitude of the orbit, the indexes of accelerometer and GPS positioning precision in recovering the Earth's gravitational field are analyzed. Compared to the cumulative geoid errors derived from the EGM96 and EIGEN-CHAMP03S models, the simulated results validate the effectiveness of the analytical simulation methods. And the optimal design of resolution indexes of high and low sensitive axes from space-borne accelerometer in the SSH-II is researched. The matching relationship between accuracy indexes of GRACE space-borne accelerometer, K-band ranging system and GPS receiver is demonstrated by the energy conservation method. The results prove to be appropriate to set the three-axis resolutions of accelerometer as  $ACC_x = (1 \sim 5) \times 10^{-9} \text{m/s}^2$ ,  $ACC_y, z = (1 \sim 5) \times 10^{-10} \text{m/s}^2$  when the published accuracy indexes are used in GRACE K-band ranging system and GPS receiver.

(4)The optimal choice of orbit altitude in SST measurement is researched. Firstly, the GRACE Earth's gravitational fields complete up to degree and order 120 are recovered based on different orbit altitude according to the energy conservation method. The simulated results show that atmospheric drag will increase 10 times approximately, and the satellite platform in unstable work environment will influence the measuring accuracy of GRACE core payloads with the decrease of orbit altitude per 100km. And the high-frequency signals of Earth's gravitational field are attenuated quickly. The attenuation factor is 0.22 at degree 20 based on 500 orbit altitude, and increase 9.6, 92.9, 419 and 1895 times at degree 50, 80, 100 and 120, respectively. And the cumulate geoid errors of the recovered Earth's gravitational field at degree 120 improve 1.6, 4.5 and 10.9 times when the orbit altitude decrease from 450km to 350km per 50km compared to 500km. So the result is that orbit altitude in SST measurement designs between 350km and 400km is benefit for recovering the Earth's gravitational field at degree 120. Furthermore, the orbit parameters of improved-GRACE satellite gravity mission in China are optimal demonstrated. The similar simulation is given with the inter-satellite range-rate error of the interferometer laser ranging system, the measurement error of GPS satellite state vector and non-conservative force of ACC based on the improved semi-analytic method. The results suggest that the relative parameters of the first improved-GRACE satellite in China are as follows: the average orbit altitude and mean inter-satellite range set to be 350km and 50km, and the space resolution and accuracy of recovered geoid are 70km and 0.4m.

(5)For determining the design specifications of SST gravity measurement system, the simulation software for major technical indicators of SST system is developed based on Visual C++ 6.0 development platform by the theory of analytical method. It is focused that software design, goal of design, software architecture and functionality, and key technologies and countermeasures of

software implementation. The simulation results show that the software can be applied to preliminary design of the major technical indicators of SST system.

(6)On the basis of (3) and (4), the signal and combined analytic error models of the GRACE Follow-On satellites' core payload measurements are established, which include inter-satellite range-rate of interferometer laser ranging system, space-borne GPS receiver and accelerometer. The influences of different matching accuracy indexes of key payloads and orbit altitudes from GRACE Follow-On satellites on the accuracies of Earth's gravitational field are demonstrated by those of GRACE on the orbit and GRACE Level 1B provided by the American Jet Propulsion Laboratory (JPL). The result is the cumulative geoid height error is  $1.231 \times 10^{-1} \text{m}$  at the resolution 50km (degree 360) using combined analytic error model based on orbit altitude 250km, inter-satellite range 50km, inter-satellite range-rate error  $1 \times 10^{-9} \text{m/s}$ , orbit position error  $3 \times 10^{-5} \text{m}$ , orbit velocity error  $3 \times 10^{-8} \text{m/s}$ , and non-conservative fore error  $3 \times 10^{-13} \text{m/s}^2$ .

#### **IV. Exploration of Theory and Method**

##### *1. Research on Basic Theory*

The research on basic theory includes geodetic boundary value problem, the definition of normal ellipsoid, the effect of topography to the gravity field of the space, theory of gravity isostasy, tide-generating force, theory of gravity field changes with time and space, inversion of gravity anomaly and sources that be caused (Yu Jinhai and Peng Fuqing, 2007; Shen Wenbin, Zhong Qiuju, et. al., 2007; Zhang Chijun, Fang Jian, et. al., 2007; Wang Haihong, Ning Jinsheng, et. al., 2009; Zhang Chuanyin, Chao Dingbo, et. al., 2009; Zhang Hanwei, Guo Zengzhang, et. al., 2010). The results show:

(1)A new method for solving the over-determined geodetic boundary value problem was proposed based on calculus of variations for functional minimization. The variation solution of boundary value problems is derived based on the variation principle. The existence, uniqueness and best approximation properties of variation solution were proved on theory. The general algorithm was discussed and variation expression was given on the ball boundary conditions. A calculated example was given using EGM96. The results show that the method can effectively improve the accuracy of gravity data processing, and can include different types of observation data into unified model.

(2)The defects of classic definition of ellipsoid were researched. According to classical theory, the shape and size of the normal ellipsoid should be closest to the global geoid, so the geoid undulation related to normal ellipsoid is the positive and negative white. When the geoid is located within the ellipsoid, geodetic boundary value problem by the classical theory is not defined. Because normal gravity potential inside the ellipsoid is not defined, the internal disturbing potential on the geoid are not defined. A program was proposed to solve this problem. The normal gravitational potential was analytically continued from the ellipsoid to the outer space of a virtual sphere in the geoid. Accordingly, a virtual normal potential filed can be defined. The virtual normal potential equals to the normal potential at outside of the ellipsoid and will be harmonic inside. Then the disturbing potential on the geoid that inside the ellipsoid can be defined in theory and the external disturbing potential function is regular and harmonic. Take the WGS84 ellipsoid as normal ellipsoid, the gravity potential  $U_0$  on the ellipsoid can be calculated with the four announced basic parameters, minus the centrifugal potential  $Q_0$ , the boundary value of attracted

potential on the surface can be derived ( $V_0=U_0-Q_0$ ). Take 6000km as the radius of the virtual sphere, using a "virtual compression recovery method", the normal potential outside the virtual sphere that contain the geoid can be defined with accuracy better than millimeter. Then, the problem of "undefined" can be solved.

(3)The inversion theory of gravity anomalies based on multi-scale edges was studied. The concept "edge" comes from image processing, refers to a variety of dramatic changes points that can be used to identify the objects' contour. In the gravity signal field, the edge may reflect the physical density discontinuity within the earth or the location of the drastic change. Multi-scale edges models of gravity anomalies for homogeneous sphere and several 2D regular bodies are derived on the potential wavelet. The features of these models are analyzed, and then a multi-scale edges based on the method is put forward for the gravity anomalies inversion. The outstanding ability of the proposed method is that geometric parameters and density parameters can be inverted without any hypothesis. This method also has high stability and good anti-noise performance. A model of 2D block is used as an example to verify the method. With multi-scale edge analysis theory, the method of multiple wavelet decomposition of gravity anomalies was studied further and the gravity anomalies separation method based on multi-scale edge was proposed. The experiments show that, the improved method not only conserves the advantages of the multiple decomposition method and makes the gravity anomalies of vertical and horizontal segregation, but also determines the orders of wavelet decomposition in accordance with the multi-scale edge distribution of every resource of field and then is well used to extract the character of single anomaly. The marine survey data in the southwest subduction zone of Ryukyu are analyzed and processed by this method, and the result are well fit to the geological structure of the region.

(4)It has studied the topographic effects on any type of gravity field measurements outside the Earth, including not only gravity anomaly, but also the disturbing potential, disturbing gravity, deflections of vertical, gravity gradient and other field quantities. The disturbing potential is decomposed into non-terrain effects and terrain effects, and the second part is broken down into the quality of a shell with its thickness equal to the height of topography and the quality of the local topography. The terrain effect expression of commonly ( $T, \Delta g, \delta g, \zeta, \eta, T_{rr}$ ) is derived using types of field quantity according to the functional relationship between various gravity field quantity and disturbing potential, respectively. In the sphere approximation, it has given the strict fast algorithm used to calculate of the disturbing potential, gravity and local topography effect. The method can be effectively used to calculate the topographic effects of ground, marine, space and satellite gravity measurements, which is the extension of classic theory of terrain correction in gravity reduction.

(5) Having re-examined and studied a variety of terrain gravity isostatic theories, the author believes Vening-Meinesz's regional isostasy theory that based on the principle of elastically template bend loading is reasonable. Meanwhile, the author studied the gravity effect of different wavelengths topography, analyzed the relationship between the wavelength of topography and isostatic compensation conditions and drew the conclusion that the short wavelength topography can neglect their compensation effect. With further analysis of the role of bending stiffness on the isostasy research, it is got that the relationship between the wavelength of topography and the degree of crustal bending compensation in the condition of bending stiffness fixed, and came to the conclusion that short-wavelength of topography which is less than a certain scale can be

without taking into account the crustal bending compensation. The topographic loading of wavelength less than 100km is essentially braced by the intensive earth's crust and that less than 50km is almost entirely braced by the crust. So it's not appropriate to interpolate and estimate the gravity value by isostatic anomalies in these regions. Finally, 4 methods were respectively used to estimate the gravity potential of Everest with short-wavelength terrain data and 12 points of gravity values. The differences of results are not large, whose value is  $(976970 \pm 7) \times 10^{-5} \text{ m/s}^2$ .

(6) It is studied the spatial and temporal changes theory in Earth's gravitational field caused by the tide-generating force. The author pointed out that the variation of gravity detected by observation instruments is only that of a single particle on the surface of the earth (Lagrangian variation), but the theoretical study was carried out based on Euler's equation of gravity and the gravitational potential field. The author made a correction of a principle mistake in the paper (Grafarend E.W. et al., The space time gravitational field of a deformable body, Journal of Geodesy. 1997, 72: 11-30). Simultaneously, adopted the same derived process as that in the paper, it is given that the corrected expression of Eulerian gravitational potential increment as well as the theoretical relationship between potential and displacement Love number. Furthermore, the expression of Lagrange, Euler and Lagrangian gravitational increment are deduced and proved.

### *2.The research and experiment of new method*

Because of the powerful numerical computing ability with the development of computer and software technology and multi-type of abundant observation data provided by satellite gravity detecting technology, many non-classical gravity field computing methods, which are impossible to realize by handworked computing technology, have been emerged in the research of gravity field's observation data process and parameter solution method, such as least-square collocation method based on statistics and random process theory, Fourier transform and convolution algorithms based on signal processing theory of spectral domain, spectral algorithm by simulating linear input-output system, and so on. These methods are mostly used for gravity field calculation less than 40 years, but still maintain a strong development activity and attract researchers to continue exploring the accuracy and efficiency potential. A variety of de-noise filtering and fast computing technology are developed, among which fast Fourier transform (FFT) technology is widely used and improved in the calculation of gravity field. Meanwhile, sophisticated fast algorithms of some new methods in determining the gravity field are produced, such as virtual point mass approach and the inverse Vening-Meinesz methods. In recent years, the achievements of research on calculation method of gravity field in our country reflect the progress. (Zhang Chuanyin, Ding Jian, et. al., 2007; Cui Lili, Luo Zhicai, et. al., 2009; Zhou Shichang, Wang Qingbin, et. al., 2009a; Zhou Shichang, Wang Qingbin, et. al., 2009b; Zhong Bo, Wang Haihong, et. al., 2009; Zhang Xiaolin, Zhao Dongming, et. al., 2009; Zhai ZhenHe and Sun ZhongMiao, 2009; Pang Zhenxing and Zhang Chuanding, 2009; Li Na and Zhang Chuanyin, 2009; Pang Zhenxing, Zhang Chuanding, et. al., 2010; Peng Zehui, Li Hui, et. al., 2010). Main results include:

(1)The linear estimation method taking into account the observation noise and data resolution is investigated. The combined effect of estimation errors leading by the observation noise and the data resolution are discussed. The general formula of optimal linear estimation and its error power spectrum that considering observation noise and data resolution are given based on the frequency form of the least mean square error criterion. Numerical simulation is undertaken with gravity anomalies estimates for example. The analysis conclusion is obtained on effects of observation

noise and data resolution on the estimated results. Meanwhile, the effect of the observation noise to the frequency domain input-output method of data fusion is studied. Taking the local geoid or gravity anomaly refined by the fusion of geoid height and gravity anomaly data as an example, the effect of observation noise level and non-stationary noise on the data fusion results is analyzed. The results show that the satisfactory results can be obtained by the fusion with double-input and single-output method.

(2)The usage of least square collocation in the establishment of airborne gravity measurement data continuation model is investigated. The covariance model of gravity anomaly (GAC) and local gravity disturbance (GDC) is respectively derived from the covariance model of local disturbing potential (DPM) established by Forsberg. Two fitting methods for parameters of GAC model are proposed and examined by actual surveying data. According to the gravity anomaly continuation based on collocation, the accuracy of upward and downward continuation based on the GAC model is about  $1.8 \times 10^{-5}$  m/s<sup>2</sup> and  $5 \times 10^{-5}$  m/s<sup>2</sup> respectively. The general expression of least squares collocation on local gravity field is researched, and a general expression of experiential covariance function is put forward, which is identical for many gravity field variables of different types and different heights. With the general expression, it can be realized that the arithmetic for interpolation, extrapolation and identical continuation least square collocation of local gravity field variables in different heights. The method of least squares collocation for making grid of discrete data was used to obtain the pattern of dynamic gravity changes. The comparison and analysis with actual surveying data show that least square collocation interpolation method can efficiently describing the morphological and characteristics of the dynamic changes of gravity field.

(3)The fast algorithms of terrain correction and aerocarft disturbing gravity are investigated. The former uses the discrete convolution having the Toeplitz matrix characteristics to expand it to vector multiplication of cyclic Toeplitz matrix and the prolonged observation data. Then the fast discrete convolution algorithm under the condition that integral radius can be controlled is realized. Using the simulated data, the latter quickly and almost real-time approximates the disturbing gravity of space points by a wide-area polynomial approximation method. The experiment results show that this method can reach the precision of 1 mGal with the 30km per step in the aspect of height.

(4)The proposal of using inverse Vening-Meinesz technique in fine terrestrial gravity anomaly structure is put forward. Based on remove-restore technology of inverse Vening-Meinesz formula on topography isostasy and considering the topographic effects, the mathematic model and algorithm for calculating terrestrial gravity anomaly is given. The numerical calculation experiment of  $1^\circ \times 1^\circ$  observation data shows that this method can restore gravity anomaly with certain precision requirement. The inverse Vening-Meinesz formula is widely used to calculate the sea gravity anomaly. According to the characteristic that sea surface topography focus on long-wave, the most effective integral radius, which can reducing the long-wave error from sea surface topography, is researched, the comparison suggest that the most suitable integral radius is between  $0.5^\circ \sim 1^\circ$ .

(5)The point mass method is introduced for accurate determination and approximation of outer disturbing gravity field. The construction of the model of point mass is proposed by gravity observations. The characteristics of each layer of point mass in terms of diffraction error, effect of

approximation are analyzed. Result shows that the disturbing gravity field is approximated accurately using the point mass method. Meanwhile, an improved fictitious compress recovery method is also applied to the approximation of outer disturbing gravity field and compared with point mass method. The simulated calculating example shows that accuracies and the computation speed of these two approaches are equivalent to each other.

## **V. The application of gravity field information in related Earth's science**

### *1. The application of satellite altimetry*

Since 1970s, multi-generation satellite altimetry missions have been implemented. Based on the abundant altimeter data, Chinese geodesists have been conducting lots of application researches in satellite altimetry and the related areas, which includes:

(1) The mean sea surface height (SSH) and sea level variations over China Sea as well as that of global were studied, and the relationship between sea level change and El Niño, La Niña events was analyzed (Zhao Xiaoyang, Li Jiancheng, et. al., 2007; Bao Lifeng, Lu Yang, et. al., 2007; Liu Guifeng, Ma Haiqin, et. al., 2007; Jiang Tao, Li Jiancheng, et. al., 2008; Deng Kailiang, Bao Jingyang, et. al., 2008a; Zhan JinGang, Wang Yong, et. al., 2009; Jiang Tao, Li Jiancheng, et. al., 2010). The  $2' \times 2'$  mean sea surface height model over China Sea was computed by forcing correction method with Geosat/GM, ERS-1/2, T/P, GFO observation data. Compared with other international global models over the same period, the discrepancy is about 7~12 cm. The accuracy and resolution of the computed SSH have greatly increased due to the waveform retracking by 5 parameters linear model and least square fit. Using girded SSH data over 14 years, the characteristics of principle components variations in time and space domain of sea level variations in Yellow Sea, East China Sea and South China Sea were given. The spatial distribution and average rising rates of sea level variations over China Sea were discussed. The sea level rising rate is estimated to be  $+3.9 \pm 0.47$  mm/a,  $+4.28 \pm 0.35$  mm/a and  $+3.5 \pm 0.4$  mm/a in Yellow Sea, East China Sea and South China Sea, respectively. Seasonal variability of global mean sea level and its eusteric component and steric component during September 2002 and April 2008 is investigated from combined GRACE time variable gravity field model and Jason-1/2 satellite altimetric data. The annual amplitudes and phases of mean sea level variation from combined satellite observations are quite consistent with that of results from WOA05 datasets. Over 6.5 years' time scale, the secular trend of global mean sea level rise is  $+2.0 \pm 0.4$  mm/a. The contribution of ocean mass sea level and steric sea level is estimated to be  $+1.4 \pm 0.4$  mm/a and  $+0.5 \pm 0.3$  mm/a, respectively. Using sea level anomaly data during 1992~2005 provided by AVISO, the secular trends of China Sea and global ocean were analyzed. The results show that the linear trends in Yellow Sea, East China Sea and South China Sea are  $+5.05$  mm/a,  $+4.8$  mm/a and  $+4.27$  mm/a respectively, all of which are great than global sea level trend ( $+2.66$  mm/a). The wavelet crossing spectrum and correlation spectrum of sea level anomaly in China Sea and global ocean were investigated as well. There are captured and analyzed that the whole process of the El Niño/La Niña phenomenon happened during the year of 1997~1998, and the El Niño phenomenon happened during the year of 2002~2003 from the observations over tropical Pacific by T/P and Jason-1 respectively. Sea level variations in tropical Pacific are calculated by collinear method based on the latest Envisat-1 altimetric data, and the monthly sea level anomalies are plotted in the resolution of  $30' \times 30'$  from which. The whole process of El Niño happened during the year of

2006~2007 are monitored and analyzed based on the figures.

(2)The variations of ocean mass and heat content as well as its relative sea level are investigated by satellite altimetric data and the combined dataset of satellite altimetry and satellite gravity measurements (Chang Jinlong, Zhong Min, et. al., 2007; Mi Renhuan, Zhong Min, et. al., 2009; Jin Taoyong, Li Jiancheng, et. al., 2010; Feng Wei, Zhong Min, et. al., 2010). Global ocean mass variations are computed using the data of satellite gravity, satellite altimetry and marine hydrology, and their spatial and temporal characteristics are also analyzed. Monthly GRACE gravity field models during the four years from January 2003 to December 2006 are selected, in which the spherical harmonic coefficients of the degree 1 and C20 are considered to be substituted. In the data processing, a filter to remove correlative errors and Gaussian filter are applied, and the leakages of land hydrological signal are corrected to obtain the mass variation component of the sea level change expressed in equivalent water thickness. The global sea level changes are computed using Jason-1 data in the same duration, and the steric variations are obtained by inversion using monthly ocean temperature and salinity data, so that the mass variations of sea water are determined. The two types of maps of the inversed mass variations agree well with each other in the characteristics of yearly variation. Compared to the secular trends derived from altimetry, GRACE and ocean data observed during 1993 and 2003, we can see that the contribution of global ocean mass variations get larger, and become the main factor affecting the global mean sea level rise. It is estimated that the ability of GRACE time variable gravity field model to inverse the global ocean mass variations. And the distribution of global thermo-steric sea level variation is investigated by combining satellite altimetric data and GRACE time variable gravity field models during Jan. 2003 ~ Dec. 2005. The conclusion is that it can be detected at the same time that seasonal variability of global ocean mass and thermo-steric sea level in large-scale by the combined dataset of two satellite measurements. The seasonal heat content changes over North Pacific and South China Sea during 2001 ~ 2007 are estimated by satellite altimetric data. Compared with the results computed from the ECCO ocean model, the results show that the observations by satellite altimetric data agree well with that from the ECCO ocean model both in the local region and the global ocean. Considering the variations of ocean bottom pressure and the influence of thermal expansion coefficient changes with ocean depth, the heat content changes of the global ocean and the China Sea are estimated by multi-altimetric data from 2003 to 2008. So, an improved method is proposed, which can improve the estimation accuracy of ocean heat content variation in mid and high latitude areas.

(3)It is investigated that marine gravity field recovering with satellite altimetric data, as well as datum unification of multi-satellite altimetric data and the accuracy verification of new satellite altimetry (Wang Hubiao, Wang Yong, et. al., 2007; Huang Motao, Wang Rui, et. al., 2007; Jin Taoyong, Li Jiancheng, et. al., 2007; Jin Taoyong, Li Jiancheng, et. al., 2008; Yang Yuande, E Dongchen, et. al., 2008; Deng Kailiang, Bao Jingyang, et. al., 2008b; Deng Kailiang, Bao Jingyang, et. al., 2009a; Wang Hubiao, Wang Yong, et. al., 2008; Wang Hubiao, Wang Yong, et. al., 2009; Guo Jinyun, Gao Yonggang, et. al., 2009). The main results are as follow. The deflection of vertical over China Sea and global ocean are determined by the along-track weighted least squares using gravity field model (EIGEN-CG01C) and multi-altimetric data during 1985~2001, which include T/P, ERS-1/GM/ERM, ERS-2 and Geosat/GM/ERM. The Geosat/GM altimetric data is reprocessed by waveform retracking. Then, gravity anomalies in the resolution of  $1.5' \times 1.5'$  grid over China Sea and its vicinity are determined using inverse Vening-Meinesz formula. Compared

with the latest shipboard gravity measurements, the standard error (STD) of difference is  $3.37 \times 10^{-5}$  m/s<sup>2</sup>. On the basis of the above results, the practical formula to compute the horizontal and vertical component of gravity gradient vector on geoid at local tangent plane coordinate system was derived. Based on the above  $2' \times 2'$  grid gravity anomaly and deflection of vertical, the three components of  $2' \times 2'$  grid gravity gradient in west Pacific Ocean were computed, the STD of which is 9.99E when compared with the earlier results. Using the multi-satellite altimetric data during 1985~2006 which include T/P, ERS-1/GM, ERS-2, Geosat/GM and GFO, the two components of the deflection of vertical in  $2' \times 2'$  grid over China Sea are computed by the direction-differential coefficient of along track geoid and the azimuth angle of altimetric crossovers. Compared with that of CLS-SHOW99 model, the root of mean square error (RMS) of the difference is 0.87" in meridian and 1.45" in prime vertical. Using the computed deflection of vertical, the  $2' \times 2'$  grid gravity anomaly model over China Sea and its vicinity is obtained by inverse Vening-Meinesz formula. Compared with that of CLS-SHOW99 model, the RMS of the difference is  $8.15 \times 10^{-5}$  m/s<sup>2</sup>. When eliminated error points that the difference is large than 20 mGal, the number of which occupy 3.3% of the total points, and the RMS of the difference is  $4.72 \times 10^{-5}$  m/s<sup>2</sup>. When compared with the shipboard gravity measurements, the RMS of the difference is  $8.91 \times 10^{-5}$  m/s<sup>2</sup>. Two  $2' \times 2'$  grid gravity anomaly models over China Sea are computed by LSC and IVM respectively, using Geosat/GM altimetric waveform data which is retracked by an improved threshold method under the cooperation with the geodesist of Chiao Tung University in Taiwan. The accuracy of the model computed by LSC is better than that by IVM, when compared with the shipboard gravity measurements. A new method is proposed to recovery marine gravity field by combined adjustment using multi-satellite altimetric data. The method reduces the traditional integral crossover adjustment to two steps. Firstly, conditional adjustment is made to the crossover observation equations. Secondly, the least square filtering and extrapolation of sea surface height are made along the altimetric tracks by new error models. Transforming the sea surface height after combined adjustment to  $2' \times 2'$  grid, the grid values of deflection of vertical and gravity anomaly are computed by the differential method and IVM respectively. It is verified that the new method can simplify the solution procedure of crossover adjustment by practical examples.

The problem of datum unification exists in the recovering of marine gravity field by multi-satellite altimetric data. That includes the parameters difference of reference ellipsoid and inconsistent of reference frame that influenced by all types of system error. The former can be solved by simplify but precise transfer formula, but the latter involves much effect estimating of many types of system error. A procedure is proposed to unify the reference frames used by multi-satellite altimetry. Firstly, precise pre-process is made on multi-satellite altimetric data. Secondly, collinear adjustment is used to eliminate the effect of system error and improve the precision of the difference of crossovers. Then, the transfer parameters of reference frame ( $\Delta x$ ,  $\Delta y$ ,  $\Delta z$ , B) are computed by the difference of crossovers, where, B is the scale factor. And the reference frames of all satellite are transferred to that of T/P. The method is verified by comparing the sea surface height model established using multi-altimetric data that unified with the transfer parameters of reference ellipsoid and frame by crossover adjustment, with KMSS04, CLS01 and WHU2000 models. The relative accuracy of Jason-1 to T/P is calibrated by collinear method using their synchronism observations during Jan. 15, 2002 ~ Jul. 2, 2002. After fitting two versions of Jason-1 observations to that of T/P in the same cycle, there are compared and analyzed that significant

wave height, backscatter coefficients, geophysical corrections and corrected sea surface height at the same fitting points. The actual observation accuracy of Jason-1 is estimated by the differences of single-satellite crossovers in each cycle. The conclusion is that the accuracies of Jason-1 and T/P are at the same level.

(4) Sea surface topography and ocean circulation are determined by combining altimetry derived mean sea surface height and gravity field model (Zhang Zizhan, Lu Yang, et. al., 2007a; Zhang Zizhan, Lu Yang, et. al., 2008; Zhou Xuhua, Wang Hubiao, et. al., 2008; Deng Kailiang, Bao Jingyang, et. al., 2009b). Main contents are as follow. The  $2' \times 2'$  grid mean sea surface height (MSSH) model over China Sea is obtained by the forcing correction method using multi-satellite altimetric data, which include Geosat/GM, ERS-1/168, T/P, ERS-2 and GFO. Then, the corresponding  $2' \times 2'$  grid geoid is derived by IVM from deflection of vertical based on the reference gravity field model of EIGEN-GL04C. So,  $2' \times 2'$  grid sea surface topography model is achieved by subtracting the geoid from MSSH, the accuracy of which is  $\pm 5.3$  cm compared with that computed by the latest GPS/Leveling measurement using oceanographic method. It is investigated that the characteristics of mean upper layer geostrophic flow in several years over China Sea and surface geostrophic in typical winter and summer monsoon over South China Sea using the static sea surface topography computed by altimeter derived MSSH and satellite gravity measurements. The results show that the Kuroshio has significant influence on the circulation over China coastal sea. The upper layer geostrophic flow over South China Sea is predominated by seasonal variations, and there are different forms of the whole circulation in winter and summer. Through the comparison of the calculated geostrophic circulation with the satellite tracking surface drifting buoy, it is found that there are in quite good agreement with each other.

Wavelet filter was used to reduce the sea surface topography noises, the geostrophic circulation results determined by wavelet filter and Gauss low-pass filter with sea surface topography in global ocean domain and Kuroshio area were compared with each other, it is proved that wavelet could keep more local characteristic than Gauss filter; Combining a new geoid model (EIGEN-GL04S) recovered from GRACE mission and the KMSS04 model, a new mean dynamic ocean topography (MDT) model are estimated over the Antarctic region. The surface Antarctic Circumpolar Current (ACC) field and its Polar Front (PF) and sub-Antarctic Front (SAF) are derived from MDT after filtering with a wavelet de-noising method. Comparing the MDT, surface ACC, PF and SAF with those from previous geoid model (EGM96) / altimetry, merged MDT and the ocean hydrological data (WOA01), separately, the results show that the ACC from GRACE agree well with WOA01 map in general, and reveal more details than all other results. These indicate that the accuracy of EIGENGL04S model has been improved greatly over pre-existing models at long wavelengths and the ACC detected by satellite measurement has reached relatively high precision at large and middle scale.

(5) A  $5' \times 5'$  grid regional tide model over China Sea ( $2^\circ\text{N} \sim 41^\circ\text{N}$ ,  $99^\circ\text{E} \sim 132^\circ\text{E}$ ) has been established by POM numerical oceanographic model. The "blending" assimilation method is implemented to assimilate 10 years of TOPEX/Poseidon altimeter data and 52 gauges into POM model. Comparison of the tide model with tide gauge records shows that the RSS of 8 constituents is 12.5 cm (Xu Jun, Bao Jingyang, et. al., 2008).

(6) The changes of the Antarctic ice sheet were determined by satellite altimetric data, and its joint dataset with satellite gravity field model (Chu Yonghai, Li Jiancheng, et. al., 2008; Yang Yuande,

E Dongchen, et. al., 2009a). Two conclusions are achieved. The average elevation model ENVISAT-DEM over Antarctic ice sheet is derived from ENVISAT altimetric data during Sep. 2002 ~ Sep. 2006 which has been applied relocation and geophysical correction. Compared with numerical elevation model RAMP-DEM from RADARSAT Antarctic Mapping Project, the mean height difference is about 18m, which means that their accuracies are close to each other. Changes of mean height in five profiles, each of which has 51 sample points, over Antarctic ice sheet are analyzed. The conclusion is that the changes vary from -0.31m to +0.17m. The time variable gravity field models from GRACE can be used to build the global mass (water) distribution change models. At present, seven models have been released by several well-known research institutions (JPL, CSR, GFZ, and GSGR), which include JPL RL02, JPL RL04, CSR RL01, CSR RL04, GFZ RL03, GFZ RL04 and GSGR GL04. These models can be used to study changes of Antarctic ice sheets, but the difference between them vary greatly from each other. In order to select a suitable model for the application in Antarctic, it is verified by the comparison of the time series of steric sea level change between that computed by WOA05 model and those derived by the sea level changes from Jason-1 altimetric data and ocean mass changes from seven GRACE models. Finally, CSR RL04, GFZ RL04, GRGS GL04 models which agree well, are select to compute the mass variations of Antarctic ice sheet. The conclusion is that the equivalent volume change of the ice and snow melting over Antarctic ice sheet varies from -76km<sup>3</sup>/a to +69km<sup>3</sup>/a during Jan. 2003 ~ Dec. 2007.

(7)The application of satellite altimetric data on monitoring water level changes of inland lakes is investigated (Li Jiancheng, Chu Yonghai, et. al., 2007; Jiang Weiping, Chu Yonghai, et. al., 2008; Gao Yonggang, Guo Jinyun, et. al., 2008). Three results are achieved. There are studied that the water level variations of Poyang Lake, Dongting Lake, Taihu Lake and Chaohu Lake on the middle and lower reaches of the Yangtze River and its relationship with climate change using Envisat-1 altimetric data from 2002 to 2005 based on appropriate edit criterion and necessary geophysical corrections. The water level of Qinghai Lake is computed using ENVISA altimetric data during 2002 ~ 2006, which has been processed by distance corrections, such as waveform retracking. The water level variations of the orthometric and normal height are derived using EGM96 model and quasi-geoid model of Qinghai respectively. Compared with the in-situ gauge record, the results show that the accuracy of altimeter range measured within inland lake can be improved by waveform retracking technique. Altimeter waveforms of T/P within Hulun Lake are analyzed. And, the conclusion is achieved that altimeter waveforms within the lakes have similar characteristics of ocean wave. When the lake freezes in winter, the altimeter waveforms are mostly awl-like waveforms. And, by the effect of accumulated snow within the lake, the energy of waveform in winter is lower than that in summer.

(8)Inversion of seafloor topography with satellite altimetric data was studied (Li Dawei, Li Jiancheng, et. al., 2009; Wu Yunsun, Chao Dingbo, et. al., 2009). On the basis of approximate linear relationship between gravity anomaly and seafloor topography, the 2'×2' bathymetry model over China Sea and its vicinity was calculated from the gravity anomalies derived by satellite altimetric data and with ETOPO2 as reference model. Compared with shipboard measured depth, it shows that the accuracy is 120-160m in different depth more than 5 km. Based on the theory of potential and flexural isostatic compensation, the relationship between ocean depth and the vertical component of gravity gradient anomalies is derived. Using the vertical component of gravity gradient anomalies computed with Geosat, ERS-1/2, T/P, Jason-1, EnviSat-1 altimetric

data, the ocean depth model of the South China Sea is predicted using FFT method. Compared with LDEO ocean depth, the RMS of the difference between the predicted model and LDEO achieves 595m when ocean depth is greater than 5000 m.

(9)The improvement of satellite altimetric data process method is studied (Liu Chuanyong, Bao Jingyang, et. al., 2008; Guo Jinyun, Gao Yonggang, et. al., 2009; Guo Jinyun, Gao Yonggang, et. al., 2010). In order to eliminate the inconsistency of the existing data from multi-satellite missions, using a new method of two steps processing procedure based on the a posteriori compensation theory of error, the normal sea surface height points from Geosat/GM are self-crossover adjusted and combing adjusted with altimetric data from T/P. Abnormal is detected in the coefficients calculating of error model. Based on the analysis of the error model and distribution characteristics of normal sea surface height points, the reason of abnormal is found. Then, a modified compute model for crossover adjustment from altimeter data is proposed, which can improve the efficiency and reliability greatly. It is developed that a new multi-sub-waveform parametric retracker (MSPR) to improve the quality of altimeter data in coastal oceans. The least squares collocation method is used to recover the residual gravity anomaly over the coastal water from altimetric data. The corresponding variance and covariance matrices are given too. The waveform data records from Geosat/GM around Taiwan Island are practically retracked with MSPR. When compared with the Taiwan geoid height, the results retracked by MSPR are more accurate than those retracked by the well-known  $\beta$ -5-parameter method and from the geophysical data records (GDRs). According to the analysis of waveform retracking methods for Envisat-1, the Threshold retracking algorithm is optimized. Taking the Mediterranean Sea as experimental area, several methods are used to retrack the altimeter waveform of Envisat-1 over coastal sea. The results show that the Threshold retracking algorithm is the most robust retracking algorithm, and suitable for the Envisat-1 waveform retracking over the Mediterranean Sea and other coastal seas.

## *2.The application of GRACE time variable gravity field information*

GRACE satellites can measure the variation of gravity field and geoid at  $\mu\text{Gal}$  and 0.01 mm level respectively, which mostly reflects the water storage redistribution on Earth surface at the time scale of years or decades. The monthly and annual variations in terms of equivalent water thickness at millimeter meter and centimeter level can be measured, and the mass redistribution of lithosphere caused by big earthquake can be reflected as well, which provides new important information for studying global climate change and strong earthquake disaster. The research on the application of GRACE time variable gravity model has attracted widely attentions. Recently in China, the research on terrestrial water storage change and geophysical application have been conducted, include:

(1)The recovery of global terrestrial water storage variations is studied (Zhu Guangbin, Li Jiancheng, et. al., 2008; Zhou Jiangcun, Sun Heping, et. al., 2009; Yang Yuande, E Dongchen, et. al., 2009b). By using RL-04 GSM gravity field models of the GRACE Level-2 product, the variations of global continental water storage are deduced. And in the deduction, the problems in the choice of Gaussian filter radius and the truncated degree are discussed. The computation result are the best when the Gaussian smoothing radius is 800km and the degree truncates till 20, and the variations of global continental water storage are in accord with those from CPC model in regional scale and seasonal scale. Using GRACE GFZ RL04 time-variable gravity field models, the seasonal and annual water storage variations of 27 valleys all over the world during January 2003

~ December 2007 were estimated and analyzed. The de-correlation filter method P3M8 is similar with that used by Chambers, and the 400 km Gaussian filter and truncation degree 60 were chosen. The results show that seasonal variations of adjacent valleys are similar with each other. The amount seasonal variation of continental water storage is about 1572.4 km<sup>3</sup> in five years. The biggest change is of the Amazon Basin River, followed by the Ob River, Niemann River and the Niger River Basin. The annual change of GRACE derived terrestrial water storage during five years is  $-75.4 \pm 40.3$  km<sup>3</sup>/a, where the Amazon River, Lena River and the McKenzie River show positive growth, but the Congo River, the Mississippi River, constant River, Yukon River and the Brahmaputra river basin are the opposite.

In order to verify the global water storage variation model from GRACE measurements, the long-term continuous gravity observations obtained by the superconducting gravimeters (SG) at seven globally-distributed stations are comprehensively analyzed. After removing the signals related to the Earth's tides and variations in the Earth's rotation, the gravity residuals are used to describe the seasonal fluctuations in gravity field. Meanwhile, the gravity changes due to the air pressure loading are theoretically modeled from the measurements of the local air pressure, and those due to land water and non-tidal ocean loading are also calculated according to the corresponding numerical models. The numerical results show that the gravity changes due to both the air pressure and land water loading are as large as  $100 \times 10^{-9}$  ms<sup>-2</sup> in magnitude, and about  $10 \times 10^{-9}$  ms<sup>-2</sup> for those due to the non-tidal ocean loading in the coastal area. On the other hand, the monthly-averaged gravity variations over the area surrounding the stations are derived from the spherical harmonic coefficients of the GRACE-recovered gravity fields, by using Gaussian smoothing technique in which the radius is set to be 600 km. Compared the land water induced gravity variations, the SG observations after removal of tides, polar motion effects, air pressure and non-tidal ocean loading effects and the GRACE-derived gravity variations with each other, it is inferred that both the ground- and space-based gravity observations can effectively detect the seasonal gravity variations with a magnitude of  $100 \times 10^{-9}$  ms<sup>-2</sup> induced by the land water loading.

(2)The recovery of terrestrial water storage variations over China and its vicinity is studied (Xing Lelin, Li Hui, et. al., 2007; Wang HanSheng, Wang ZhiYong, et. al., 2007; Zou Zhengbo, Xing Lelin, et. al., 2008; Zhai Ning, Wang Zemin, et. al., 2009; Zhong Min, Duan Jianbin, et. al., 2009). Using 43 monthly gravity models observed by GRACE satellites, water storage variations of Yangtze River basin are estimated. The geocentric variations and C20 effects are considered in the computation. The results show remarkably good agreement with that computed from CPC model. 22 monthly water storage changes are predicted for the supply water systems of the Three Gorges Reservoir from GRACE time-variable gravity data. Gaussian averaging radius is selected as 1000 km in the computation. The results are compared with CPC hydrological models and true average results of CPC models respectively. It is found that the first comparison has overestimated the effectiveness of GRACE. Nevertheless, the monthly water storage changes can be also determined with the accuracy of 1~2 cm from GRACE data in this area. On the basis of the 100 degree time-variable gravity field model of GRACE, the monthly variation of the water storage in China and its vicinity is inversed during January and November in 2005. The effects of C20 are ignored. The analysis of results shows that time variable gravity field of GRACE can be used to monitor the variation of water storage with the accuracy of several centimeters in terms of equivalent water thickness, and reflect regional climate conditions during monitoring period as well. By near 5-years' GRACE time variable gravity field observation data, the long spatial scale continental

water storage trends in China are investigated. The results show that trends of terrestrial significant reduction in water exist in five typical regions, which are region of Beijing-Tianjin in North China, Qinghai-Tibet Plateau region, the Three Gorges Reservoir, border region of Qinghai-Sichuan-Gansu, and Altun Mountain Nature Reserve in Xinjiang. The trend of continental water (ice) storage decrease obviously in the first two regions. In the region of Beijing-Tianjin in North China, the continental water storage declines at a rate of about 2.4 cm/a from 2003 to 2007. In 120,000 km<sup>3</sup> area of the Three Gorges reservoir, the average water storage variation in terms of equivalent water thickness can achieve 5.0 cm before and after water storing in Jun. 2003, which is captured by GRACE gravity satellite. In addition, in the border region of Qinghai, Sichuan and Gansu, the water storage increases at a rate of about 1.1 cm/a, which shows that the regional climate in recent years the trend has gradually become moist.

(3)The application in the field of geophysics is investigated (Zhang ZiZhan, Lu Yang, et. al., 2007b; Chen Wei, Shen Wenbin, et. al., 2009; Duan Hurong, Zhang Yongzhi, et. al., 2009; Xing Lelin, Li Jiancheng, et. al., 2009; Zou Zhengbo, Luo Zhicai, et. al., 2010; Liao Haihua, Zhong Min, et. al., 2010; Wang WuXing, Shi YaoLin, et. al., 2010). Using RL-04 GSM 60 degree monthly gravity model of GRACE published by CSR, and taking 500km as the Gaussian average radius and the GGM02S gravity model as a reference, the co-seismic and post-seismic deformation of inner mass density redistribution caused by Sumatra-Adaman MS9.1 earthquake that happened on December 26, 2004, are computed in the terms of equivalent water thickness. The numerical results show that co-seismic and post-seismic deformation information about -20~10 cm equivalent water thickness can be detected by GRACE satellite gravity surveying. Based on the monthly GRACE gravity field model between 2006 and 2008, taking 666 km as the Gaussian average radius and the EIGEN-GRACE02S gravity model as a reference, it is calculated and compared that the gravity field in Chinese continent before and after the Wenchuan MS8.0 earthquake happened on May. 12, 2008. By the comparison of three-month gravity field (May, June and July) in 2008 with the ones in 2006 and in 2007, those are found that in the areas of Lanzhou and Kunming, there are obviously positive gravity potential variations between 2006 and 2007, and large region of high values. But the values decline sharply in 2008 and they are the trend of reversing to negative on the edge of areas. Taking 800km as Gaussian smoothing radius and the average of 78 monthly gravity filed changes as reference, annual gravity changes in China mainland and its vicinity are calculated from RL-04 GSM(60 degree and order) produced from GRACE monthly gravity field data between April 2002 and December 2008. The characteristics of annual changes are discussed as well. By analyzing the gravity changes before and after several strong earthquakes larger than Ms7.5 between 2003 and 2008, the results show that the gravity in the epicenter zone appears positive before the earthquake and converts to negative after the shock. The calculation of the gravity before and after the Wenchuan earthquake shows the same phenomenon. The gravity changes related to the Wenchuan Ms8.0 earthquake are observed by GRACE satellite. Time variable changes of gravity field and the surface density in Chinese Mainland and its vicinity before and after the Wenchuan Ms8.0 earthquake are obtained from the GRACE satellite gravity data. Time series of monthly gravity changes at typical locations are also obtained. Results from GRACE indicate that after the Sumatra Ww9.3 earthquake along the Himalaya arc, the satellite gravity decreases rapidly, particularly during the period of 2006 to 2008; while along the northwestern boundary of the Xiyu block, post seismic gravity decrease significant too. And along the northern and eastern boundaries of the Tibetan plateau, there

appeared an arc along the tectonic boundary with significant gravity increase in 2007. But in 2008 there was also significant increase in gravity in the southern and middle segments of the North-South seismic belt. This trend in gravity variations changed only after the Wenchuan earthquake.

The impacts of the temporal second-order potential coefficients on the Earth's principal axes and moments of inertia as well as variations of length of day (LOD) are studied. By using the wavelet analysis, the monthly-averaged GRACE gravity model is processed. The Earth's principal axes and moments of inertia are obtained from the processed and non-processed second-order potential coefficients respectively; it is found that the related mass redistribution of the Earth system lead to a decreasing tendency of LOD during the recent 6 years. The results of  $J_2$  from GRACE do not agree well with that from SLR measurements. The maximum entropy spectral analysis and wavelet analysis are used to assess the data sets  $J_2$  from GRACE and SLR. The results show that the inter-annual amplitude of the  $J_2$  signal from GRACE is only 25% of that from SLR, and GRACE  $J_2$  signals contain inputted system information and great phase difference, but the former reveals stronger short-term (2~6 months) signals than the later. These differences might be caused by the un-synchronism of the global measurements from GRACE and SLR.

Climate driven surface annual vertical deformation is studied by the GRACE time-variable gravity data. Seasonal vertical deformation signals of the solid Earth in China and neighboring areas are calculated from GRACE monthly time-variable gravity field coefficients truncated to degree and order of 60, and the results are compared with seasonal signals measured at 42 GPS sites located in the same region. In calculating we use de-stripes and de-stripes plus Gaussian smoothing respectively, and we find the former filtering result is better than the latter one. These results demonstrate that GRACE can be a new effective tool for monitoring annual vertical deformation on a large scale in China and neighboring areas, and the surface deformation monitored by GRACE is more accurate than one simulated by surface fluid model such as continent water.

### *3.Application in other relative fields*

These related areas include the images of changes in gravity field in China and its geodynamic characteristics, the information technology of Earth gravity field, gravity information aided inertial navigation and applications in the deep geophysical. Main research results include:

(1) Geodynamic characteristics reflected by time-variable gravity field in Mainland of China and new statistic parameters of gravity field in China are analyzed (Zhu Yiqing, Liang Weifeng, et. al., 2007; Li Yuefeng and Ding Xingbin, 2008; Li Hui, Shen Chongyang, et. al., 2009; Li Shanshan, Wu Xiaoping, et. al., 2010). The spatial evolution of gravity field in Mainland of China is computed using absolute gravity and relative gravity measurements in 1998~2000 by the Crustal Movement Observation Network of China, which includes 23 reference stations, 56 base stations and more than 200 regional stations. Robust estimation method is used in data processing. And the character of dynamic gravity change in China and its relationship with crust movement and geologic structure movement are analyzed combined with Bouguer gravity anomaly field, geologic structure movements and the earthquake epicenters. The image and characteristics of gravity field changes in Mainland of China during 1998-2007 are researched based on observations of the dynamic gravity network. The dynamic gravity network covered the mainland of China contains gravity networks of crustal movement network and digital seismic network. The

former whole network has about 400 points, and completed 3 times absolute gravity observation (1998, 2001 and 2004), and 4 times relative gravity observations (1998, 2000, 2002 and 2005), whose measuring one-way line is about 35000km. The latter network construction began in 2004, which is based on expansion in the former, has increased 11 absolute gravity points and 146 monitoring points, whose one-way survey line extends about 11000km. The first time measurement is completed in 2007. After rigorous data processing and weak base adjustment, the precision of gravity change between any 2 times observations is about  $20 \times 10^{-8} \text{m/s}^2$ . Accordingly, the dynamic images of the gravitational field are constructed and mapped, and the differential dynamic characteristics and the accumulated dynamic characteristics are analyzed. Gravity changes response to 4 large earthquakes ( $> \text{Ms}7.0$ ) from 198 to 2008 in China are analyzed combining with the inner dynamic movement. Based on intensive gravity and topographic data of a pilot area, the new statistics are constructed, such as the covariance and representative error model parameters between complete Bouguer anomaly and the free-air anomaly. The corresponding practical calculation model, programs and algorithms are proposed, and the program is extended to the national large-scale, multi-region statistical calculations. The variance, covariance, and representative error model parameters between complete Bouguer anomaly and complete free-air anomaly in 6 regions of different terrain are given. The results show that grid values and contour values of local gravity field statistical parameters of any terrain type in the whole nation can be calculated by observations based statistical models, algorithms and ideas given by the author, which can be used for a variety of calculation of the local gravity field based on statistical methods. Several formulas to compute the Plumb Line Variations (PLV) are discussed. It is probed into the measuring precision about PLV, which can be attained to  $0.005''$  in theory, and whose variation is about  $0.02''$  in measuring. It appears that the PLVs at Tangshan, which are determined using the 46 batch repeated gravity observations of the Beijing-Tangshan network during the years 1987~1998, are related with the 38 earthquakes ( $\text{Ms}>4.0$ ) in this period. The relationship between PLV and earthquake is given.

(2)The establishing of gravity surveying information system and relative technique problems of software are studied (Wu Xing, Li Ming, et. al., 2007; Zhang Hao, Li Shanshan, et. al., 2006). Aiming at the information construction of gravity surveying, a detailed study has been done on the multi-source information service of the gravity field as well as the applications through analysis of the gravity field information. Based on multi-source gravity field information, a service system which integrated data storage, processing, distribution and application is built, which satisfy the requirements of gravity field research and application departments, and realize the automation of the collection, processing and management of enormous gravity data and enhanced work efficiency. It is introduced that the design and the basic function of land gravity precision technology software. The key technique of each part is analyzed and expounded. The software is composed of three parts, including gravity field data processing, data applying and analyzing, data visualizing. The software, which is main component of gravity field information system, has realized the management of gravity observation data and provided automated processing of gravity field data and simulation of field gravimetric survey laying station as well as graphics visualization of gravity field information.

(3)The applications of gravity field information in the underwater and aerial inertial navigation are studied (Dai Quanfa, Hsu Houze, et. al., 2008; Jin Jihang and Bian Shaofeng, 2010). Simulations of realize the gravity matching aided inertial navigation underwater using high-resolution marine

gravity data (gravity anomaly and deflection of vertical) by satellite altimetry are being done. Simulation which employs the true gravity anomalies on the Chinese coastal waters is designed by two different algorithms, multiple model adaptive Kalman filter and the method of the absolutely difference's square. The simulation is implemented in two routes that have different changing magnitude in the gravity anomalies. The feasibility of gravity anomaly matching technology is verified through the simulation. And the influence of gravity disturbance on aircraft inertial navigation system position is analyzed. Starting from the physical geodesy and Newton's second law, an error dynamics equation of inertial navigation system, including the influence of gravity disturbance, is presented. Then, taking single-axis inertial navigation system as an example, the position error caused by the deflection of vertical and corresponding characteristics of error propagation in three situation were analyzed. And simulation is done on  $1' \times 1'$  deflection of vertical database. From the simulation result, the horizontal error of inertial navigation system caused by deflections of vertical on the sailing course can reach as large as 3km.

(4)The inner core's super rotation and its influence on gravity field are investigated (Shen WenBin, Liu Lin, et. al., 2007). It is dissertated that the inner core has three main characters: is has ellipsoidal shape; the anisotropic symmetric axis of the inner core coincides with its self-rotation axis; the rotation axis of the inner core is tilted to and processes around the Earth's rotation axis. The inner core's super rotation gives rise to the mass redistribution of the Earth system, and consequently results in the variation of the gravity field. By investigating the motion of the inner core's super rotation, a model of gravity change caused by the inner core's super rotation is established. Calculation results are provided about the gravity variations on the whole surface of the Earth caused by the inner core's super rotation. Under the assumption of the super rotation rate  $1^\circ/a$ , the maximum gravity variation in one year is around 0.37 micro Gal.

(5)The undulation of geoid influenced by loading of neighboring buildings and there effect on elevation are investigated (Wang Jiexian, Ji Shanbiao, et. al., 2008). Based on the loading tides theory, the ground vertical deformation and the geoid undulation caused by loading of neighboring buildings are studied using the building distribution of Shanghai provided by Shanghai Surveying and Mapping Institute. The influence on elevation is also considered. The results show that the ground vertical deformation and the geoid undulation both reach millimeter magnitude. Therefore, it is obvious that the building loading significantly affects the precise engineering surveying, and it must be seriously considered in application.

## **VI. Progress of the research**

In the past four years, the research on the Earth's gravity field is still focused on the used of satellite gravity data in china. The research on applications was extended combined with determination of local gravity field with high-resolution and high-precision and the relevant basic theory, and explore new methods and new technologies. Further efforts are still need to refine the Chinese regional geoid in order to achieve centimeter-level precision. At the same time, the environmental issues were studied by the measurements of satellite altimetry, GRACE and surface gravity, such as changes in sea level, ocean currents and the dynamic equilibrium of surface water storage that associated with climate in Chinese mainland and water area.

During this period, more strictly practical SST ranging observation equation was derived, the approaches used to refinement process of SST observation data were proposed. Three new series

of satellite gravity models were released, including XISM-CHAMP, IGG-GRACE and SWJTU-GRACE. Energy conservation principle for gravity field determination from satellite observations was studied further. Close formula for computing the differences of Kinetic energy between two satellites using the KBR relative line of sight rate observation method directly was derived. The least squares adjustment method for calculation of the coefficients was proposed and tested based on energy conservation principle and Variance component estimation. The new method for computing the satellite average acceleration with onboard GPS satellite phase data directly was proposed. The method for determination of Earth's gravity field based on dynamics method using the double difference phase observations of onboard GPS and IGS data was studied. In the simulation research of the recovery of the earth's gravity using SGG data, the complex combination formula for computing disturbance gravity gradient of single-point, grid points and average of grid network with the gravity models was derived. The new methods for computing generalized spherical harmonics and its definite integral as well as a new method for fast simulation of GOCE gravity gradient observations along track were proposed. The magnitude and contribution of GOCE orbit and main perturbation acceleration were simulated based on dynamic orbit integration. The generalized torus harmonic analysis method for determination of gravity using the combination of the energy components of GOCE gravity gradient and the construction of point mass model for gravity gradient data were studied. In the field of error analysis of satellite gravity measurements, based on the satellite dynamic orbit determination and the theory of coefficient calculation, the effect of the satellite initial state and force model to the orbital integral was studied. At the same time, the effect of ocean tide and the adjusted precision of the mass center of GOCE and its accelerometer to the recovery of gravity field were studied.

In the field of preliminary research on the development of Chinese satellite gravity measurement system, the relationship between error spectrum of gravity field and noise spectrum of SST-LL distance variability observations was studied and established. Accordingly, the effect of accuracy variations of satellite distance, orbit height and distance variability on the accuracy of gravity recovery was studied and the optimal design of orbital altitude and the resolution index of the accelerometer high-low axis were researched in this model. The major technical indicators of SST-HL model were simulated, analyzed and tested, and SGG. As an alternative model, the effect of orbital altitude, inclination, gradient measurement accuracy and data sampling rate to the accuracy of gravity field recovery was studied too.

In the research on basic theory, the solution of super-posed boundary value problem based on variation method is studied; the analysis of well-posedness and solution model of the problem is given, as well as the theoretical deficiency of the classic definition of the Normal Ellipsoid and solution approach. The inversion theory of gravity anomaly based on multi-scale edge is investigated, and we give the expression and fast algorithm of topographic effect on any type of the Earth's external gravity field observations, re-examine and research the equilibrium theory of a variety of terrain gravity, and propose new academic viewpoints. In the aspect of new approach research and test, the main investigation is linear estimation method in frequency domain considering the noise and resolution, the downward continuation application of least square collocation method in airborne gravity data, and general expression of empirical covariance combining observations of multi-type and different height as well.

In the research on application, the seasonal changes and long-term trends of the global mean sea

level and its mass and steric components are studied by jointly using satellite altimeter and GRACE data between 2002 and 2009. In the time-scale over 6.5a, the rising rate of global mean sea level is  $+2.0\pm 0.4\text{mm/a}$ , the contribution of mass change and steric variation are  $+1.4\pm 0.4\text{mm/a}$  and  $+0.5\pm 0.3\text{mm/a}$  respectively. In addition, using the dataset of GRACE, satellite altimeter, ocean temperature and salinity between 2003 and 2006, the changes of global mean sea level, ocean mass and steric are obtained, which are  $+2.4\pm 0.2\text{mm/a}$ ,  $+1.8\pm 0.2\text{mm/a}$  and  $-0.5\pm 0.2\text{mm/a}$  respectively, and the characteristics of ocean mass annual changes derived from GRACE agrees well with that from satellite altimeter and ocean temperature and salinity data.

Using 14 years altimeter data in China coastal areas, the spatial and temporal variations over Yellow Sea, East China Sea and South China Sea are obtained. The mean sea level rise rate over three seas is  $+3.9\pm 0.4\text{mm/a}$  during 1993 and 2007. Based on multi-generation satellite data and EIGEN-GL04C geoid model, the  $2'\times 2'$  grid sea surface topography model of China coastal seas is produced, the accuracy of which is coarsely estimated to be  $\pm 5.3\text{cm}$ . Meanwhile, the multi-year upper layer geostrophic flow in China coastal seas and surface geostrophic in typical winter and summer monsoon over South China Sea are studied using static sea surface topography. At the same time, the Antarctic Circumpolar Current is determined using satellite gravity associated with satellite altimetric data. Based on the satellite altimetric data between 1985 and 2006, the  $2'\times 2'$  gravity anomaly model over China coastal seas is established. The RMS of the difference between the model and shipboard measurements is  $8.9\times 10^{-5}\text{m/s}^2$ . There are two other similar achievements. The  $5'\times 5'$  ocean tide model over China coastal seas is derived by 10 years T/P altimetric data. Other applications of satellite altimetry research include the studies of the Antarctic ice sheet changes, variations in water level of inland lakes, and submarine topography inversion.

Using GRACE time-variable gravity field model, the changes of global continental water storage distribution are obtained in the 5-year period, the magnitude of whose seasonal change is  $1572\text{km}^3$ , and annual change is  $-75.4\pm 40.3\text{km}^3/\text{a}$ . The continental water storage variations of China and its vicinity are also studied. And the tendency of Chinese continental water storage variation with medium and long spatial scale in recent 5 years is analyzed, associated with the relationship between geographical and climatic factors. The characteristics of gravity field variation in Chinese mainland is studied by many authors using GRACE time-variable gravity field model, especially the relationship with earthquakes that great than  $M_s 7.5$  between 2003 and 2008.

The applications in other related areas include: the characteristics of geodynamics and its relationship between crustal movement and tectonic activity which is reflected by the Chinese mainland time-variable gravity field, the inner core's super rotation and its influence on the time-variable gravity field, gravity aided inertial navigation and the establishment of gravity measurement information system, etc.

In recent five years, China has made a lot of jobs in the field of the Earth gravity field, and achieved rich results, which objectively and comprehensively reflect the current situation and development level of our research in this area.

## Reference

- [1] Xiao Yun, Xia Zheren, and Wang Xingtao, Recovering the Earth Gravity Field from Inter-satellite Range-rate of GRACE. *Acta Geodaetica et Cartographica Sinica*, 2007. 36(1): p. 19-25.
- [2] Luo Jia, Ning Jinsheng, Shi Chuang, and Zou Xiancai, Establishment of observation equation for satellite-to-satellite tracking. *Geomatics and Information Science of Wuhan University*, 2008. 33(6): p. 619-622.
- [3] Xu Tianhe and Ju Xiangming, CHAMP Gravity Field Recovery Based on Variance Component Estimation. *Geomatics and Information Science of Wuhan University*, 2007. 32(3): p. 242-245.
- [4] Xu Tianhe and Gan Yuehong, CHAMP Gravity field recovery based on the improved energy conservation approach. *Progress in Geophysics*, 2008. 23(1): p. 63-68.
- [5] Wang ZhengTao, Li JianCheng, Jiang WeiPing, and Chao DingBo, Determination of earth gravity field model WHU-GM-05 using GRACE gravity data. *Chinese Journal of Geophysics*, 2008. 51(5): p. 1364-1371.
- [6] Zheng Wei, Hsu Houze, Zhong Min, Yun MeiJuan, et al., Effective processing of measured data from GRACE key payloads and accurate determination of Earth's gravitational field. *Chinese Journal of Geophysics*, 2009a. 52(8): p. 1966-1975.
- [7] Xu Tianhe, He Kaifei, and Wu Xianbin, Comparison of time-wise approach and space-wise approach for CHAMP gravity field recovery. *Progress in Geophysics*, 2009. 24(2): p. 456-461.
- [8] 8. You Wei, Fan Dongming, and Guo Jiang, Gravity field recovery by using energy conservation approach. *Journal of Geodesy and Geodynamics*, 2010. 31(1): p. 51-55.
- [9] Guo Jinyun, Hwang Cheinway, Hu Jianguo, and Li Jiancheng, Determination of Earth Gravity Field Model from GPS Phase Double-Different Data Onboard CHAMP. *Geomatics and Information Science of Wuhan University*, 2007. 32(1): p. 11-14.
- [10] Zhao Qile, Guo Jing, Liu Xianglin, and Shi Chuang, Gravity Field Modeling on the Basis of Satellite Accelerations Directly Derived from Onboard GPS Measurements. *Geomatics and Information Science of Wuhan University*, 2009. 34(10): p. 1168-1171.
- [11] Wu Xing, Zhang Chuanding, Ye Xiusong, and Han Zhichao, Simulation of Satellite Gravity Gradient Tensor Observations. *Journal of Geomatics Science and Technology*, 2008. 25(6): p. 391-395.
- [12] Xu Xinyu, Li Jiancheng, Jiang Weiping, and Zou Xiancai, Rapidly Computing Satellite Gravity Gradient Observations Along Orbit from Gravity Field Model. *Geomatics and Information Science of Wuhan University*, 2009. 34(2): p. 226-230.
- [13] Wu Xing, Zhang Chuanding, and Zhao Dongming, Generalized Torus Harmonic Analysis of Satellite Gravity Gradients Component. *Acta Geodaetica et Cartographica Sinica*, 2009a. 38(2): p. 101-107.
- [14] Wu Xing, Zhang Chuanding, and Liu Xiaogang, Point-Mass Model Construction Based on Satellite Gravity Gradients. *Journal of Geomatics Science and Technology*, 2009b. 26(6): p. 414-417.
- [15] Luo Zhicai, Zhong Bo, Ning JinSheng, and Yang Guang, Numerical simulation and analysis for GOCE satellite orbit perturbations. *Geomatics and Information Science of Wuhan University*, 2009. 34(7): p. 757-760.

- [16] Luo Zhicai, Wu Yunlong, Zhong Bo, and Yang Guang, Pre-processing of the GOCE satellite gravity gradiometry data. *Geomatics and Information Science of Wuhan University*, 2009. 34(10): p. 1163-1167.
- [17] Zhou JiangCun and Sun HePing, Effect of ocean tide on recovery of satellite gravity field. *Chinese Journal of Geophysics*, 2007. 50(1): p. 115-121.
- [18] Xu Xinyu, Li Jiancheng, Wang Zhengtao, and Zou Xiancai, Calibration of GRACE Accelerometer Using Reference Gravity Field Model Based on Energy Balance Approach. *Geomatics and Information Science of Wuhan University*, 2008. 33(1): p. 72-75.
- [19] Wang Zhengtao, Jin Xiangsheng, Dang Yamin, and Jiang Weiping, Numerical Integration Error Analysis of Initial Orbit Vectors and Force Model Parameters in Precise Orbit Determination. *Geomatics and Information Science of Wuhan University*, 2009. 34(6): p. 728-731.
- [20] Zheng Wei, Hsu Houze, Zhong Min, Yun Meijuan, et al., Mutual verification of two methods on evaluating accuracy of GRACE Earth's gravitational field. *Journal of Geodesy and Geodynamics*, 2009b. 29(5): p. 89-93.
- [21] Zheng Wei, Hsu HouZe, Zhong Min, Yun MeiJuan, et al., Influence of the adjusted accuracy of center of mass between GRACE satellite and SuperSTAR accelerometer on the accuracy of Earth's gravitational field. *Chinese Journal of Geophysics*, 2009c. 52(6): p. 1465-1473.
- [22] Zhang Xingfu and Shen Yunzhong, The influence of LEO satellite s initial state errors on gravity field recovery. *Science of Surveying and Mapping*, 2009. 34(3): p. 46-48.
- [23] Zou Zhengbo, Luo Zhicai, Xing Lelin, Wu Yunlong, et al., Time domain least squares method for recovering Earth's gravity field by satellite gravity gradient. *Journal of Geodesy and Geodynamics*, 2007. 27(3): p. 44-49.
- [24] Ning Jinsheng, Zhong Bo, Luo Zhicai, and Luo Jia, Establishment and Analysis of the Spectral Relationship Between Range-Rate and Gravity Potential Based on Energy Conservation. *Geomatics and Information Science of Wuhan University*, 2008. 33(3): p. 221-225.
- [25] Zhong Bo, Luo Zhicai, Luo Jia, and Wu Yunlong, Simulation Analysis and Verification for Major Indexes of High-Low Satellite-to-Satellite Tracking Mission *Geomatics and Information Science of Wuhan University*, 2008a. 33(8): p. 864-867.
- [26] Zhong Bo, Luo Zhicai, Wu Yunlong, and Luo Jia, Design and realization of the simulation analysis software for the major technology indexes of satellite-to-satellite tracking mission. *Science of Surveying and Mapping*, 2008b. 33(3): p. 146-148.
- [27] Zheng Wei, Hsu HouZe, Zhong Min, Yun MeiJuan, et al., Demonstration on the optimal design of resolution indexes of high and low sensitive axes from space-borne accelerometer in the satellite-to-satellite tracking model. *Chinese Journal of Geophysics*, 2009d. 52(11): p. 2712-2720.
- [28] Zheng Wei, Hsu Houze, Zhong Min, Yun Meijuan, et al., Optimal design of orbital altitude in satellite-to-satellite tracking model. *Journal of Geodesy and Geodynamics*, 2009e. 29(2): p. 100-105.
- [29] Zheng Wei, Hsu Houze, Zhong Min, Yun Meijuan, et al., Research on optimal selection of orbital parameters in Improved-GRACE satellite gravity measurement mission. *Journal of Geodesy and Geodynamics*, 2010a. 30(2): p. 43-48.
- [30] Zheng Wei, Hsu Houze, Zhong Min, Yun MeiJuan, et al., Efficient and rapid estimation of

- the accuracy of future GRACE Follow-On Earth's gravitational field using the analytic method. *Chinese Journal of Geophysics*, 2010b. 53(4): p. 796-806.
- [31] Yu Jinhai and Peng Fuqing, Variational solution about over-determined geodetic boundary value problem and its related theories. *Science in China(Series D:Earth Sciences)*, 2007. 37(1): p. 39-45.
- [32] Shen Wenbin, Zhong Qiuju, and Li Jin, The normal field determination and a theoretical problem. *Science of Surveying and Mapping*, 2007. 32(2): p. 12-14.
- [33] Zhang Chijun, Fang Jian, Bian Shaofeng, and Gao Jinyue, Gravity(Crust) Isostasy and Topographic Wavelength—On Isostatic Isn t Suitable for Gravity Estimation on Qumolangma Peak. *Geomatics and Information Science of Wuhan University*, 2007. 32(3): p. 229-233.
- [34] Wang Haihong, Ning Jinsheng, Luo Zhicai, and Luo Jia, Separation of Gravity Anomalies Based on Multiscale Edges. *Geomatics and Information Science of Wuhan University*, 2009. 34(1): p. 109-112.
- [35] Zhang Chuanyin, Chao Dingbo, Ding Jian, and Zhang Liming, Precision Topographical Effects for any Kind of Field Quantities for any Altitude. *Acta Geodaetica et Cartographica Sinica*, 2009. 38(1): p. 28-34.
- [36] Zhang Hanwei, Guo Zengzhang, and Li Aiguo, Theoretical research on the space-time changes of the Earth's gravitational field produced by tidal force. *Science of Surveying and Mapping*, 2010. 35: p. 5-7.
- [37] Zhang Chuanyin, Ding Jian, and Chao Dingbo, General Expression of Least Squares Collocation in Local Gravity Filed. *Geomatics and Information Science of Wuhan University*, 2007. 32(5): p. 431-434.
- [38] Cui Lili, Luo Zhicai, Zhong Bo, and Wang Haihong, Effect of observation noise on data fusion bby frequency domain inpu-output method. *Journal of Geodesy and Geodynamics*, 2009. 29(1): p. 79-82.
- [39] Zhou Shichang, Wang Qingbin, and Zhang Chuanding, Simulation experiment of quickly determination of disturbing gravity using wide-area polynomial approximation. *Science of Surveying and Mapping*, 2009a. 34(4): p. 153-154.
- [40] Zhou Shichang, Wang Qingbin, and Zhu Leiming, Research of improved fictious compress recovery approach for approximating locally disturbing gravity. *Journal of Geodesy and Geodynamics*, 2009b. 29(1): p. 88-90.
- [41] Zhong Bo, Wang Haihong, Luo Zhicai, and Cui Lili, Research on Linear Estimation Method Considering Observation Noise and Data Resolution *Geomatics and Information Science of Wuhan University*, 2009. 34(3): p. 273-276.
- [42] Zhang Xiaolin, Zhao Dongming, and Wang Qingbin, Precise Determination and Approximation Analysis of Disturbing Gravity Field. *Journal of Geomatics Science and Technology*, 2009. 26(3): p. 212-215.
- [43] Zhai ZhenHe and Sun ZhongMiao, Continuation model construction and application analysis of local gravity field based on least square collocation. *Chinese Journal of Geophysics*, 2009. 52(7): p. 1700-1706.
- [44] Pang Zhenxing and Zhang Chuanding, Terrain correction computation by controlling the integral radius using the FFT method. *Science of Surveying and Mapping*, 2009. 34(4): p. 188-190.

- [45] Li Na and Zhang Chuanyin, Option of integral radius in inversion of sea gravity with inverse Vening-meinesz formula. *Journal of Geodesy and Geodynamics*, 2009. 29(6): p. 126-129.
- [46] Pang Zhenxing, Zhang Chuanding, and Xiao Yun, The research of calculating the land gravity anomaly by using the inverse Vening Meinesz formula. *Science of Surveying and Mapping*, 2010. 35(3): p. 34-36.
- [47] Peng Zehui, Li Hui, Shen Chongyang, and Sun Shaoan, Interpolation method based on least squares collocation for dynamic gravity changes. *Journal of Geodesy and Geodynamics*, 2010. 30(3): p. 43-46.
- [48] Zhao Xiaoyang, Li Jiancheng, Wang Zhengtao, and Jin Taoyong, Using Satellite Altimetry Technique for Monitoring ElNino and LaNina Phenomenon *Hydrographic Surveying and Charting*, 2007. 27(1): p. 41-44.
- [49] Bao Lifeng, Lu Yang, Wang Yong, and Xu Houze, Coastal mean sea surface height by retracking ERS-1 altimeter waveform data. *Progress in Geophysics*, 2007. 22(2): p. 427-431.
- [50] Liu Guifeng, Ma Haiqin, and Zhang Guoyu, Trends and wavelet correlation analysis of sea level changes in the China Seas and the global area from satellite altimetry. *Science of Surveying and Mapping*, 2007. 32(6): p. 56-58.
- [51] Jiang Tao, Li Jiancheng, Wang Zhengtao, and Jin Taoyong, Monitoring El Niño Phenomenon during 2006-2007 in Satellite Altimetry. *Marine Science Bulletin*, 2008. 27(5): p. 105-109.
- [52] Deng Kailiang, Bao Jingyang, Xu Jun, and Zhang Chuanyin, Establish the average sea level model of the Chinese Coastal Waters using forced correct method. *Geomatics and Information Science of Wuhan University*, 2008a. 33(12): p. 1283-1287.
- [53] Zhan JinGang, Wang Yong, and Cheng YongShou, The analysis of China Sea Level change. *Chinese Journal of Geophysics*, 2009. 7: p. 1725-1733.
- [54] Jiang Tao, Li Jiancheng, Wang Zhengtao, Jin Taoyong, et al., Global sea level variations from combined Jason-1 and GRACE data. *Acta Geodaetica et Cartographica Sinica*, 2010(02).
- [55] Chang Jinlong, Zhong Min, Duan Jianbin, Yan Haoming, et al., On seasonal steric sea level variations combining GRACE with satellite altimetry data. *Journal of Geodesy and Geodynamics*, 2007. 27(5): p. 44-48.
- [56] Mi Renhuan, Zhong Min, Yan Haoming, Peng Peng, et al., On ocean heat content changes by using satellite altimetry data. *Journal of Geodesy and Geodynamics*, 2009. 29(5): p. 58-61.
- [57] Jin Taoyong, Li Jiancheng, Wang Zhengtao, and jiang Weiping, Global ocean mass variation in recent four years and its spatial and temporal characteristics. *Chinese Journal of Geophysics*, 2010. 53(1): p. 49-56.
- [58] Feng Wei, Zhong Min, Jiang Min, and Xu Houze, Inferring ocean heat content variations from satellite altimetry and model data. *Chinese Journal of Geophysics*, 2010. 53(7): p. 1562-1570.
- [59] Wang Hubiao, Wang Yong, and Lu Yang, High Precision Vertical Deflection over China Marginal Sea and Global Sea Derived from Multi-satellite Altimeter. *Geomatics and Information Science of Wuhan University*, 2007. 32(9): p. 770-773.

- [60] Huang Motao, Wang Rui, Zhai Guojun, and Ouyang Yongzhong, Integrated data processing for multi-satellite missions and recovery of marine gravity field. *Geomatics and Information Science of Wuhan University*, 2007. 32(11): p. 988-993.
- [61] Jin Taoyong, Li Jiancheng, Wang Zhengtao, Xing Lelin, et al., Cross-calibration and validation of Jason-1 and T/P altimetric data in their synchronous cycles. *Journal of Geodesy and Geodynamics*, 2007. 27(6): p. 72-76.
- [62] Jin Taoyong, Li Jiancheng, Xing Lelin, and Chu Yonghai, Research on datum unification of multi-satellite altimetric data. *Journal of Geodesy and Geodynamics*, 2008. 28(3): p. 92-95.
- [63] Yang Yuande, E Dongchen, Hwang Cheinway, and Wang Haihong, Chinese Coastal Gravity Anomalies from Waveform Retracked Geosat/GM Altimetry. *Geomatics and Information Science of Wuhan University*, 2008. 33(12): p. 1288-1291.
- [64] Deng Kailiang, Bao Jingyang, Zhang Chuanyin, Liu Yanchun, et al., Determination of vertical deflection over China Sea by combination of multi-satellite altimeter data. *Hydrographic Surveying and Charting*, 2008b. 28(3): p. 15-17.
- [65] Deng Kailiang, Bao Jingyang, Liu Yanchun, Zhang Chuanyin, et al., Determination of gravity anomalies over China sea by combination of multi-satellite altimeter data. *Science of Surveying and Mapping*, 2009a. 34(1): p. 78-80.
- [66] Wang Hubiao, Wang Yong, Lu Yang, and Zhou Xuhua, Gravity Anomalies with Resolution of 1.5'×1.5' Over China Sea and Its Vicinity Derived from Multi-Satellite Altimeter. *Geomatics and Information Science of Wuhan University*, 2008. 33(12): p. 1292-1295.
- [67] Wang Hubiao, Wang Yong, Lu Yang, and Bao Lifeng, Determination of gravity gradients in the Western Pacific Ocean by combining multi-altimeter data. *Progress in Geophysics*, 2009. 3: p. 852-858.
- [68] Guo Jinyun, Gao Yonggang, Hwang Cheinwei, and Sun Jialong, A multi-subwaveform parametric retracker of the radar satellite altimetric waveform and recovery of gravity anomalies over coastal oceans. *Science in China(Series D:Earth Sciences)*, 2009(09).
- [69] Zhang Zizhan, Lu Yang, and Xsu Houze, Detecting surface geostrophic currents using wavelet filter from satellite geodesy. *Science in China(Series D:Earth Sciences)*, 2007a. 37(06): p. 753-760.
- [70] Zhang Zizhan, Lu Yang, Hsu Houze, and Chen Hongxia, The Antarctic circumpolar current derived from the satellite gravity geoid and altimetry data. *Chinese Journal of Polar Research*, 2008. 20(1): p. 14-22.
- [71] Zhou Xuhua, Wang Hubiao, and Zhan Jingang, Study on upper layer geostrophic circulation on China marginal sea by use of data of satellite gravity and satellite altimetry. *Journal of Geodesy and Geodynamics*, 2008. 28(4): p. 83-88.
- [72] Deng Kailiang, Bao Jingyang, Zhang Chuanyin, Liu Yanchun, et al., The determination of quasi-stationary Sea Surface Topography over China Sea by using multi-altimeter data. *Acta Geodaetica et Cartographica Sinica*, 2009b. 38(2): p. 114-119.
- [73] Xu Jun, Bao Jingyang, Liu Yanchun, and Tang Yan, A Regional Tide Model Around China Developed by POM and Blending Assimilation Method. *Hydrographic Surveying and Charting*, 2008. 28(6): p. 15-17.
- [74] Chu Yonghai, Li Jiancheng, Zhao Xiangfang, Ma Jing, et al., On ice sheet heigh changes over antarctic from altimetry data. *Journal of Geodesy and Geodynamics*, 2008. 28(2): p.

- 67-70.
- [75] Yang Yuande, E Dongchen, and Chao Dingbo, Antarctic ice mass loss from gravity satellite. *Chinese Journal of Polar Research*, 2009a. 21(2): p. 109-115.
- [76] Li Jiancheng, Chu Yonghai, Jiang Weiping, and Xu Xinyu, Monitoring level fluctuation of Lakes in Yangtze River Basin by altimetry. *Geomatics and Information Science of Wuhan University*, 2007. 32(2): p. 144-147.
- [77] Jiang Weiping, Chu Yonghai, Li Jiancheng, and Yao Yongshun, Water level variation of Qinghai Lake from altimetric data. *Geomatics and Information Science of Wuhan University*, 2008. 1: p. 64-67.
- [78] Gao Yonggang, Guo Jinyun, and Yue Jianping, Lake level variations measurement with satellite altimetry. *Science of Surveying and Mapping*, 2008. 33(6): p. 73-75.
- [79] Li Dawei, Li Jiancheng, Feng Hai, and Jiang Tao, research on inversion of seafloor topography of China Sea and its adjacent areas from satellite altimetric data. *Journal of Geodesy and Geodynamics*, 2009. 29(4): p. 70-73.
- [80] Wu Yunsun, Chao Dingbo, Li Jiancheng, and Wang Zhengtao, Recovery of Ocean Depth Model of South China Sea from Altimetric Gravity Gradient Anomalies. *Geomatics and Information Science of Wuhan University*, 2009(12).
- [81] Liu Chuanyong, Bao Jingyang, Huang Motao, Ouyang Yongzhong, et al., The application of posteriori compensation theory of error in altimeter data set from Geosat/GM crossover adjustment. *Hydrographic Surveying and Charting*, 2008. 28(1): p. 5-8.
- [82] Guo Jinyun, Gao Yonggang, Chang Xiaotao, and Hwang Cheinway, Optimal threshold algorithm of EnviSat waveform retracking over coastal sea. *Chinese Journal of Geophysics*, 2010. 53(4): p. 807-814.
- [83] Zhu Guangbin, Li Jiancheng, Wen Hanjiang, and Wang Jianqiang, Study on variations of global continental water storage with GRACE gravity field models. *Journal of Geodesy and Geodynamics*, 2008. 28(5): p. 39-44.
- [84] Zhou Jiangcun, Sun Heping, and Xu Jiangqiao, Validating global hydrological models by ground and space gravimetry. *Chinese Science Bulletin*, 2009. 54(9): p. 1282-1289.
- [85] Yang Yuande, E Dongchen, Chao Dingbo, and Wang Haihong, Seasonal and inter-annual change in land water storage from GRACE. *Chinese Journal of Geophysics*, 2009b. 52(12): p. 2987-2992.
- [86] Xing Lelin, Li Hui, Liu Dongzhi, and Zhou Xin, Monthly water distribution in China and its adjacent area from time-variable gravity field of GRACE. *Journal of Geodesy and Geodynamics*, 2007. 27(4): p. 35-37.
- [87] Wang HanSheng, Wang ZhiYong, Yuan XuDong, Patrick Wu, et al., Water storage changes in Three Gorges water systems area inferred from GRACE time-variable gravity data. *Chinese Journal of Geophysics*, 2007. 50(3): p. 730-736.
- [88] Zou Zhengbo, Xing Lelin, Li Hui, Kang Kaixuan, et al., Research on GRACE satellite gravity changes in Chinese mainland and its vicinity. *Journal of Geodesy and Geodynamics*, 2008. 28(1): p. 23-27.
- [89] Zhai Ning, Wang Zemin, Wu Yue, and Ye Congyun, Recovery of Yangtze River Basin Water Storage Variations by GRACE Observations. *Geomatics and Information Science of Wuhan University*, 2009. 34(4): p. 436-439.
- [90] Zhong Min, Duan Jianbin, and Hsu Houze, Trend of China land water storage redistribution

- at medi- and large-spatial scales in recent five years by satellite gravity observations. Chinese Science Bulletin, 2009. 54(9): p. 1290-1294.
- [91] Zhang ZiZhan, Lu Yang, and Xu HouZe, Maximum entropy spectral analysis and wavelet coherence analysis of the dynamic ellipticity of the earth from GRACE and SLR measurements. Chinese Journal of Geophysics, 2007b. 50(5): p. 1383-1389.
- [92] Chen Wei, Shen Wenbin, Li Jin, and Han Jiancheng, Variations of LOD inferred from temporal GRACE gravity data. Journal of Geodesy and Geodynamics, 2009. 29(6): p. 119-124.
- [93] Duan Hurong, Zhang Yongzhi, Liu feng, and Kang Ronghua, Study of the gravity variance in Chinese Mainland before and after Wenchuan Earthquake with GRACE gravity models. Journal of Seismological Research, 2009. 32(3): p. 295-298.
- [94] Xing Lelin, Li Jiancheng, Li Hui, and Sun Wenke, Detection of Co-seismic and Post-seismic Deformation Caused by the Sumatra-Andaman Earthquake Using GRACE. Geomatics and Information Science of Wuhan University, 2009. 34(9): p. 1080-1084.
- [95] Zou Zhengbo, Luo Zhicai, Li Hui, Shen Chongyang, et al., Detection of gravity change before and after strong Earthquake by GRACE. Journal of Geodesy and Geodynamics, 2010. 30(2): p. 6-9.
- [96] Liao Haihua, Zhong Min, and Zhou Xuhua, Climate-driven annual vertical deformation of the solid Earth calculated from GRACE. Chinese Journal of Geophysics, 2010. 53(5): p. 1091-1098.
- [97] Wang WuXing, Shi YaoLin, Gu GuoHua, Zhang Jing, et al., Gravity changes associated with the Ms8.0 Wenchuan earthquake detected by GRACE. Chinese Journal of Geophysics, 2010. 53(8): p. 1767-1777.
- [98] Zhu Yiqing, Liang Weifeng, Li Hui, and Sun Heping, On Gravity Field Variations and Geodynamic Characteristics in Mainland of China. Geomatics and Information Science of Wuhan University, 2007. 32(3): p. 246-250.
- [99] Li Yuefeng and Ding Xingbin, Progress in studying plumb line variations. Chinese Journal of Geophysics, 2008. 23(6): p. 1736-1745.
- [100] Li Hui, Shen Chongyang, Sun Shaoan, Wang Xiaoquan, et al., Dynamic gravity change in recent years in china continent. Journal of Geodesy and Geodynamics, 2009. 29(3): p. 1-10.
- [101] Li Shanshan, Wu Xiaoping, Zhang Chuanding, Sun fenghua, et al., Calculation and analysis of the new statistical character parameters of gravity field in China. Chinese Journal of Geophysics, 2010. 53(5): p. 1099-1108.
- [102] Wu Xing, Li Ming, and Li Shanshan, Construction of Multi-Source Gravity Field Information System. Journal of Zhengzhou Institute of Surveying and Mapping, 2007. 24(6): p. 391-394.
- [103] Zhang Hao, Li Shanshan, Chang Liling, Li Ming, et al., The Design and Realization of Land Gravity Precision Technology Software. Journal of Institute of Surveying and Mapping, 2006. 23(6): p. 422-424.
- [104] Dai Quanfa, Hsu Houze, Xu Daxin, and Wang Yong, Simulation of gravity matching navigation system. Geomatics and Information Science of Wuhan University, 2008. 33(2): p. 203-207.
- [105] Jin Jihang and Bian Shaofeng, Analysis of inertial navigation system positioning error caused by gravity disturbance. Geomatics and Information Science of Wuhan University,

2010. 35(1): p. 30-32.
- [106] Shen WenBin, Liu Lin, and Ning JinSheng, The inner core's super rotation and its influences on the gravity field. *Chinese Journal of Geophysics*, 2007. 50(2): p. 430-436.
- [107] Wang Jiexian, Ji Shanbiao, Cao Yueling, and Yu Meiyi, Geoid Deformation and Elevation Affection Caused by Building Loading. *Geomatics and Information Science of Wuhan University*, 2008. 33(6): p. 616-618.

## Progress in Geoid Determination Research Areas in China

LI Jiancheng<sup>1,2</sup>, CHAO Dingbo<sup>1,2</sup>, SHEN Wenbin<sup>1,2</sup>, ZHANG Shoujian<sup>1,2</sup>,  
ZOU Xiancai<sup>1,2</sup>, JIANG Weiping<sup>1</sup> and YAO Yibin<sup>1,2</sup>

1 School of Geodesy and Geomatics, Wuhan University, Wuhan 430079, China

2 The Key Laboratory of Geospace Environment and Geodesy, Ministry of Education,

Wuhan University, Wuhan 430079, China

### I. Introduction

The quasi-geoid is used as the datum of normal height system in China. The accurate geodetic height can be obtained by GPS technology, combining with high-resolution and high-precision quasi-geoid model, as an integrated positioning technology, the normal height of ground points can be determined at corresponding accuracy. Then, it is realized that the three dimension GPS positioning in “Gravity Space”, which has been expected by geodesy and geomatics workers for a long time. So, the traditional leveling mode can be substituted by the integrated positioning technology, the difficulty and obstacle of the technology is to improve the resolution and accuracy of the geoid model to approach the accuracy of leveling before. The spectrum of geoid is dominant by long waves and the key issue is to improve the accuracy of long wavelength geoid to centimeter level or better. The regional geoid with corresponding accuracy can be recovered using terrestrial gravity data with sufficient density, high resolution DEM and a few GPS observations.

The above problem has been solved by the integrated gravity model that constructed with the new generation satellite gravity and terrestrial gravity data. Therefore, it is particularly active that the researches on determination of high-resolution and centimeter-level accuracy regional geoid model taking high degree and high precision gravity field model as reference, combining with terrestrial gravity observations, GPS leveling data and high-resolution DEM. China has made this effort for nearly 10 years, and continued to expand the research and engineering practice in this area in last 4 years. The main achievements include: improving the theory and method used to determine the regional geoid, making it practical and standardized gradually, extending to variety of engineering and construction services. Meanwhile, the new approach of determining global centimeter-level geoid was studied. All the researches have reflected China’s progress in this field.

### II. General progress

#### *1. The methods for regional geoid determination*

In order to determine the elevation using GPS combined with the geoid model instead of the conventional leveling technique, extensive studies on local and regional geoid refinement were conducted in China during the past 20 years, and high resolution, centimeter level geoid models

have been computed for many provinces and cities. Recently, some new developments have been made, including the study of cm level geoid model determination, refinement of the long-wavelength geoid using new satellite-only gravity field model, determination of medium and short wave length geoid using combined ultra-high resolution DTMs and terrestrial gravity data, refinement of the mathematic model of direct and indirect topographic effect, etc.. And also some progresses have been made in investigations of the fitting method to determine the gravimetric geoid and GPS-leveling geoid, the experiment of recovering geoid by airborne gravity, and the unification of local height datum. (Zhang Chuanyin, Chao Dingbo, et. al., 2006; Li Jiancheng, 2007; Sun Zhongmiao, Xia Zheren, et. al., 2007; Zhang Liming, Li Fei, et. al., 2007a; Zhang Liming, Li Fei, et. al., 2007b; Guo Chunxi, Ning Jinsheng, et. al., 2008; Zhao Jianhu, Wang Zhenxiang, et. al., 2008; Jin Shaohua, BaoJingyang, et. al., 2008; Liu Zuanwu, Tao Daxin, et. al., 2008; Chen Luying and Xu Houze, 2008; Qiu Bin, Zhu Jianjun, et. al., 2008; Zhang Liming, Li Fei, et. al., 2009; Song Lei, Fang Jian, et. al., 2009; Lin Miao, Zhu Jianjun, et. al., 2009; Tian Bin, Li Jin, et. al., 2009; Wang Jianqiang, Li Jiancheng, et. al., 2010; Wang Rui and Li Houpu, 2010). And the achievements include:

(1)For the first time, the digital gridding quasi geoid model of the Qomolangma area with a resolution of  $2.5' \times 2.5'$  and a precision  $\pm 9$  cm was determined, in which 2501 gravity points and 44 GPS leveling points, SRTM3, 1: 50000 DEM and GTOPO30 DTM in that area were used, and gravity model EGM96, WDM94, IGG05B, DQM2000D and CGM03C were selected as reference model. In this study, the  $2.5' \times 2.5'$  mean free air anomaly grids were interpolated from topographical isostatic gravity anomalies, based on the remove-compute-restore principle and Molodensky series expressions with consideration of the first two terms (zero-order and first-order terms); the  $2.5' \times 2.5'$  mean height anomaly grids were computed by Stokes formula from Faye anomalies, and the optimal selection of the integration radius and compensation depth of the Airy-Heiskanen topographical isostatic reduction model was investigated. The two-parameter second-order polynomial was used as a fitting function to fit the gravimetric quasi geoid and GPS-leveling geoid, thus, a  $2.5' \times 2.5'$  quasi geoid model in Qomolangma area in consistent with China height system was determined, and the conversion between the height anomaly and the geoid undulation was studied as well. Numerical results show that the quasi geoid is located at the position 1.22m higher than the geoid at the peak of Qomolangma.

(2)Local geoid refinement using high order and ultra-high degree geopotential model was studied, and there are several papers about the computation algorithms, the evaluation and selection of the geopotential model and some practical results. The Clenshaw summation which is used to speed up the computation of the geoid undulation from ultra-high gravity models was investigated. Clenshaw method is not used to compute the Legendre function individually, but used to compute the summation of series directly. By comparing with the standard forward column method and analyzing the stability of the two methods, a better algorithm using the semi-normalized associated Legendre function to improve the computation efficiency and stability was introduced. There are two papers on the problem of the optimal model selection. One paper compared the geoid error degree variance of EGM2008, EGM96 and GGM, and the accuracies of the three models were compared with each other with 56 GPS points in Mainland China as reference value. The conclusion is that the three gravity models are comparable with each other in precision at long wave length, and at short wave length, EGM2008 provides the most accurate results. In other paper, 33 GPS-leveling points were used to evaluate 7 gravity

models. Using EGM2008 gravity model and SRTM topography data, a  $15' \times 15'$  quasi geoid model in Xinjiang was computed by Molodensky method. It is noted that the geodetic heights of the grids were approximately computed from SRTM data, and the comparison results with height anomalies of 15 GPS-leveling points show that the model precision reached 0.2 m.

(3)The methods for processing the airborne gravimetry data are summarized. The effects of the downward continuation approaches and the filtering amount on the precise local air-borne geoid determination are discussed in details. The results show that the accuracy of an air-borne geoid with 3 cm can be obtained by all three downward continuation approaches, namely by the direct representation method, Tikhonov regularization, and point-mass model. However, the direct representation method may be optimal since it is not limited by the observed area and has little edge effect. It is also shown that the filtering amounts of 100-250 s can be suitable for airborne geoid determination, but a smaller amount e.g. 100 s will preferable due to less edge effects. The geoid determined from airborne gravity achieves the accuracy level of 3 cm compared to a  $5' \times 5'$ -grid reference geoid.

(4)The effects of the accuracy and resolution of the disturbance gravity data on the determination of the high-resolution local geoid through solution of the GPS / Gravity Boundary Value were studied. Firstly, using 1175 points of GPS/gravity data in the mountain area with altitude fluctuations of about 2km, resolution of about 3km, four random errors in the range of 0.1 ~ 2.0 mGal were imposed on the true gravity value. The results show that, when the precision value of the disturbance gravity is larger than 1 mGal, the impact on the height anomaly calculated by Hotine formula, will be more than 1 cm, and can only achieve centimeter level. 4823 GPS points and gravity data with resolution about 1 km ( $0.5' \times 0.5'$ ) in Shenzhen city with the topographic undulation less than 250m were used and the original data set were gridded into two data sets with lower resolution which are  $1' \times 1'$  and  $2' \times 2'$  respectively. Then the height anomalies of the different data sets were calculated using Hotine formula. The results indicate that the differences between the results with different resolution data have strong correlation with the topography undulation. In plains and hilly areas, the differences between the results computed from the data with resolution of  $0.5' \times 0.5'$  and  $1' \times 1'$  are less than 1 cm, and both of the accuracy can reach centimeter-level. In flat areas, a centimeter-level accuracy can also be obtained for the data with the resolution of 4km (corresponding to  $2' \times 2'$ ), but in the areas with large topography undulations the differences will be greater than 1cm and the extreme value will reach 14cm. The conclusion is that, in the areas with large topographic undulation, in order to achieve centimeter-level accuracy of the height anomalies, the resolution of the disturbance gravity data should be at least 2 km (corresponding to  $1' \times 1'$ ).

(5)Recently, the fitting method of the geoid determined by gravity data and the geoid determined by GPS leveling continues to attract the concern of researchers in China. Three related papers were published, in which new methods were proposed. ①Bayesian Regularized BP Neural network fitting was studied. Because of evident difference between the two different kinds of geoids and their different and complicate errors, there usually exist model errors when using polynomial surface fitting method. But, BP neural network method, which can be considered as a special kind of function approximator, can significantly reduce this kind of errors. The gravimetric quasi-geoid with a resolution of  $2.5' \times 2.5'$  was calculated based on Molodensky series expression at the test area ( $115^\circ\text{E} \sim 120^\circ\text{E}$ ,  $35^\circ\text{N} \sim 38^\circ\text{N}$ ), and 63 GPS Leveling points were

used to fit the gravity quasi-geoid, and the other 16 points are used to evaluate the precision. The gravity quasi-geoid was fitted using the third degree and fourth degree surface polynomial and 4 kinds of BP neural network fitting, and then all the four kinds of geoids were fitted using BP neural network fitting. The external precision and the internal accuracy of the fitting residuals were assessed. Both the internal and external accuracy of polynomial surface fitting are about 0.2m, while the new fitting method provides the corresponding accuracies of 0.1 m and 0.07m, respectively. The contour figure of the fitting residual of the latter is much closer to that of the raw data. ②A new fitting method considering the gravity information of stations is proposed. The characteristics of the geoid height variations are analyzed through the series expansion of the measured gravity values by Bruns formula. The analysis indicates that the vertical deflection is the linear correction about the inclination of the geoid to the normal level ellipsoid, and the gravity anomaly is the linear correction about the bending of the geoid to the normal level ellipsoid. The second order variation of the geoid is corresponding to the variation of the topography. Accordingly, a least square fitting method, which can be used to extrapolate the geoid on the grid using the observations on the GPS/Leveling points including the geoidal undulation and the gravity values, is put forward. It should be noted that this method is different from the fitting method in common sense, which avoids the gravimetric geoid computation. The confirmation of the reliability of this method is in further investigations. ③A fitting method to combine the two kinds of the above-mentioned geoids at land-sea interface area is discussed. The mean of the difference between the gravimetric geoid and the GPS/Leveling derived geoid for the land points, as well as the difference for the grid points on the sea are calculated, and the weight value is determined by the reciprocal of the distance between the GPS/Leveling points to the grid points. Taking EGM96, WDM94 and GFZ as reference model, a  $2' \times 2'$  gravity quasi-geoid was calculated using 1045 gravity points at the test area. The measured height anomaly of 43 GPS leveling points were taken into account. Through comparison and accuracy assessment, the accuracy of the determined geoid using this method, which is about 3 cm, is better than that determined by the linear regression interpolation method.

(6)The join of the mainland geoid and ocean geoid is investigated. The mainland geoid is derived mainly from land gravity data and GPS measurements, and the ocean geoid is derived mainly from the satellite altimeter data. The difference between the mainland geoid and ocean geoid along their merge boundary area is due to the sparse gravity data and the poor quality of the satellite altimeter data. Taking account of the physical characteristics of the geoid, and according to the physical geodesy equations of the geoid in a local area, we transform the mainland-ocean merge geoid problem into the Laplace boundary value problem. Then, the ideas of the mathematics joining the mainland geoid and the ocean geoid along their merge boundary area are discussed based on the finite element method, and a relevant mathematical model is given.

(7)Research of the innermost area effects in the altimetry gravity recovery is based on the inverse Stokes formula. In order to improve the precision of the altimetry gravity computed by the inverse Stokes formula, the geoidal height of the innermost area is expressed as double cubic polynomial, and a formula to calculate gravity anomaly of this area is derived after the non-singular transformation is introduced. The analysis based on the theoretical model of the geoidal height shows that the accuracy of this formula is quite high. A practical calculation is done based on the geoidal height data with a resolution of  $2' \times 2'$ , and the results indicate that the contribution of the innermost area to the gravity anomaly recovery should not be ignored. The

formula derived could provide theoretical basis for the gravity anomaly recovery with high precision.

(8)Regional height datum unification including the unification between geodetic height datum and normal height datum is investigated. Two papers discussed and solved the problem of the height datum unification through practical cases. The geodetic height datum is different from the independent GPS leveling networks established by different departments, for these independent networks commonly have different datums with different accuracies. The consistency of the geodetic height datum will also be affected if the observations are of different periods in the same GPS network. According to the invariance of difference of the height anomaly in an independent network and the parallelism of the geodetic datum surface and WGS84 ellipsoid, a two-step method used to unify the datum was proposed: Firstly, the constant deviations between two different networks were determined using their common points. Accordingly, all other independent networks' datums can be unified to a selected datum. Secondly, in the large area covered by independent networks, one GPS point was chosen as reference datum, and then the differences of the height anomaly between all other GPS points and reference datums was calculated. A model about the differences of the height anomaly was built using polynomial fitting in the large area. The least square method was used to calculate the fitting coefficients. The reference surface of the large area will be unified to the WGS84 ellipsoid represented by the reference GPS points using this two-step method. The unification of the GPS networks' datum in the north of Yangtze Delta is completed using the above method. Another example is the height datum unification of the Shenzhen and Hong Kong. The method is the solution of the GPS/gravity boundary problem and GPS/Leveling. The height anomalies corresponding to the global height datum and local height datum which is from the GPS/Leveling observables are computed for the height datum points at Shenzhen and Hong Kong, and then the differences between the two height datum are computed for the points at Shenzhen and Hong Kong, and finally, the differences between the local height datum between Shenzhen and Hong Kong can be determined. So, the Hong Kong height datum can be unified to the Mainland China height datum.

#### *2.A new method for global geoid determination with an accuracy of centimeter-level*

As the successful implementation of the gravity measurement task taken by low-orbit satellite during this century, a new series of satellite-only gravity model or combined gravity model are released, in which the precision of long-wave is largely improved. In particular, combining high-resolution ocean satellite altimetry and improved continental gravity data, ultra-high degree (2160 degree) global 5'×5' gravity model EGM2008 is produced, with an accuracy of full band geoid up to 0.2 m (in China). With the successful launch of GOCE, a precision of 1°×1° geoid model is expected to reach centimeter-level. Thus, using the new generation gravity model, it is possible to realize the global geoid with an accuracy of centimeter-level, but there are still theoretical and methodological difficulties which need to be investigated and solved. The global gravity field model is expressed by harmonic functions defined in the Earth's outer space. However, outside the continental geoid, about 30% global area has terrain mass, which is not in the definition space of the Earth gravity model. So, in theory, we cannot directly use the Bruns formula to determine the geoid by gravity model. At present, we generally adopt spherical approximation approach, ignoring the terrain effects, to calculate the disturbing potential in a

spherical area with the radius of the Earth's average radius, and the corresponding accuracy is limited to meter- or decimeter-level. Also, the methodology considering the topographical impacts to geoid needs to be investigated, which has been achieved new preliminary results in our country (Chao Dingbo, Shen Wenbin, et. al., 2007; Han Jiancheng and Shen Wenbin, 2007; Shen Wenbin and Chao Dingbo, 2008). The theory and method of this research can be summarized as follows. If given a high-degree (upper than 180 degree) global gravity model (for example, EGM2008) with the geoid accuracy of centimeter-level, a high-resolution high-precision global digital topographical model (for example, SRTM 3"×3"), and a global crustal density model (for example, CRUST2.0), then, the solid earth  $\Omega$  can be divided into two parts. The first part, containing geoid inside, is shallow mass layer  $\Omega_1$  of ground surface with thickness lower than 10km, and the other part is the Earth solid  $\Omega_0$  excluding  $\Omega_1$ . That is to say,  $\Omega = \Omega_0 + \Omega_1$ . The surface of  $\Omega_0$  is presented as  $\partial\Gamma$ , and its outside space is  $\bar{\Gamma}$ . The ground surface is  $\partial\Omega$ , its outside space is  $\bar{\Omega}$ . Firstly, using terrain model and crustal density model, the gravitational potential  $V_{\Omega_1}$  of the shallow mass layer  $\Omega_1$  in space  $\bar{\Gamma}$  can be calculated by numerical integration approach according to Newton's gravitational potential integration formula. Then, in space  $\bar{\Omega}$ , the gravitational potential is  $V_{\Omega_1}^e$ . The gravitational potential in space  $\bar{\Omega}$  and that of  $\Omega_0$ , denoted by  $V_{\Omega_0}^e$  and  $V_{\Omega}^e$  respectively, can be determined from a high-degree Earth gravity field, and thus one has  $V_{\Omega_0}^e = V_{\Omega}^e - V_{\Omega_1}^e$ . Our aim is to determine the inner gravitational potential  $V_{\Omega}^i(\Omega_1)$  of the whole Earth solid  $\Omega$  inside  $\Omega_1$ . Given that the inner gravitational potential of solid  $\Omega_0$  and mass layer in space  $\Omega_1$  are  $V_{\Omega_0}^i(\Omega_1)$  and  $V_{\Omega_1}^i(\Omega_1)$  respectively, then  $V_{\Omega}^i(\Omega_1) = V_{\Omega_0}^i(\Omega_1) + V_{\Omega_1}^i(\Omega_1)$ , where  $V_{\Omega_0}^i(\Omega_1)$  is determined by  $V_{\Omega_0}^e$ , and  $V_{\Omega_1}^i(\Omega_1)$  is unknown. The key problem is to determine  $V_{\Omega_1}^i(\Omega_1)$ . There are two methods. The first method is: make a minimal spherical area  $\partial K$  (for example Brillouin sphere) surrounding the Earth, calculate the grid values of  $V_{\Omega_0}^e$  in spherical area  $\partial K$ , and expand the corresponding  $V_{\Omega_0}^e$  to be spherical harmonic series using harmonic analysis method. It can be proved that the series can be analytically extended to space  $\Omega_1$  and is equal to  $V_{\Omega_0}^i(\Omega_1)$ . The second method is using the improved Bjerhammar downward extension method. Within space  $\Omega_0$ , make a Bjerhammar spherical area  $\partial K_0$  approximating to  $\partial\Gamma$ , its outside space is  $\bar{K}_0$ , and determine  $V_{\Omega_0}^e$  using grid values of spherical area  $\partial K$  by "fictitious compress recovery method" proposed by Shen Wenbin. Then, the geopotential in space  $\Omega_1$  can be determined from  $w_{\Omega_1} = V_{\Omega_1}^i(\Omega_1) + Q(\Omega_1)$ , where  $Q(\Omega_1)$  is particle's centrifugal potential in  $\Omega_1$ . Under the assumption that the potential constant  $w_0$  of geoid is given, based on the equation  $w_{\Omega_1}(\varphi, \lambda, h) = w_0$ , where  $(\varphi, \lambda, h)$  are geodetic

coordinates, one could determine  $h$  by numerical approximation approach, denoted by  $h_0$ , that is the geoid difference  $N = h_0(\varphi, \lambda)$ . The potential constant  $W_0$  can be chosen as the value released by IAG, or calculated using EGM2008 model and global satellite altimetry mean sea surface height model under the concept that geoid should closely approximate the mean sea surface.

Preliminary results of determining a global  $1^\circ \times 1^\circ$  geoid by numerical simulative experiments suggest that the accuracy of above geoid determination approach can reach centimeter-level or even better.

### **III. The method for local geoid determination and project practice in China**

With continuous advances of the globalization process, the ancient discipline of surveying and mapping plays an irreplaceably important role as always in national economic constructions and social developments. With the developments of the space technology, computer technology, information technology and communication technology, there have been "3S" technologies as the representatives of the modern surveying and mapping technologies, so that there have fundamental changes in this ancient discipline from theory to method.

As a typical representative of the 3S technologies, GPS led the overall prosperity of the positioning with the space technology since the 20th century 70's. The comprehensive application of the GPS pushed forward the Geodesy from the independent branches to the integrated, from the static to the dynamic, from the surveying and mapping in a local reference coordinate system to the one in a unified earth-center global reference coordinate system. Because of its superior data collection capabilities and incomparable advantages, the space positioning technology, with the GPS as a typical one, developed rapidly and the scope and objects of its services also expanded continuously.

Satellite navigation and positioning is a "disruptive" technology in the positioning on a plane, while the leveling still adopts the method invented 150 years ago. The problem of the leveling is the final hurdle in the modernization of geodesy. The general directions to break through the difficulties are to construct a geoid model, converting the ellipsoidal height to the orthometric height. As a result, the satellite positioning technology can obtain not only the planar coordinates, but also the orthometric height. In this sense, satellite-positioning technology is a real 3D positioning technology.

The establishment of high-precision high-resolution geoid model is not only the key of the modernization of elevation measurement in the geodetic discipline, which can be integrated into the GPS technique, then to substitute the traditional leveling technique which is very costly and inefficient, but also is very important to several branches of the geoscience such as Oceanography, Hydrology, Tectonics, Geophysics, for example, the usage of the marine geoid and mean sea surface height model to study the changes of the distribution of global water reserves. At the end of last century, the IAG suggests that the determination of a global geoid with 1 cm level accuracy is the strategic objective of the geodetic development. And in the recent 10 years, the determination of the cm-level accuracy of the geoid is the most active research fields in physical geodesy.

#### *1. The development background of China's regional geoid determination*

Because of the important role of the geoid model, Chinese State Bureau of Surveying and

Mapping proposed the task of refining the geoid model first in the “Eighth Five-Year Science and Technology Plan”, and then, in the “Tenth Five-Year Plan of the National fundamental Surveying and Mapping”, it requires clearly that “Combing the gravimetric data, GPS/Leveling, Digital Terrain Model, satellite altimetry, airborne gravimetry and satellite gradiometry, improves the accuracy of the quasi-geoid model, ..... , replace the laborious leveling in the height control by GPS altimetry in the middle and small scale mapping”.

At the same time, land and sea height datum unification and the surveying and mapping of the island (reef) have been listed as the strategic focuses in the fundamental surveying and mapping in the national "Eleventh Five-Year" plan, of which the core technology is to establish a unified geoid model for the land and sea. To this end, the State Bureau of Surveying and Mapping organized some related units in "land and sea base unification and the production test on the surveying and mapping of the island (reefs)", which aims to unify the reference base of the surveying and mapping in the land and on the sea, the methods for the surveying and mapping of the island (reefs), completes the design of the general program and its demonstration, and provides technical supports for the production test.

On May 12, 2008, the WenChuan earthquake brought serious damages to the ground benchmarks for the surveying and mapping. So we recognized that the traditional mode, maintaining the base of the surveying and mapping by the stones on the ground, couldn't resist the disaster. Taking into account the fact that the changes of the regional quasi-geoid can be ignored, and the regional quasi-geoid model address the rapid determination of the heights in the post-disaster reconstruction, some experts and scholars proposed that according to the principle "unified planning, overall Layout", pre-build high precision digital quasi-geoid model covering the scope of the seismic areas are important items in the construction of the service platform in the integrated disaster reduction and relief GIS.

## *2.Theories and methods*

In this context, after the years' research on the theories and methods by the Chinese scholars, several difficult problems have been conquered and a series of key technologies on the refinement of the regional quasi-geoid have been proposed, developed and successfully used in China's cm level accuracy of geoid determination, including mainly:

(1)It is derived that the strict integration formula on the sphere in the ground gravity data reduction taking the earth curvature into account. This method can effectively improve the numeric accuracy in the computation of the terrain isostatic anomaly. It is proposed a strict algorithm on the unification of the land and sea, assuring the consistency of the accuracy of the grid gravity anomalies in these areas.

(2)It is proposed the curvature continuous tensor spline algorithm for the interpolation and prediction of the grid gravity anomalies. By introducing the tension parameter in the elastic plate bending equation, the points with deformation in the fitting of the surface can be eliminated. At the same time, the minimum curvature gridding algorithm can be promoted to a more general one by introducing a tension parameter, which is very suitable for the areas with sparse, very unevenly distributed gravimetric measurements and difficult terrain. Practice shows that the gridding of the potential field and the terrain with this method can maintain more high frequency information in data meanwhile avoid over-smoothing, and can better reflect the Spatial

autocorrelation of the data than the minimum curvature method.

(3) It is adopted the Helmert's second condensation method to determine the geoid in China for the first time, and computed the direct and indirect effects on the potential and gravity of the various kinds of topography by the derived strict integration formula on the sphere taking into account the curvature of the earth. The Helmert's second condensation method can effectively estimate the mass above the co-geoid and its effects on the external potential and gravity of the condensed topography.

(4) It is investigated the unification of the gravimetric geoid model and the discrete GPS/leveling, and proposed and applied a new analysis method using the spherical cap harmonic functions as the fitting base and satisfying the potential theory strictly. This method can overcome the limitations of the geometric surface fitting or polynomial fitting, and is not only strict in theory but also can greatly improve the computation efficiency.

Based on the achievement, in the recent 10 years, the geoid refinement of more than 40 different provinces or cities has been conducted. Before the year 2007, the method to build the quasi-geoid is to use the first order solution of the Molodensky's series expression with a resolution of  $2.5' \times 2.5'$ . Among the urban quasi-geoid models, the accuracy of those built during 2003-2005 in the Wuxi, Qingdao, Changzhou, Datong, Jinzhong, Changzhi, Suozhou and the northern district of Harbin are about 2cm. In 2006, the first urban quasi-geoid model with 1cm accuracy was built in Dongguan, followed by the next one in Guangzhou, which symbolized that the technology on the building of the urban quasi-geoid model with 1cm accuracy is mature. After the year 2007, the method to build the quasi-geoid model is mainly the Helmert's second condensation method, and the resolution is  $2.0' \times 2.0'$ . Tens of urban quasi-geoid models in Wuhan, Nanjing, Shenyang, Suzhou, Ningbo, Fuzhou, Baotou, Huhehaote, Shaoxing, Zengcheng, Foshan, Zhuhai, Xian are all with the accuracy better 1cm, realizing the cross-age development in the accuracy of the urban quasi-geoid models in China.

Meanwhile, with improvement of the accuracy of the quasi-geoid, their applications have also been greatly expanded. In addition to the establishment provinces or cities quasi-geoid on the needs of the basic surveying and mapping, the regional quasi-geoid meeting the needs of individual engineering construction also appeared.

### *3. The project practice of establishment of local quasi-geoids*

#### *3.1 Quasi-geoid models for provincial regions*

The second Helmert agglutination was used to compute the Chifeng quasi-geoid based on 9856 gravity data points and 72 GPS leveling results. In another place, the point numbers is 1069 and 32 in Xing'an'meng quasi-geoid. The computation of quasi-geoid also needs the SRTM  $3'' \times 3''$  digital terrain model for gravity calculation, and the earth EIG01C gravity field model as the reference gravity field. The Airy-Haiskanen terrain isostatic correction is used in the interpolation or estimate of the grid gravity anomalies, where the terrain correction (i.e.: Helmert aggregation layer produced by gravitational effects) and the isostatic correction are applied to the close spherical integral formula taking into account the curvature of the Earth, with a radius of 300 km. Chifeng, Xing'an'meng gravity geoids are compared independently with 72 and 32 GPS leveling data, respectively, the accuracies are about  $\pm 0.044\text{m}$  and  $\pm 0.046\text{m}$ , respectively.

Combing the gravity geoid with the GPS leveling, the derived 2'30"×2'30"-grid geoid with accuracies of  $\pm 0.030\text{m}$  and  $\pm 0.022\text{m}$  are obtained using harmonic analysis of the spherical cap method (Li Jiancheng, 2007).

Using the same or similar method, technology of the quasi-geoid determination and the same numerical terrain model, the quasi-geoid of the Gansu, Jiangxi and Fujian provinces are determined one after another. And in Gansu quasi-geoid determination, 355467 gravity data, 135 high-precision GPS/Leveling data and 95 state grade B GPS/Leveling data are used, and the reference gravity field model is GGM02C, the accuracy of the gravimetric quasi-geoid is  $\pm 0.13\text{m}$ , the accuracy of the 2'×2' grid quasi-geoid, obtained after the integration of the GPS/Leveling data and the gravimetric quasi-geoid, is  $\pm 0.08\text{m}$ ; In Jiangxi province, 82904 gravity data are used, and the accuracies of the gravimetric quasi-geoid and quasi-geoid are  $\pm 0.07\text{m}$  and  $\pm 0.03\text{m}$  respectively; In Fujian province, 70734 gravity data and 192 GPS/Leveling data are used, and the accuracies of the gravimetric quasi-geoid and quasi-geoid with a resolution of 2'×2' are  $\pm 0.09\text{m}$  and  $\pm 0.07\text{m}$  respectively.

### 3.2 Quasi-geoid models for cities

Using the same or similar method, technology of the quasi-geoid determination and the same numerical terrain model, the quasi-geoid model with precision of 1 cm level for 13 cities are determined, and the Suzhou quasi-geoid model have been determined twice. The used data, reference model and the corresponding resolution and accuracy values are listed in Table 1.

Table 1 The relative indexes of quasi-geoids determined in several cities

City	Number of the gravity anomaly points	Number of the GPS/Leveling points	reference gravity field model	Resolution (arcminute)	accuracy (m)	
					Gravimetric geoid	Integrated geoid
Zhenjiang	965	32	EIGEN03C	2.5'	$\pm 0.015$	$\pm 0.008$
Suzhou	1048	60	EIGEN03C	2.5'	$\pm 0.015$	$\pm 0.006$
Wuhan	2939	164	GGM02C	2.5'	$\pm 0.012$	$\pm 0.007$
Nanjing	1309	143	GGM02C	2.0'	$\pm 0.014$	$\pm 0.008$
Ningbo	1543	53	GGM02C WDM94	2.0'	$\pm 0.014$	$\pm 0.006$
Guangzhou	5472	116	EGM08	2.0'	$\pm 0.015$	$\pm 0.009$
huhhot	100	100	GGM02C WDM94	2.0'	$\pm 0.019$	$\pm 0.007$
Baotou	192	51	EIGEN04C	2.0'	$\pm 0.014$	$\pm 0.007$
Fuzhou	1526	72	EIGEN03C	2.0'	$\pm 0.014$	$\pm 0.008$
Suzhou (whole city)	4156	102	EGM08	2.0'	$\pm 0.014$	$\pm 0.009$

Zengceng	1261	43	EIGEN04C	2.0'	±0.009	±0.005
Zhuhai	728	42	EIGEN04	2.0'	±0.012	±0.005
Foshan	3329	70		2.0'	±0.013	±0.008
Shaoxing	1644	75	EIGEN03C	2.0'	±0.012	±0.009

In the sequel it will be introduced the determined local quasi-geoid that serves the bridge, highway construction and the disaster area reconstruction, and the approach and numerical terrain model used are as same as the above mentioned.

#### IV. Local quasi-geoids for serving engineering projects

##### 1. Bridge engineering

In 2008, the Qingdao Gulf Bridge quasi-geoid are determined by the second method of Helmert condensation, using 1364 gravity points data, 4 periodic observations of 15 high precision GPS/Leveling data, and the EIG04C gravity field model which is used as the reference gravity field model. Compared with the independent 4 periodic observations of 15 high precision GPS/Leveling data, the accuracy of the grid gravimetric quasi-geoid is  $\pm 0.004\text{m}$ .

In the determination of the HongKong-Zhuhai-Macao quasi-geoid, 106 gravity data and the SRTM 3"×3" numerical terrain model are used, and the terrain isostatic correction is computed with Airy-Haiskanen model, and the 2'×2' grid gravity anomaly data are interpolated and estimated with the curvature continuous tensor method. The GGM02C and WDM94 combined the Earth gravity field model are chosen as the reference gravity field model, and the local quasi-geoid is computed with the second method of Helmert condensation. Compared with 16 high precision GPS/Leveling points, the accuracy of the grid gravimetric quasi-geoid is  $\pm 0.016\text{m}$ , and the accuracy of the 2'×2' grid quasi-geoid, which is the integration of the gravimetric quasi-geoid and GPS/Leveling data using the spherical cap harmonic analysis method, is  $\pm 0.006\text{m}$  (Li Jiancheng, Ning Jinsheng, et. al., 2009).

The combination of the high-precision local quasi-geoid model and the GPS technique has been a novel leveling technique in China's large-scale cross-sea bridge construction.

##### 2. Highway engineering

In the determination of the high-precision zonal quasi-geoid of Yiwu-Mingshui-Luotuojuanzi road which is located in Xinjiang, 3360 gravity data and 7 high-precision GPS/Leveling data are used, and the reference gravity field model is EGM08. Compared with 7 high precision GPS/Leveling points, the accuracy of the grid gravimetric quasi-geoid is  $\pm 0.040\text{m}$  (Li Jiancheng, Ning Jinsheng, et. al., 2009).

In the determination of the Mianzhu-Maoxian local quasi geoid, 576 gravity data and 20 high precision GPS/Leveling points are used, and the reference gravity field model is EIGEN04C. Compared with 20 high precision GPS/Leveling points, the accuracies of the grid gravimetric quasi-geoid and the quasi-geoid are  $\pm 0.045\text{m}$  and  $\pm 0.015\text{m}$  respectively (Li Jiancheng, Ning Jinsheng, et. al., 2009).

### *3. Disaster area reconstruction*

In the determination of the quasi-geoid of the 2008 Wenchuan seismic area, the EIGEN04C is selected as reference gravity field model, and 2997 gravity data and 122 high precision GPS/Leveling points are used. Compared with independent 122 high precision GPS/Leveling points, the accuracies of the grid gravimetric quasi-geoid and the quasi-geoid are  $\pm 0.051\text{m}$  and  $\pm 0.020\text{m}$  respectively.

In 2010, in the determination of the quasi-geoid of the Yushu seismic area, 729 gravity data and 7 high-precision GPS/Leveling points are used, and the EIGEN03C gravity field model are chosen as reference gravity field model. Compared with 7 high precision GPS/Leveling points, the accuracy of the grid gravimetric quasi-geoid is  $\pm 0.046\text{m}$  (Li Jiancheng, Ning Jinsheng, et. al., 2009).

The National State Bureau of Surveying and Mapping (SBSM) recognizes that the determination of the quasi-geoids of the Wenchuan seismic area the Yushu seismic area may guarantee the basic surveying and mapping for the fast reconstruction of the seismic areas. And the quasi-geoid of the Wenchuan seismic area provides an accurate height datum for the emergence in surveying and mapping, and then the traditional leveling, which is costly and inefficient, is to be substituted by the GPS integrated with precise quasi-geoid model, which is economical and efficient. After a precise quasi-geoid model is determined, the altitude can be determined easily using GPS technique, and the combination of the geoid model and GPS is a great technological advances in determining the elevation for the areas with complex terrain.

## **V. The evaluation and test of EGM2008 over China Mainland**

With its ultra-high resolution ( $5' \times 5'$ ), EGM2008 has attracted the worldwide geodetic researcher's attention to carry out extensive testing and evaluation about its accuracy and applicability. In 2008, invited by the IAG/IGFS Joint Working group, Wuhan University of China participated in the testing and evaluation of EGM2008, meanwhile the National SBSM and Xi'an Research Institute of Surveying and Mapping also did the similar work (Li Jiancheng, Ning Jinsheng, et. al., 2009; Zhang Chuanyin, Guo Chunxi, et. al., 2009; Rong Min, Zhou Wei, et. al., 2009). The main results are stated as follows:

### *1. The results from National State Bureau of Surveying and Mapping*

The observed data applied to evaluation include 4 sets of GPS/leveling data: national 858 GPS A/B grade GPS-leveling data; 1305 GPS/leveling data in north China; 918 GPS/Leveling data in south China and 4707 GPS/leveling data in east and central China, and 583932 ( $2.5' \times 2.5'$ ) mean free-air anomaly grid data.

The results indicate: (1)The accuracy of the EGM 2008 height anomalies achieves 20 cm in Mainland China, 12 cm in Central East China, and even 9 cm in North China; (2)The general accuracy of the EGM 2008 free-air gravity anomalies is  $10.5 \times 10^{-5} \text{ m/s}^2$  in China; (3)The EGM 2008 accuracy is very high and its global precision is similar to that of Mainland China; (4)Compared with China's WDM 94, QDM model series and EGM 96, the accuracy of the EGM 2008 height anomalies is increased by 3~5 times, also by above 2 times compared with IGG05b and EIGEN-5c, especially in gravity anomalies. Based on the research of EGM 2008, it has been significantly improved to better understand the gravity field structure in China, especially in west

China.

## *2.The results from Wuhan University*

The evaluation of both PGM07A and EGM08 has been carried out in China using the observed data sets and high-resolution regional geoid models including the observations of 652 GPS/Leveling points within Chinese National A/B-order GPS Networks and 1160 GPS/Leveling points distributed over seven provincial regions, as well as the data sets of 183201 2'×2'-gridded mean gravity anomalies collected from five provincial regions. In the evaluation of PGM07A and EGM08, the other recent released Earth Geopotential Models (EGMs) including EIG01C, EIG03C, EIG04C, GGM01C, GGM02C, GGM01C\* and GGM02C\* are also used for comparisons.

The statistic results of the comparisons show that the RMS and Std.D of the differences between the quasi-geoid heights derived from PGM07A/EGM08 and their corresponding ones determined from the GPS/Leveling data of 652 A/B-order testing points are  $\pm 0.358\text{m}$ ,  $\pm 0.338\text{m}$  for PGM07A, and  $\pm 0.284\text{m}$ ,  $\pm 0.257\text{m}$  for EGM08 respectively, which are remarkably less than the indices of RMS and Std.D corresponding to the other EGMs used in the comparisons. The RMS and Std.D of the differences between the quasi-geoid heights derived from PGM07A/EGM08 and their corresponding ones determined from the GPS/Leveling data of total 1160 points in seven provinces-wide networks are in the range of  $\pm 0.09\text{m} \sim \pm 0.31\text{m}$  with a mean of  $\pm 0.19\text{m}$  for PGM07A, and  $\pm 0.07\text{m} \sim \pm 0.24\text{m}$  with a mean of  $\pm 0.16\text{m}$  for EGM08. For the other seven EGMs, however, the corresponding range of the statistics is  $\pm 0.26\text{m} \sim \pm 0.80\text{m}$  with a mean of  $\pm 0.44\text{m}$ . The synthetic comparisons of the quasi-geoid derived from PGM07A and EGM08 as well as the other EGMs with those determined from the GPS/Leveling data of all 1812 points within both A/B-order GPS/Leveling networks and seven provinces-wide ones are also made. The RMS and Std.D of the differences obtained from the comparisons are  $\pm 0.269\text{m}$ ,  $\pm 0.243\text{m}$  for PGM07A, and  $\pm 0.222\text{m}$ ,  $\pm 0.186\text{m}$  for EGM08 respectively, and for the other seven EGMs, the corresponding statistics is in the range of  $\pm 0.375\text{m} \sim \pm 0.680\text{m}$ . According to the above results of the comparisons, it shows that the quasi-geoid derived from PGM07A and EGM08 can provide a better approximation to the quasi-geoids determined from Chinese GPS/Leveling data including both the data of the national A/B-order networks and the data of the province-wide GPS/leveling networks than an approximation to the same quasi-geoids provided by the quasi-geoids derived from other seven EGMs. According to all statistical indices of the comparisons between the EGMs-derived quasi-geoids and GPS/Leveling-derived ones, however, it indicates that EGM08 is better than PGM07A as applied in Mainland Chinese. The quasi-geoid heights derived from EGM08 are more accurate than those derived from PGM07A by a range of  $\pm 0.01\text{m} \sim \pm 0.07\text{m}$  with an average of  $\pm 0.03\text{m}$  in the sense of the RMS or Std.D of the differences by comparisons.

In addition, the comparisons of the gravity anomalies derived from PGM07A and EGM08 with those measured in five provincial regions are made, and the statistic results of the comparisons show that the RMS and Std.D of the differences between PGM07A/EGM08-derived gravity anomalies and those measured in the regions are within the range of  $\pm 13 \sim 29 \text{ mGal}$ , with a mean of  $\pm 18 \text{ mGal}$ . It also indicates that the gridded mean anomalies derived from EGM08 are more accurate than those derived from PGM07A by a range of  $\pm 1 \sim 4 \text{ mGal}$  with a mean of  $\pm 2.7 \text{ mGal}$  in the sense of the RMS or Std.D of the differences by comparison.

In general, the quasi-geoid and gravity anomalies computed from PGM07A and EGM08 have significantly improved the representation of the Chinese local gravity field as compared with other seven models used in the evaluation. However, our testing results show that for both EGM08 and PGM07, there are some large (or small) biases in the determined quasi-geoids, which deviate from the general bias level in some regions.

In 2009, the application results for the above areas (e.g. Jiangxi, Fujian, Guangzhou and Suzhou, etc) indicate that the precision of the geoid have been improved.

### *3.The results from Xi'an Research Institute of Surveying and Mapping*

The accuracies of the EGM2008 and EGM96 are compared with 854 GPS/Leveling observations in China area. The results show that the evident systematic errors between the geoid heights derived from EGM2008 and EGM96 are significantly improved. The 289 GPS/Leveling observations in the western China are calculated, and it is demonstrated that EGM2008 is better than EGM96 in the western China.

## **VI. Conclusions**

After more than 10 years' research and practice, Chinese geodesists have conquered a series of relative problems in regional geoid determination systematically, put forward effective ways to determine the regional geoid, and established many regional geoids of provinces with several centimeters-level accuracy, dozens of urban geoids with the accuracy better than 1 cm, and several regional geoids for bridge and highway engineering, including especially the high-precision local geoids of the Wenchuan and Yushu seismic areas. These regional geoids have provided important support for the basic surveying and mapping tasks, the bridge and highway project construction and the fast reconstruction of the seismic areas.

In the near future, with continuous improvement of the theories and methods and the enrichment of the data, and combined with the new cm-level satellite gravity field model, it is possible to determine the new generation national geoid model with high accuracy. And it is expected that the absolute accuracy of the elevation determination will reach 5 cm in the east, and 30 cm level in the west; and the accuracy of the geoid for provinces will obtain 3~5 cm in the east and 10~20 cm in the west; the accuracy of the geoid for cities will be better than 1 cm. Integrated with the new geoid model, the GPS can substitute the second-order leveling overall, and realize the revolutionary changes of the elevation determination in China.

## **References**

- [1] Zhang Chuanyin, Chao Dingbo, Ding Jian, Wen Hanjiang, et al., Arithmetic and Characters Analysis of Terrain Effects for CM-order Precision Height Anomaly. *Acta Geodaetica et Cartographica Sinica*, 2006. 35(4): p. 308-314.
- [2] Li Jiancheng, Study and progress in theories and crucial techniques of modern height measurement in China. *Geomatics and Information Science of Wuhan University*, 2007. 32(11): p. 980-987.

- [3] Sun Zhongmiao, Xia Zheren, and Wang Xingtao, Determining Accuracy of Local Geoid Determined from Airborne Gravity Data. *Geomatics and Information Science of Wuhan University*, 2007. 32(8): p. 692-695.
- [4] Zhang Liming, Li Fei, and Chen Wu, Influence of Gravity Disturbance Resolution on GPS/Gravity Boundary Value Problem. *Geomatics and Information Science of Wuhan University*, 2007a. 32(6): p. 523-526.
- [5] Zhang Liming, Li Fei, and Yue Jianli, Effect of Gravity Disturbance Precision on GPS/Gravity Boundary Value Problem. *Geomatics and Information Science of Wuhan University*, 2007b. 32(1): p. 15-18.
- [6] Guo Chunxi, Ning Jinsheng, Chen Junyong, Wang Bin, et al., Improvement of regional quasi-geoid in Qomolangma [MT.Everest] and determination of orthometric elevation. *Chinese Journal of Geophysics*, 2008. 51(1): p. 101-107.
- [7] Zhao Jianhu, Wang Zhenxiang, Wang Shengping, and Dong Jiang, Determination of a Quasi-geoid in Large Region with Datum of Continuous GPS Networks. *Geomatics and Information Science of Wuhan University*, 2008. 31(1): p. 68-71.
- [8] Jin Shaohua, BaoJingyang, Liu yanchun, You Baoping, et al., Determination of high precision quasi-geoid in boundary of land and sea. *Journal of Zhengzhou Institute of Surveying and Mapping*, 2008. 25(2): p. 101-103.
- [9] Liu Zuanwu, Tao Daxin, Yao Hong, Yu Jinhai, et al., Joining the mainland geoid and the ocean geoid by the finite element method. *Progress in Geophysics*, 2008. 23(4): p. 1138-1142.
- [10] Chen Luying and Xu Houze, Fitting geoidal height regarding for gravity field information on stations. *Geomatics and Information Science of Wuhan University*, 2008. 33(7): p. 701-705.
- [11] Qiu Bin, Zhu Jianjun, and Le Kejun, Evaluation and optimal selection of high-order earth's gravity field models. *Science of Surveying and Mapping*, 2008. 33(5): p. 25-27.
- [12] Zhang Liming, Li Fei, Chen Wu, and Zhang C, Height datum unification between Shenzhen and Hong Kong using the solution of the linearized fixed-gravimetric boundary value problem. *Journal of Geodesy*, 2009. 83(5): p. 411-417.
- [13] Song Lei, Fang Jian, Zhou Xuhua, and Huang Teng, Application of Bayesian Regulation BP Neural Network to Fit Two-Kind Quasi-geoid. *Geomatics and Information Science of Wuhan University*, 2009. 34(5): p. 552-555.
- [14] Lin Miao, Zhu Jianjun, Yang Jinhao, and Qiu Bin, Comparison of the regional geoid undulations determined by geopotential models. *Geomatics and Information Science of Wuhan University*, 2009. 34(10): p. 1194-1198.
- [15] Tian Bin, Li Jin, and Shen Wenbin, The quasi-geoid of Xinjiang area determined based on the EGM2008 and SRTM model and its accuracy evaluation. *Science of Surveying and Mapping*, 2009. 34(supplement): p. 5-6,20.
- [16] Wang Jianqiang, Li Jiancheng, Zhao Guoqiang, and Zhu Guangbin, Geoid Undulation Computed Based on Clenshaw Summation. *Geomatics and Information Science of Wuhan University*, 2010. 35(3): p. 286-289.
- [17] Wang Rui and Li Houpu, Calculation of Innermost Area Effects in Altimetry Gravity Recovery Based on the Inverse Stokes Formula. *Geomatics and Information Science of Wuhan University*, 2010. 35(4): p. 467-471.

- [18] Chao Dingbo, Shen Wenbin, and Wang Zhengtao, Investigations of the possibility and method of determining global centimeter-level geoid. *Acta Geodaetica et Cartographica Sinica*, 2007. 36(4): p. 370-376.
- [19] Han Jiancheng and Shen Wenbin, Simulation test for determination  $1^{\circ} \times 1^{\circ}$  global geoid with centimeter-level accuracy. *Journal of Geodesy and Geodynamics*, 2007. 27(5): p. 38-43.
- [20] Shen Wenbin and Chao Dingbo, An Approach of Realizing the Global  $1^{\circ} \times 1^{\circ}$  Geoid at Centimeter-Level Accuracy. *Geomatics and Information Science of Wuhan University*, 2008. 33(6): p. 612-615.
- [21] Li Jiancheng, Ning Jinsheng, and Chao Dingbo, Evaluation of the Earth Gravitational Model 2008 using GPS-leveling and gravity data in China. *Newton's bulletin*, 2009(4): p. 252-275.
- [22] Zhang Chuanyin, Guo Chunxi, Chen Junyong, Zhang Liming, et al., EGM 2008 and Its Application Analysis in Chinese Mainland. *Acta Geodaetica et Cartographica Sinica*, 2009. 38(4): p. 283-289.
- [23] Rong Min, Zhou Wei, and Chen Chunwang, Evaluation of gravity field models EGM2008 and EGM96 applied in Chinese area. *Journal of Geodesy and Geodynamics*, 2009. 29(6): p. 123-125.

# National Report on Absolute and Superconducting Gravimetry

*SUN Heping, WANG Yong, XU Jianqiao, ZHANG Weimin and ZHOU Jiangcun*

Institute of Geodesy and Geophysics, Chinese Academy of Sciences, Wuhan, 430077

By now, there are four FG5 and two A-10 style absolute gravimeters (AG in abbr.) in China which are used to set up the base of absolute gravity fiducial network with accuracy of  $2\sim 5\times 10^{-8}$  ms<sup>-2</sup>. Meanwhile, there are three high accuracy superconducting gravimeters (SG in abbr.) which are being applied in long-term continuous gravity surveying. The observational data obtained by these gravimeters are supporting the researches on time-variable gravity field, Earth's tides, mass transportation and loading on Earth's surface, crustal movement, geodynamics as well as on the structure in the Earth's interior.

In recent years, the researches on crustal movement, for example the construction of Chinese Continent Tectonic Environment Monitoring Network (CCTEMN in abbr.) and the corresponding studies have been developed in China. It is comprised of three parts including fundamental network, regional network and data system. It is an integrated monitoring network combing space techniques of GPS, fix and mobile gravimetry, VLBI and SLR to obtain broad images of crustal movement and gravity field variation with high accuracy and high spatial-time resolution.

In the frame of CCTEMN, the Institute of Geodesy and Geophysics, Chinese Academy of Science (IGGCAS in abbr.) set up several gravity and GPS continuous observatories such as Lasha, Zhanjiang, Wanzhou, Jian and Lingzhi among which one high accurate SG was installed at Lasha in the end of 2009. Consequently, a network on continuous gravity surveying with high spatial resolution was formed by collecting Wuhan field observatory on dynamic geodesy and other station in CCTEMN. CASIGG also took part in the construction of gravity data analysis software for CCTEMN and is now building the branch of gravity data center in China mainland.

Recently, the units to which the instruments belong have been exploring actively the international co-operations, such as Global Geodynamics Project (GGP in abbr.) which aims to share the data observed by different SG in the world and the China-Japan joint project of gravity survey in east Asia. With the advanced AGs and SGs, some important developments have been gained as follows:

## **I. Survey with AG**

By the FG5 AG, IGGCAS accomplished the fourth round of gravity survey under national absolute gravity network and also conducted repeat surveys at some stations in south-west China.

The FG5 AG belonging to Xi'an Research Institute of Survey and Mapping, State Bureau of Surveying and Mapping is mainly responsible to national gravity fiducial stations, which includes maintenance and update of the benchmarks. Since 2007, about 50 times absolute gravity surveys have been conducted.

The FG5 AG belonging to the Institute of seismology, China Earthquake Administration (ISCEA

in abbr.) took part in the 2nd international comparative absolute gravity survey held in Walferdange, Luxemburg at the end of 2007. The observational results showed that the relative deviation, about  $1.4 \times 10^{-8} \text{ ms}^{-2}$ , by the gravimeter was the smallest one among all the participants (Xing et al, 2009). By the efforts in recent years, the absolute gravity benchmarks of the Chinese gravity network for earthquake have been preliminary established (Liu et al, 2007). After the big Wenchuan Ms8.0 and Yushu Ms7.1 earthquakes, several FG5 AGs were immediately organized to set up 15 absolute gravity control points in those areas to obtain co-seismic and analyze post-seismic gravity changes.

During the course of the implementation of CCTEMN, in order to better construct absolute gravity fiducial network and further to conduct surveys, a coordination committee on gravity survey was organized specially for CCTEMN. And a round of co-site comparative observations by 4 FG5 AGs was organized at Wuhan fiducial station to make the data obtained by the 4 instruments comparable and to make the data obtained at different stations successive.

## **II. Surveys with SG**

Since IGGCAS imported the first SG in China in 1980s, high accuracy long-term continuous gravity data as well as barometric and hydrological data have been obtained at Wuhan station which is located in Mt. Jiufeng in Wuhan. In the end of 2009, in order to investigate the mechanism of Tibet Plateau, a new SG observatory has been set up and has run for more than one year. By FG5 AG, a calibration was done to transfer the digitally acquisitions to gravity variations. And now the two instruments are working well.

ISCEA set up another SG station in Wuhan in Sep. 2008 as well as the necessary facilities. By now, there are about 2 year continuous gravity data. A calibration was also done by FG5 AG there. And now the instrument is working well.

## **III. Application of the AG observations in gravity variation and its mechanism**

Recently, by using high accuracy absolute gravity data, some investigations have been carried out, for example, the investigation on crustal movement and mass transportation in Earth's interior over earthquake monitoring area, which is benefit to earthquake prediction; on the determination of uplift velocity of Tibet Plateau and its mechanism; and on gravity field variation due to environmental changes.

Li et al (2009) gave the dynamic change of gravity in China mainland on the time scale of 2~3 years according to mobile gravity surveys of crust movement observation network in China and Chinese digital earthquake observation network since 1998 and analyzed this variation by combing the dynamic tectonic environment and strong earthquake activities (see Fig.1). The dynamic changes of gravity preliminarily reflect mass transportation in crust and the basic profile of strong earthquake activities in China mainland.

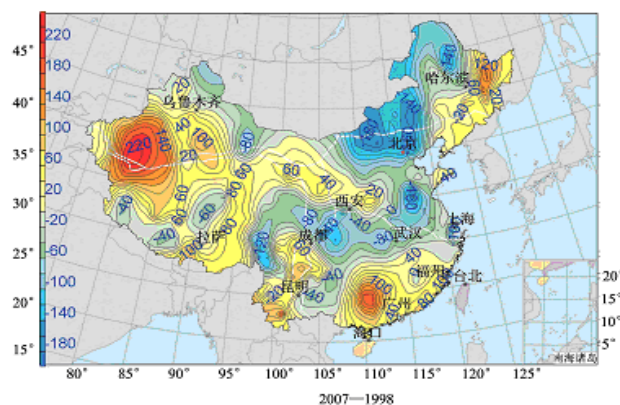


Fig.1 Changes in gravity in China mainland (unit:  $10^{-8} \text{ ms}^{-2}$ )

Shen et al (2009) analyzed the characteristics of gravity field before the Wenchuan Ms8.0 earthquake according to the dynamic changes of gravity in China mainland. The properties of gravity changes reflect the mass transportation in crust on regional large spatial scale, which may implicate the process of gestation and occurrence of earthquake and provide investigations on medium-term earthquake prediction with references. Zhang et al (2007) analyzed about 10 years of AG data at Wuhan station and pointed that the gravity was increasing with mean velocity of  $1 \times 10^{-8} \text{ ms}^{-2}/\text{a}$  which corresponds to the vertical displacement velocity of  $-0.38 \text{ cm}/\text{a}$  in accordance with GPS results (Zhu et al, 2007). Xing et al (2008) analyzed the absolute gravity data spanning about 15 years in Pi county of Hebei province and concluded that the gravity increased greatly with velocity of about  $5.0 \times 10^{-8} \text{ ms}^{-2}$  which was similar to the situation during Tangshan earthquake.

Wang et al (2009) analyzed absolute gravity data at Changchun fiducial station and hydrological data and showed that the water level variation directly affect the gravity results up to  $15.4 \times 10^{-8} \text{ ms}^{-2}$  extremely. This effect caused the gravity deviation with a magnitude of  $6.7 \times 10^{-8} \text{ ms}^{-2}$  at the station. And gravity increased with velocity of  $0.6 \times 10^{-8} \text{ ms}^{-2}/\text{a}$  averagely during the past 7 years.

Through two experiments on gravity changes due to disturbing mass by FG5 AG, Wang et al (2009) obtained the gravitational constant  $G$  of  $(6.6665 \pm 0.0554) \times 10^{-11} \text{ m}^3/(\text{kg} \cdot \text{s}^2)$  by appropriate error controlling method and plenty of repeat surveys.

#### IV. Application of the SG observations in tidal, non-tidal gravity and Earth's normal modes

Under the project of GGP, the SG data and the auxiliary data at all the GGP stations since 1997 were gathered and a database was constructed after preprocessing on the data by the recommended software. Meanwhile, the stacking method and the wavelet method were developed to enhance the signal-noise ratio corresponding to different dynamic processes.

An accurate tidal correction model for gravity was constructed by considering together the solid Earth tides by theoretical and experimental tidal models and ocean tide loading by global and regional tidal maps. The accuracy of the model is better than  $0.5 \times 10^{-8} \text{ ms}^{-2}$ , which can be applied to gravity survey as a correction provider (Zhou et al, 2009).

By using convolution technique according to load Green's function theory and considering the temperature on Earth's surface, the effects of atmosphere on gravity observations were estimated.

A new quasi-3d computation scheme was put forward for atmosphere loading computation, which not only saved computation time but also overcame the lack of 3D atmospheric pressure data (Luo et al, 2009). Chen et al (2008) estimated the effect of self-consistent equilibrium pole tides on tidal parameters firstly in China. The relative magnitude of this effect exceeded 1%, which is the main source of difference between the theoretical and observational values. Chen et al (2009) later accurately determined the tidal parameters for pole tides by using SG data and taking both the 3D atmospheric pressure data and hydrological data into consideration.

By using long-term continuous SG data as well as AG and GPS data at Wuhan station, the long-term non-tidal characteristics of gravity variation and its relation with regional air pressure and water storage as well as vertical crustal movement were investigated. The results showed that there was an obvious seasonal variation, and about 70% of this variation and about 95% of annual signal were due to regional air and water storage variations. By comparative experiments with SG and AG, a long-term drift of  $17.13 \times 10^{-9} \text{ ms}^{-2}/\text{a}$  was derived. At the same time, according to the GPS results, the crust over the regional area where the station locates was subsiding slowly with velocity of  $3.71 \pm 0.16 \text{ mm}/\text{a}$ , which corresponded to gravity variation of  $13.88 \pm 0.22 \times 10^{-9} \text{ ms}^{-2}/\text{a}$ . In the other words, as a result from crustal movement, the ratio of consequent gravity variation to consequent height variation was about  $-37.41 \times 10^{-9} \text{ ms}^{-2}/\text{cm}$ , which implicated that the vertical crustal movement was accompanied by huge mass adjustment. However, it's mechanical mechanism need to be investigated (Xu et al, 2008).

By using SG data, spheroidal fundamental modes of medium and low degrees and plenty of overtones as well as coupling of toroidal free oscillation were obtained completely and accurately, which further perfected long-period seismic chart (with frequency lower than 1 mHz) and accumulated abound of basic data for investigations on elastic characteristics of Earth's mantle. It is noted that the anomalous triplet of low degree spheroidal oscillation due to ellipticity and Earth's rotation was found (see Fig.2). The results showed that the stiffness in the top of Earth's inner core was smaller than the theoretical evaluation while the anisotropy of velocity of compression wave was bigger than the corresponding evaluation. It was the first time that the coupling between torodal modes, 1T2 and 1T3 for instance, and spheroidal modes was found, which verified the role of Coriolis force in coupling of toroidal oscillation. Additionally, the sensitivities of frequencies of fundamental modes for different degrees to parameters in different depth, such as density and Lamé constants were investigated, which was benefit to the inversion on physical parameters in Earth's interior (Yang et al, 2010).

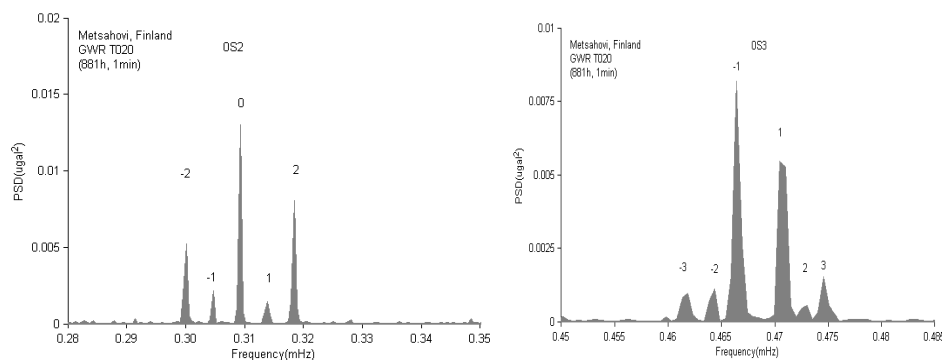


Fig.2 Triplet of  ${}_0S_2$  and  ${}_0S_3$

According to the features of nearly diurnal resonance, the resonance parameters were determined accurately by application of stacking technique in SG data (Ducarme et al, 2007). Xu et al (2009) found the decadal variation of period of Earth's free nutation. And Liu et al (2007) estimated that the dynamic ellipticity of core-mantle boundary was 5% larger than the one under the approximation of hydrostatic equilibrium. The dynamic viscosity on the bottom of core-mantle boundary was also estimated about 103 Pa·s, which is an important constraint to mechanism of core-mantle coupling (Sun et al, 2009).

The possibility of existence of Slichter triplet was scouted by stacking technique using continuous SG data obtained by 6 SGs in GGP in the same time band according to the features of Slichter triplet (see Fig.3). The results showed that in the sub-tide frequency band, i.e. 0.162~0.285cph, the Slichter modes might exist. Any a signal with amplitude of  $0.0152 \times 10^{-9}$  ms<sup>-2</sup> could be detected, which implicated that the Slichter modes would be identified by SG provided they existed. Accordingly, through plenty of tests, a group of signals whose periods were 5.310, 4.995 and 4.344 h respectively were found. The characteristics of these signals were in accordance with the ones of triplet of Slichter modes, which implicated that this group of signals must have been induced by translational oscillation of Earth's inner core. As a result, the density difference between inner and outer core must be in the middle of the values predicted by the models of PREM and 1066A (Xu et al, 2009).

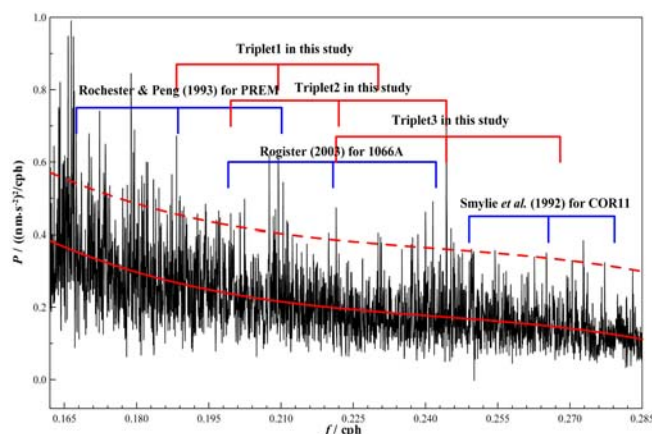


Fig.3 Search for the triplet of Slichter modes

## References

- [1] Chen Xiaodong, Ducarme Bernard, Sun Heping, Xu Jianqiao, 2008. Loading effect of a self-consistent equilibrium ocean pole tide on the gravimetric parameters of the gravity pole tides at superconducting gravimeter stations [J]. *Journal of Geodynamics*, 45: 201-207
- [2] Chen Xiaodong, Kroner Corinna & Sun Heping, et al, 2009. Determination of gravimetric parameters of the gravity pole tide using observations recorded with superconducting gravimeters [J]. *Journal of Geodynamics*, 48(3-5):348-353
- [3] Ducarme Bernard, Sun He-Ping, Xu Jian-Qiao, 2007. Determination of the free core nutation period from tidal gravity observations of the GGP superconducting gravimeter network [J]. *J. Geodesy*, 81: 179-187
- [4] Li Hui, Shen Chongyang, Sun Shaoan, et al. Dynamic gravity change in recent years in

- China continent [J]. *Journal of Geodesy and Geodynamics*, 2009, 29(3): 1-10. (in Chinese)
- [5] Liu Dongzhi, Li Hui, Xing Lelin, et al. analysis of absolute gravimetry result of China earthquake gravity network [J]. *Journal of Geodesy and Geodynamics*, 2007, 27(5): 88-93. (in Chinese)
- [6] Liu Mingbo, Sun Heping, Xu Jianqiao, et al. Determination of the Earth's free core nutation parameters by using tidal gravity data [J]. *Acta Seismologica Sinica*, 2007, 20(6):708-711
- [7] Luo Shaocong, Sun Heping, Xu Jianqiao, 2009. An investigation of the quasi 3-D atmospheric loading response on gravity—Implementation and evaluation [J]. *Journal of Geodynamics*, 48(3-5): 366-370
- [8] Shen Chongyang, Li Hui, Tan Hongbo, et al. Dynamic gravity changes and Wenchuan Ms8.0 big earthquake [J]. *Recent development in world seismology*, 2009, 4: 26
- [9] Sun Heping, Cui Xiaoming, Xu Jianqiao, et al. Preliminary application of superconductive gravity technique on the investigation of viscosity at core-mantle boundary [J]. *Chinese Journal of Geophysics*, 52(2): 311-321
- [10] Wang xiaobing, Zhang weimin, Zhong min. Impact on absolute gravity observation at Changchun fiducial of Jingyuetan reservoir impoundment [J]. *Journal of Geodesy and Geodynamics*, 2009, 30(5): 72-75. (in Chinese)
- [11] Wang Yong, Ke Xiaoping, Zhang Weiming, et al. Measurement of the Newtonian gravitational constant based on the principle of free fall [J]. *Chinese Science Bulletin*, 2009, 54(6): 1019-1025
- [12] Xing Leli, Li Hui, He Zhitang, et al. Analysis of repeat absolute gravimetric results at chengdu seismostation [J]. *Journal of Geodesy and Geodynamics*, 2008, 28(6): 38-42. (in Chinese)
- [13] Xing Leli, Shen Chongyang, Li Hui, et al. Comparative observation of absolute gravimeters in Walferdange [J]. *Journal of Geodesy and Geodynamics*, 2009, 29(3): 77-79. (in Chinese)
- [14] Xu Jianqiao, Sun Heping, 2009. Temporal variations in free core nutation period. *Earthq Sci*, 22: 331-336
- [15] Xu Jianqiao, Sun Heping, Zhou Jiangcun. Experimental detection of the inner core translational triplet [J]. *Chinese Science Bulletin*, 2010, 55(3) : 276-283
- [16] Xu Jianqiao, Zhou Jiangcun, Luo Shaocong, et al. Study on characteristics of long-term gravity changes at Wuhan station [J]. *Chinese Science Bulletin*, 2008, 53(3): 2033-2040
- [17] Yang Zhao, Sun Heping, Lei Xiange, et al. Study of normal mode based on the changes of stratified structure parameters [J]. *Chinese Journal Geophysics*, 2010, 53 (4): 807-814
- [18] Zhang Weimin, Wang Yong. Absolute gravity measurement in dynamic geodesy center experiment station at Jiufeng [J]. *Journal of Geodesy and Geodynamics*, 2007, 27(4): 44-46. (in Chinese)
- [19] Zhou Jiangcun, Xu Jianqiao, Sun Heping. Accurate correction models for tidal gravity in Chinese continent [J]. *Chinese Journal Geophysics*, 2009, 52(6):1474-1482 (in Chinese)
- [20] Zhu Yiqing, Liang Weifeng, Li Hui, et al. On gravity field variations and geodynamic characteristics in mainland of China [J]. *Geometrics and Information Science of Wuhan University*, 2007, 32(3) 246-250, (in Chinese)

## Progress of Underwater Gravity-aided Inertial Navigation

*WU Xiaoping, LI Shanshan*

Zhengzhou Institute of Surveying and Mapping, Zhengzhou, P.R.China

Inertial navigation is currently the most popular technology adopted by underwater submarine navigation, its primary principle is using inertial sense organ to survey the linear and rotational movement parameters of the underwater submarine relative to inertial space, and work out the submarine's attitude, orientation and positioning on certain initial movement conditions. Inertial navigation has several technical advantages such as high precision, good reliability and it is basically immune to environment disturbance. The new-style peg-top module has high integration, little volume, wide surveying range for attitude and course angle, good dynamic capacity, and can work in bad environment. But the disadvantage of this technology is that the system error is accumulating along with time when calculating track and location, the positioning error will increase limitlessly if the system error is not re-adjusted periodically, and it is not fit for long time self-navigation for underwater submarine. At present, the inertial navigation system is calibrated by GPS (Global Positioning System), wireless navigation and astronomical navigation. These technologies need the submarine to come out of the ocean surface or get close to it, or transmit signal, consequently it makes the submarine to be detected and discovered. Therefore, a technology, which makes the submarine not to get close to ocean surface and transmit signal, is needed to amend the inertial navigation system, and this technology is automatic gravity-aided inertial navigation.

The automatic gravity-aided inertial navigation is developed on the basis of surveying and compensation for gravity anomaly and deflection of the vertical. It is a figure tracking navigation technology realized by gravity surveying. It consists of inertial navigation system, gravity data-base, gravity surveying sensor, matching calculation computer and so on. The basic working principle can be described as follows: the gravity distributing figure is made out in advance, and every path in the figure has special gravity distribution, the gravity distribution is stored in the navigation system, the gravity information is surveyed by gravimeter on the submarine to search and match the path for navigation and positioning. This method doesn't radiate and use outside coordinate, and can finally solve the concealment requirement of submarine. Several key questions must be solved if put this technology into practicality: the construction of global ocean gravity background field model in high resolution and precision, the realization of underwater real-time gravity surveying (including gravity sensor and data processing method in high precision) and gravity matching algorithm.

At present, the automatic gravity-aided inertial navigation at home is at the stage of principle exploring and simulation argumentation. Beijing University and Navy Equipment Academe had some progress in the systematic study of global gravity field model fitting for gravity-aided navigation, gravity real-time surveying theory and method, two-dimension random field interpolation theory and gravity anomaly matching theory; Haerbin Engineering University put

forward the ICCP (the iterated closest contour point) algorithm that the Ou-distance is replaced by Ma-distance and the Kriging algorithm in geological statistics should be used for gravity evaluation; Southeast University studied the gravity matching navigation algorithm based on velocity azimuth flat; Surveying and physical geography academe of CAS (Chinese Academy of Science) studied the SITAN (Sandia inertial terrain-aided navigation) gravity matching algorithm and the construction of ocean background field model based on satellite altimetry data under the support of national natural science fund; Xi'an Research Institute of Surveying and Mapping explored the ocean physical geography navigation theory and method, and put forward the technological approach of ocean gravity-aided navigation; Navy Engineering University and Navy Ocean Surveying Academe studied the gravity-aided navigation and index argumentation; Beijing Mailing and Electricity University studied the theory and model of micro-system in underwater gravity-aided inertial navigation; Wuhan University discussed the gravity compensation technology of inertial navigation system in high precision; Institute of Surveying and Mapping, Information and Engineering University studied and designed the combination pattern of automatic gravity-aided inertial navigation in the mass, Gravity map reconstruction, data preprocessing, analysis of matching algorithms and capability evaluation are made, the intelligentized data is syncretized, and the simulation design of the automatic underwater navigation modules is completed, it could be a reliable technology for the precise navigation of underwater submarine in the ocean.

#### **I. Construction of global gravity background field model in high resolution and precision**

Satellite altimetry is one of the satellite-ground observation technologies in recent a few decades years, and it is also the most sophisticated technology in the observation of the earth gravity field, and the main means to obtain global ocean gravity data and construct ocean gravity background field model. Since the experiment success of the Skylab satellite schlepping with the altimetry facility in 1972, the altimetry satellites such as GEOS-3(1975), SEASAT(1978), GEOSAT(1985 ~ 1990), ERS-1(1991~1996), TOPEX/POSEIDON (1992 ~) and ERS-2(1995 ~) were launched one after the other. Satellite altimetry is using the radar altimetry facility fixed on board the satellite to survey the vertical distance between the satellite and instantaneous ocean surface just below the satellite. It can scan the entire ocean in several periods during the satellite circulation, and can determine the detailed ocean surface shape and its changement in very high time and space resolution, the ocean geoid can be obtained by correcting the ocean surface topography and other parameters, according to different observation tasks of all kinds of satellites, the geoid in different resolution and precision can be obtained. At present, the optimal ocean geoid estimation in  $2' \times 2'$  resolution and 10cm precision can be obtained by combination process of the data of several observation missions.

Altimetry satellite is the modern high-tech surveying and monitoring system that integrating the space technology, micro-wave technology, remote sensing technology and the construction of precise facility, the South China Sea's floor topography was deduced by satellite altimetry data, improved model of statistical algorithm was put forward, the influence of lithosphere equilibrium compensation effect was considered, and its precision was in accordance with world level. The global average ocean surface height in  $2' \times 2'$  grid was determined according to the Seasat, Geosat, ERS-1 and T/P's altimetry data by Taiwan scientists. The mean square errors of the average ocean surface of multi-satellites compared to T/P's average ocean surface and ERS-1's average ocean

surface were 4.6cm and 6.5cm.

At the aspect of ocean gravity field study, the gravity network adjustment problem was solved by Xi'an Research Institute of Surveying and Mapping, the dynamic system error's changement was described by choosing mathematical model, the to be determined coefficients were confirmed while adjusting the surveying line's crossing points, therefore the error compensation was achieved and the better effect could be obtained in the actual application. The methods, which used the Stokes formula and the Vening-Meinesz formula to deduce ocean gravity anomaly, were studied, and the deduced results were compared with ship surveying data. The results show that the average value's precision of gravity anomaly in  $15' \times 15'$  resolution obtained by satellite altimetry data was not less than 5mGal, the gravity anomaly in  $30' \times 30'$  resolution was not less than 4mGal, and the gravity anomaly in  $1^\circ \times 1^\circ$  resolution was not less than 3mGal. The formulae of Molodensky to deduce height anomaly and the ocean gravity deflection of the vertical's gridding value calculated by altimetry section plane gradient data were used to compute the offing altimetry (quasi)geoid of our country, the inner checkage show that the standard deviation could achieve  $\pm 0.025\text{m}$ .

## II. Gravity compensation technology of inertial navigation system in high precision

To distinguish the gravity acceleration and movement acceleration of underwater submarine, the inertial navigation must have gravity field mathematical model. In generally the actual inertial navigation chooses the reference ellipsoid to describe gravity field model, namely the actual gravity field is replaced by normal gravity field to make the mechanic arrangement equation's gravity field correction. But the changement of the swing value of gravity anomaly in China Sea and adjacent region is rather bigger, the maximum is  $378 \times 10^{-5} \text{ms}^{-2}$ , and the minimum is  $-356 \times 10^{-5} \text{ms}^{-2}$ . At present, along with the increase of inertial navigation precision requirement and the improvement of inertial facility cell organ precision, for example, the precision of static peg-top is  $10^{-6} / h$ , and the precision of acceleration is  $10^{-9} g$ , therefore the difference between actual gravity field and normal gravity field—the disturbing gravity and deflection of the vertical will be the maximum residual error in high-powered inertial navigation.

Institute of Surveying and Mapping, Information and Engineering University and Xi'an Research Institute of Surveying and Mapping validated the influence of disturbing gravity vector to inertial system precision quantitatively and qualitatively, the influence to the inertial navigation system's level position and velocity is surging error in Schuler period, its maximum swing is in direct ratio with the disturbing gravity vector's weighting integral average and integral average, if the disturbing gravity error is 5mGal, the maximum level position error will be 60m. Therefore, the gravity compensation based on known gravity anomaly figure is the effective way to improve the inertial navigation precision, and its engineering realization is rather simple. The gravity benchmark figure needs to be drawn previously, and the errors of benchmark figure and gravity vector estimation of inertial navigation reference position directly affect the precision of gravity compensation. The gravity compensation based on gravity gradiometer doesn't need to draw gravity benchmark figure previously, and it is fit for all the zones that the inertial navigation system can reach, the gravity compensation precision is much higher, but the gravity gradiometer must be equipped in inertial navigation system.

### **III. Real-time acquisition technology of underwater gravity surveying data**

The normal working precondition of automatic gravity-aided inertial navigation system is the ocean gravity field characteristic information surveyed by gravimeter or gravity gradiometer, if the facility has bigger time delay or surveying error, the precision of matching point position will descend, and even the false positioning will be generated, therefore the matching navigation has strict requirements for the surveying precision and real-time character of gravity sensor. The actual ocean gravimeter can't directly apply to the gravity navigation, development of ocean sensor in high precision and the real-time processing technology of sensor surveying data to fulfill the automatic gravity-aided inertial navigation's real-time and high precision requirements to gravity surveying data is another key supporting technology for putting gravity matching navigation into the application of underwater actual navigation.

The hardware, technologies and data processing level of the dynamic gravity surveying at home are comparatively sophisticated, the underwater real-time gravity surveying technologies mainly use the theories and methods of on-board the ship for reference. But the difference is that the gravity surveying of on-board the ship is strictly implemented according to gravity surveying criterion at sea, and real-time requirement of the gravity surveying system of aided inertial navigation is very high, the positioning message is supported by inertial navigation which should be corrected because it has accumulated navigation error, the correction of zero drift can't be accomplished, and so on. Therefore the present ocean gravity sensor can't be used to survey the gravity real-timely, and the modules of compensation, correction, filter and stabilization should also be increased. The real-time gravity surveying system for underwater robot R-One, which is developed by Tohoku and Tokyo University, is on the base of CG-3M ocean gravimeter of Canadian Scientrex company. Although the hardware facility has some differences with ocean gravimeter to fulfill the underwater real-time gravity surveying, the disturbing influence difference is very little in the process of dynamic surveying, and the data processing theory is in accordance with ocean gravity surveying.

### **IV. Study of gravity matching algorithm**

Matching algorithm is one of the core technologies in gravity-aided inertial navigation. This algorithm uses the more sophisticated topography matching technology for reference, and it consists of serial iteration and single point iteration. The single point iteration algorithm takes the SITAN algorithm as typical representative, and the inertial error's increase is restrained by matching every sampling point by extended Kalman filter technology. Serial relative matching algorithm is matching one time while the observation sampling serial reach a certain length, and the correction information is supplied to inertial navigation after the finish of matching, include the ICCP and correlative extremum matching algorithm.

At present, the theories and methods successfully applied to gravity matching mainly are extended Kalma filter and ICCP method based on figure matching theory, from the abroad experience, the positioning precision of Kalman filter is higher than ICCP algorithm, but the error statistic model of Kalman filter can't be easily acquired, and the divergence of filter can't be easily controlled neither, along with the maturity and perfection of little wave and the extensive application of all kinds of optimized computational algorithm, it is necessary to study the new matching algorithm.

Furthermore, study of the quantitative analysis of gravity positioning precision and every error

factor can on the one hand supply necessary theoretical support for improvement and increase of the algorithm precision, and on the other hand supply necessary specification requirements for development of gravity surveying facility and system, construction of gravity field electric maps, and make preparation for engineering and practicality of gravity-aided navigation.

# **Crustal Deformation Monitoring and Geodynamic Mechanism Study in China**

*XU Caijun and WEN Yangmao*

School of Geodesy and Geomatics, Wuhan University, 430079, China

This report briefly outlines remarkable advances during last period 2007-2010 in the studies on crustal deformation monitoring and geodynamic mechanism in China, including an overall description of crust deformation in China revealed from GPS measurements, investigations on present-day movement and strain-stress field in Tibet, Sichuan-Yunnan region and Beibu gulf area, works of kinematic model and dynamic mechanism on China continent, and is finished with coseismic displacement observations of Wenchuan and other earthquakes derived from GPS and SAR data.

## **I. Present-day Crustal Movement in China**

Widespread Cenozoic tectonic deformation in Asia and creation of the Tibet-Plateau are the grandest products of the collision and subsequent penetration of India into Eurasia. Late Quaternary active faults different in lengths and mechanisms are broadly distributed over the continental China. The upper crust has been sliced into a number of tectonic blocks by a network of major active faults. The present-day tectonic deformation of continental China is characterized by a combination of rigid-block movement and continuous deformation. For example, the Tarim Basin, the Ordos, and South China behave as coherent blocks similar to ocean plate without or with minor internal deformation, while the Tibetan Plateau and Tianshan seem to deform continuously with significant internal deformation. The latest GPS velocity fields processed by different groups reveal various active tectonic feature of China (Yao, 2008; Jiang et al., 2008; Wang et al., 2008; Ding and Xu, 2009; Wen and Xu, 2009; Liao and Wu, 2009).

Since 1992, China has established a number of high precision GPS crustal deformation monitoring networks, including the China national GPS A-order network, the Crustal Movement Observation Network of China (CMONOC), the Tibetan Plateau crustal deformation monitoring network, GPS network of North China, GPS network along the southeast of China Sea area, GPS network of Xinjiang etc. Combining original data from these GPS network, Yao (2008) used a multi-quadric equation interpolation method to establish a velocity field of China mainland crustal movement on International Terrestrial Reference Frame ITRF97. Inferred from the GPS site velocities, the crustal movement of China is mainly occurred in the southwest region. In particular, Himalayas and Lhasa block is with obvious northward movements. The absolutely movement of blocks in western China is in direction of northward and with fan-shaped opening. However, the Qiangtang, Sichuan and western of Yunnan block are with obvious clockwise rotation. The eastern region of Qiangtang block moves eastward dominantly. And the Sichuan-Yunnan block moves in the direction of southeastward, whereas western Yunnan block moves southwestward at a rate of 10~25 mm/a, which is a more active deformation zone. The rotation pole of western China is

(28°N, 97°E), with an average rate of 15 mm/a. The deformation in east region of north-south seismic belt is relatively small, which is dominated by southeastward movement with average rate of 5 mm/a. Heilongjiang sub-block moves at a rate of 3 mm/a, and south China block moves at rate of 8 mm/a.

The main feature of late Quaternary tectonic deformation in southern Qinghai-Tibet plateau is a series of nearly north-south fault graben systems, and discontinuous NWW dextral strike-slip faults. Jiang et al. (2008) have analyzed all campaigns and continuous GPS data collected in the Tibetan Plateau from 1993 to 2002, using GAMIT/GLOBK software in a single, self-consistent reference frame. The precision of GPS velocity field and strain field are better than previous estimates, especially in vertical velocity field. Their results show that the Himalayan block is mainly under compressing strain, and the maximum compressing rate is  $-98.5 \pm 4.2 \times 10^{-9}/a$  and with the extension rate of  $26.7 \pm 2.8 \times 10^{-9}/a$  in the direction of  $N127.1 \pm 0.7^\circ E$ . Its maximum shearing strain reaches up to  $62.6 \pm 2.6 \times 10^{-9}/a$ , and areal dilatation up to  $-78.1 \pm 5.1 \times 10^{-9}/a$ . The middle part of the Tibet block is mainly under compressing strain indirection of  $N39.0 \pm 2.0^\circ E$ , and the maximum compressing rate is  $-20.3 \pm 1.2 \times 10^{-9}/a$  in the direction of  $N37.1 \pm 0.7^\circ E$  and with the extension rate of  $10.8 \pm 1.6 \times 10^{-9}/a$  in the direction of  $N129.0 \pm 2.0^\circ E$ . Its maximum shearing strain reaches up to  $15.6 \pm 1.0 \times 10^{-9}/a$ , and areal dilatation up to  $-9.5 \pm 2.2 \times 10^{-9}/a$ . Both principal compressing strain rate and extension rate trail off from the Himalayan block to the middle part of the Tibet block. Besides, GPS result shows that the Tibetan Plateau uplifts with 3~5 mm/a, which is 2~3 mm less than the previous estimates.

The Sichuan-Yunnan region is located in the southeast of Tibetan Plateau where devastating earthquakes mostly occurred in the history. The region is divided into four first order blocks, namely, the Maerkang block, the Sichuan-Yunnan rhombic block, the Baoshan-Pu'er block and the Mizhina-Ximeng block. Cut by subordinate NE-trending active faults, the Sichuan-Yunnan rhombic block can be further divided into two sub-blocks: the north-western Sichuan sub-block and the middle Yunnan sub-block, and the Baoshan-Pu'er block into three sub-blocks: the Baoshan, Jinggu and Mengla sub-blocks. The north-western Sichuan sub-block is mainly enclosed by NW-trending Ganzi-Yushu-Xianshuihe Fault (the northern boundary), Lijiang-Xiaojinhe Fault (the southern boundary), and Jinshajiang Fault (the western boundary). The middle Yunnan sub-block is a triangular region, which is enclosed by Lijiang-Xiaojinhe Fault, Anninghe-Xiaojiang Fault and Honghe (Red River) Fault. Except the NW-trending Tengchong-Jinhong fault which serves as the boundary between the Baoshan-Pu'er block and the Mizhina-Ximeng block is the newly generated fault, other faults belong to the prior existing active fault.

A linked-fault-element model is employed to invert for contemporary slip rates along major active faults in the Sichuan-Yunnan region ( $96^\circ-108^\circ E$ ,  $21^\circ-35^\circ N$ ) using the least squares method (Wang et al. 2008). Their results support a model attributing the eastward extrusion of the Tibetan Plateau driven mainly by the north-northeastward indentation of the Indian plate into Tibet and the gravitational collapse of the plateau. Resisted by a relatively stable south China block, materials of the Sichuan-Yunnan region rotate clockwise around the eastern Himalayan tectonic syntaxis. During the process the Ganzi-Yushu, Xianshuihe, Anninghe, Zemuhe, Daliangshan, and Xiaojiang faults, the southwest extension of the Xiaojiang fault, and the Daluo-Jinhong and Mae Chan faults constitute the northeast and east boundaries of the eastward extrusion, with their left slip rates being 0.3-14.7, 8.9-17.1,  $5.1 \pm 2.5$ ,  $2.8 \pm 2.3$ ,  $7.1 \pm 2.1$ ,  $9.4 \pm 1.2$ ,  $10.1 \pm 2.0$ ,  $7.3 \pm 2.6$ , and  $4.9 \pm 3.0$

mm/a respectively. The southwestern boundary consists of a widely distributed dextral transpressional zone other than a single fault. Right slip rates of  $4.2\pm 1.3$ ,  $4.3\pm 1.1$ , and  $8.5\pm 1.7$  mm/a are detected across the Nanhua-Chuxiong-Jianshui, Wuliangshan, and Longling-Lancang faults. Crustal deformation across the Longmenshan fault is weak, with shortening rates of  $1.4\pm 1.0$  and  $1.6\pm 1.3$  mm/a across the Baoxing-Beichuan and Beichuan-Qingchuan segments. Northwest of the Longmenshan fault lies an active deformation zone (the Longriba fault) with  $5.1\pm 1.2$  mm/a right slip across. Relatively large slip rates are detected across a few faults within the Sichuan-Yunnan block:  $4.4\pm 1.3$  mm/a left slip and  $2.7\pm 1.1$  mm/a shortening across the Litang fault, and  $2.7\pm 2.3$  mm/a right-lateral shearing and  $6.7\pm 2.3$  mm/a shortening across the Yunongxi fault and its surrounding regions.

By using 84 seismic moment tensors, collected from the Harvard centroid moment tensor between 1903 and 2003, and 214 GPS velocity observations, derived from the crustal motion observation network of China between 1998 and 2004, Ding and Xu (2009) fixed the weight scaling factor of these two kinds of data in the joint inversion through Helmert method of variance components estimation (VCE), and inverted for current crustal motion in Sichuan-Yunnan area. Using VCE method, the weight scaling factor of GPS observations with a value of 0.833 is higher than that of seismic data, with a value of 0.167. It shows the importance of GPS observations with high accuracy and relatively uniform distribution in joint inversion. The crustal strain field in Sichuan-Yunnan area shows that the direction of compression strain is EW in the areas above  $30^{\circ}\text{N}$  and below  $30^{\circ}\text{N}$ , NE in the west of  $100^{\circ}\text{E}$ , and NW in the east of  $100^{\circ}\text{E}$ .

Wen and Xu (2009) studied the crustal motion and fault slip rate in Sichuan-Yunnan region using high precision GPS horizontal velocities and gravity data. Due to the influence of India-Tibet block's eastnorthward extrusion, and the gravitational buoyancy force associated with the sharp topographic gradient across the region, the first-order features of crustal deformation are the prominent clockwise rotation around East Himalaya Syntax (EHS), and leads left-slip motion along the Xianshuihe-Xiaojiang fault system (east boundary) and right-slip motion along the Jinshajiang-Honghe fault system (west boundary). The Xianshuihe-Anninghe-Zemuhe-Xiaojiang fault system is the most active left-lateral fault in the region, with a rate of  $12.1\pm 0.6$ ,  $9.0\pm 1.2$ ,  $6.4\pm 1.0$ ,  $6.0\pm 1.2$  and  $9.0\pm 1.2$  mm/a respectively. The Longmenshan fault system is with a rate of  $2.6\pm 1.1$  mm/a right-lateral slip, and  $1.3\pm 1.2$  mm/a extruded. Their result suggested that the pattern of crustal deformation in the region support the continuous deformation hypothesis.

The South China is a stable block in the views of geologic structure and seismicity and behaves as a coherent tectonic unit. In order to monitor present-day crustal motion and tectonic characteristics in Beibu gulf area, repeated GPS campaigns (1998-2009) are used to calculate the 3D velocity field on ITRF2000 and internal deformation pattern under a regional reference frame (Liao and Wu, 2009). Their results show that Beibu gulf area along South China block is moving in  $\text{NE}115^{\circ}$  direction, the average horizontal velocity is at rate of 33.5 mm/a. And the average vertical velocity is at rate of 3.5 mm/a.

## II. Kinematic Model and Dynamic Mechanism

Some theoretic studies were aiming at proving kinematic model and dynamic mechanism theories. Focusing on the tectonic blocks and kinematic model, Wang and Xu (2009) proposed rigid block motion model and strain rate model in a geodetic coordinate system as well as those in a spherical

coordinate system under the framework of tensor analysis. Both eccentricity and local tangential moving frame are now considered in these models, which is not the case for previous modeling. Their study show that the eccentricity has minor effects on determining Euler pole and strain rate tensor, indicating that it is reasonable not to consider crustal motion and deformation models in a geodetic coordinate system. On the contrary, the local tangential moving frame plays a big role in changing both of them, meaning that the local frame of velocity being different at each observation site should be taken account of when one builds up strain model in a curvilinear coordinate system. They suggested that the conventional Savage's crustal deformation model should be refurbished.

Active faulting and folding are widespread throughout the Tianshan despite far from the collision zone at the Himalaya to the south, obviously as a consequence of the collision between India the rest of Eurasia. Based on the multiple-term horizontal velocity solutions of 230 GPS monitoring sites in Tianshan and its adjacent region, the crustal shortening rate of Tianshan, with the longitude ( $77^{\circ}\pm 1^{\circ}$ ) E as the boundary, gradually decreased towards two sides, from the south to the north, which indicates that the pushing force of plate becomes weaker along with the fold deformation decreasing of the Tianshan (Wang et al., 2007). The direction of principal compressive strain of Tianshan and its adjacent area, nearly NNW, is basically perpendicular to the Tianshan cordillera trend, which suggests the distribution and variation of maximum principal compressive stress in Tianshan and its adjacent region resulted from collision and extrusion of Indian Plate. Their result indicates that the maximum shear strain field mainly concent rates on two areas, one is Isyk lake of North Tianshan, Kyrgyzstan, and the other is the juncture of Jiashi (South Tianshan) and Pamir arc faults.

Moreover, Yang et al. (2008) presented the current crustal movement velocity field for approximately 400 sites in the Tianshan Mountains and their adjacent areas and estimate slip rates on the major faults using a 2-D elastic dislocation model using GPS measurements conducted from 1992 to 2006. Their studies show slip rates within the range of 1-4 mm/a on the NW-SE trending strike-slip faults (such as Talas-Fergana fault) in the Tianshan Mountains. The slip rates on the approximately WE-SN trending gently-dipping detachment fault vary from 10-13 mm/a in the southwest Tianshan Mountains to 2-5 mm/a in the eastern Tianshan Mountains, and to 6-12 mm/a in the Kyrgrz Tianshan. This first-order feature of strain pattern is explained best by underthrusting of adjacent blocks beneath the Tianshan Mountains along a basal detachment fault. The elastic strain confined in the upper crustal layer above the detachment ultimately releases through infrequent great earthquakes in the Tianshan Mountains, resulting in considerable folding and faulting at their margins.

GPS data of 37 stations during 1997-2005 is used to study present-day crustal deformation in the northeast China. The velocities of northeast China related to Eurasia plate are generally small, with a rate of 1.58 mm/a on average (Meng et al., 2007). Several stations in the southwestern corner of the studied region are consistently moving towards the southeast, which is most probably a distant effect of the eastward motion of Qinghai-Tibet plateau. Small velocities of the stations near the epicenters of the 1999 Mw 7.1 and 2002 Mw 7.3 deep-focus earthquakes in Wangqing county show that the two earthquakes did not cause broad deformation of shallow crust. The horizontal velocities of the stations in the Northeastern Heilongjiang province may reflect the effect of the North America plate's invasion on the Eurasia plate.

Basing on Highly precise temporal deformation measurements across the Xianshuihe fault from two pairs of continuous GPS stations straddling the fault, Wang et al. (2008) proposed a kinematic fault model composed of a brittle layer in the upper crust, a ductile layer in the lower crust, and a transition zone in between to interpret the baseline vector changes. The slip in the transition zone of the south segment of the Xianshuihe fault is steady. The slips in the transition zones of the north and Daofu segments of the Xianshuihe fault, however, are not steady, and the average slip rates there are higher than that of the south segment. The difference in deformation behavior is probably associated with the rheological properties of the fault interface, suggesting that the overall fault strength of the south segment is greater than those of the north and Daofu segments, corresponding to longer earthquake recurrence time.

### III. Coseismic Displacement

#### 1. Wenchuan Earthquake

The 12, May 2008 Mw 7.9 Wenchuan earthquake was the largest seismic event in China in more than 50 years, causing fatalities of more than 80,000 and about 48 million people homeless. The earthquake epicenter was (103.186°E, 30.969°N) with focal mechanism solution in strike 238°, dip 59° and rake 128°. The scalar seismic moment is  $7.6 \times 10^{20}$  Nm (moment magnitude Mw 7.9). Field investigations (Xu et al., 2008) show that there are two NW-dipping imbricate reverse faults, the Wenchuan earthquake ruptured, along the Longmenshan Fault zone at the eastern margin of the Tibetan Plateau. This earthquake generated a 240 km long surface rupture along the Beichuan-Yingxiu Fault characterized by right-lateral oblique faulting and a 90km long surface rupture along the Guanxian-Jiangyou Fault characterized by dip-slip reverse faulting. Maximum vertical and horizontal displacements of 6.2 m and 4.9 m, respectively, were observed along the Beichuan-Yingxiu Fault, whereas a maximum vertical displacement of 3.5 m occurred along the Guanxian-jiangyou Fault. Its surface rupture length is the longest among the coseismic surface rupture zones for reverse faulting events ever reported.

Working Group of the CMONOC (2008) derived GPS coseismic deformation field from GPS mobile station along Longmenshan fault area conducted by CMONOC and Working Group of dynamic process on active block boundary and earthquake prediction, various-order control points of surveying and mapping conducted by State Bureau of Surveying and Mapping and GPS continuous network for Real Time Kinematic (RTK) services constructed by Earthquake Administrations of Sichuan and Chongqing. The GPS data is processed using GAMIT/GLOBK software with 30 s sampling interval, 24 h period and double differential strategy. The GPS coseismic displacement field shows that crustal deformation of Wenchuan earthquake is centered in Yingxiu - Beichuan fault, with opposite movement on both sides and strong horizontal shorten. Moreover, the magnitude of eastward movement on east margin of the Tibetan Plateau is bigger than westward movement on the Sichuan Basin. In addition, the earthquake is also with a dextral strike-slip component. GPS measurements revealed that horizontal displacement of south segment of Yingxiu fault is very small. And the north segment to north Beichuan County is with a clear right-lateral displacement, but the rate is still less than rate of horizontal shorten. The vertical coseismic displacements in the Chengdu Plain at east of the Longmenshan fault zone are dominated by subsidence. The hanging wall presents uplift close to fault and turns to subsidence shortly, which is similar with the elastic displacement field causing by a high-angle thrust fault.

Based on the segmenting fault model, Xu et al. (2009) derived the fine slip distribution by utilizing a sensitivity-based iterative fitting method to GPS datasets mainly from the CMONOC, with the two models of the homogeneous half space and the stratified crustal structure. The inversion results considering the stratified crustal structures are superior to them from the homogeneous, half space in the mass. The coseismic slip is concentrated to above the 10~19 km depth. There exist five slip peak zones and obvious slip distribution at the lower part of SW Beichuan fault, in line with the field investigations and the aftershocks, also can resolve the GPS observations better. The Qingchuan fault experienced distinct right-lateral slip, and the magnitude of mean slip is 1.99 m. However, the Beichuan fault mainly experienced thrust slip, and the magnitude of mean slip is 3.35 m. The magnitude of mean slip for Guanxian fault is 0.65 m. The inverted moment is  $8.74 \times 10^{20}$  Nm ( $M_w$  7.90), consistent with seismic estimates.

Li et al (2009) derived a reliable coseismic deformation field of Wenchuan earthquake from GPS network conducted by the State Bureau of Surveying and Mapping (SBSM) and China Earthquake Administration (CEA) using the highly precise data processing method. The larger deformations are in Wenchuan, Qingchuan and Beichuan Counties rather in the epicenter, while the largest magnitude is up to 2.3 m in the horizontal and 0.7 m in the vertical direction in Beichuan. They also inverted coseismic fault slip distributions using the elastic half-space homogeneous model with distributed slip model. The inversion results show that the non-constrained fault slip is most according with the GPS observed co-seismic deformation and the seismic fault is not only right-lateral and thrust slip, but also with a little left-lateral slip and normal slip slide. The moment tensor is about  $2.38 \times 10^{21}$  N·M and the main forwardly inverted coseismic deformations are in Dujianyan-Wenchuan county and also in Beichuan, Qingchuan areas at the greatest deformation of about 4.5m in the east direction and 0.8m in the north direction with a strongly right-lateral characteristic, which are almost consistent with the wide geological survey results.

Overcoming bald relief and dense vegetation in the Longmenshan mountain area, Wen (2009) used six adjacent ascending tracks JAXA ALOS L-band SAR data to generate coseismic displacements covering whole rupture zone of 2008 Wenchuan earthquake. Basing fault trace derived from high precision range change offset, a uniform slip distribution is estimated by using dislocation model in elastic half-space and genetic algorithm. A distributed slip model is derived by utilizing a sensitivity-based iterative fitting method. The inverted slip is concentrated to 0-19 km along dip direction including Yingxiu, Xiaoyudong, Beichuan and Nanba regions. The inverted geodetic magnitude is  $M_w$  7.89, consistent with seismic results. Meanwhile, Zhang et al. (2010) inverted coseismic dislocation parameters of Wenchuan earthquake using five-segment fault model with InSAR data. Their favored fault model contains five segments with varied dips, based on the seismogenic structure of precise aftershock relocation. The inverted slip distribution is concentrated in the depth of 0~20 km and the maximum slip is 10 m. Among the largest-slip area Beichuan area has relatively more concentrated slip at shallower depth than other area. The inverted rake distribution shows that there is a transition along the direction of SW-NE. It's mainly reverse and some right-lateral slip at Wenchuan and Beichuan area, but it is dominantly right-lateral with some thrusting in Qingchuan area, with the mean rake of  $97^\circ$  and  $138^\circ$  respectively. The inverted seismic moment  $M_0$  is  $7.7 \times 10^{20}$  N·m, and the moment magnitude  $M_w$  7.9.

## 2. *Other Earthquakes*

Coseismic displacement data obtained from the GPS and InSAR measurements made before and after the earthquake to invert for November 14, 2001 mountain pass west earthquake rupture distribution by Wan et al. (2008). Comparing with previous studies, their results agree better with the field survey results on horizontal surface offsets. The coseismic displacement amplitudes are asymmetric across the seismic fault, with the displacements south of the fault about 10%~20% larger in amplitude than that north of the fault. This observation can be explained by the fault dipping  $80^{\circ}\sim 81^{\circ}$  to the south. They demonstrated the first time that a left step of about 50 km length located between the west end of the rupture on the East Kunlun fault and the east end of the Sun Lake fault absorbed 0.1~0.2 m of normal faulting, and the Kunlun Pass fault absorbed about 0.8 m thrust faulting. The seismic moment release is estimated  $9.3\times 10^{20}$  N·m, corresponding to an Mw 8.0 earthquake.

On November 8, 1997, an Ms 7.9 Manyi earthquake was occurred in Qinghai-Tibet. Using InSAR coseismic deformation acquired by ESA ERS2 satellite, and combining with the fault trace derived from the correlation data and azimuth offset map and basing on dislocation model in elastic half-space, Wen and Xu (2009) derive the slip distribution by utilizing a sensitivity-based iterative fitting method. Their distributed-slip model indicated that the coseismic slip reaches about 6.78 m. The slip is concentrate to 12-112 km along the strike direction, with most of the moment release located on the shallow part above 16 km depth. The geodetic estimate of seismic moment is  $2.01\times 10^{20}$  Nm (Mw 7.50), which is consistent with seismic estimates.

Taking the InSAR coseismic deformation field as a constraint and adopting the isotropic elastic half-space dislocation model, Tan et al. (2009) made the optimum simulation for the fault geometry of the Gaize Ms 6.9 earthquake occurred in 2008. The residual deformation of one fault model is about 30 cm. And the residual deformation of two faults model is 15 cm. The dip-slip in 95% confidence interval is 1.6~2.4 m based on 20 repeated simulations. Their results suggest that the coseismic deformation of the event is caused by two ruptures.

Qiao et al. (2009) used three scenes Envisat images from ESA to derive the preseismic and coseismic deformation interfereograms caused by the Damxung Ms 6.6 earthquake on Oct. 6, 2008. Their results indicated that InSAR could not detect notable crustal motion more than 4 months before the event which caused distinct displacement in an area of  $20\text{ km}\times 20\text{ km}$  with a maximum LOS change about 0.3 m. The deformation field was symmetrically distributed and separated by a NS axis, where the west subsided and the east rose. A linear elastic dislocation model in half space and nonlinear constraint optimized algorithm is used to estimate the dislocation model of the earthquake fault. The inversion suggested that the epicenter locate at ( $E90.374^{\circ}$ ,  $N29.745^{\circ}$ ) with a seismic moment tensor Mw 6.35. The earthquake is dominated by a normal fault fracture with the maximum slip of 3 m on the  $12\text{ km}\times 11\text{ km}$  rupture surface striking  $S189^{\circ}W$ , dipping  $60^{\circ}$  to NW at the bottom of 9.5 km, located at a sub-fault of the southeastern piedmont of the Nyainqentanglha Mountains. The shallow depth of epicenter is related to crust thermal status of seismic region.

## References

- [1] Yao Y., 2008, Analysis of crustal movement characteristic in China mainland by high

- precision repeated measurements of GPS network, *Progr. Geophys.*, 23(4): 1030-1037
- [2] Jiang W., X. Zhou, J. Liu, et al., 2008, Present-day crustal movement and strain rate in the Qinghai-Tibetan Plateau from GPS data, *Acta Geodaetica et Cartographica Sinica*, 37(3): 285-292
- [3] WANG Y., E. WANG, Z. SHEN et al., 2008, GPS-constrained inversion of present-day slip rates along major faults of the Sichuan-Yunnan region, China, *Science in China Series D: Earth Sciences*, 38(5): 582-597
- [4] Ding K. and C. Xu, 2009, Current crustal strain field in the Sichuan-Yunnan area by joint inversion of GPS and seismic moment tensor, *Geomatics and Information Science of Wuhan University*, 34(3): 265-268
- [5] Wen Y. and C. Xu, 2009, Contemporary Crustal Deformation in Sichuan-Yunnan Region from GPS and Gravity Data, *Geomatics and Information Science of Wuhan University*, 34(5): 568-572
- [6] Liao C. and J. Wu, 2009, Study on characteristic of present-day crustal movement in Beibu gulf area, *J. Geodesy and Geodynamics*, 29(5): 22-26
- [7] Wang J. and C. Xu, 2009, Analyses of crustal motion and deformation models in a curvilinear coordinate system, *Chinese J. Geophysics*, 52(11): 2721-2728
- [8] Wang X., Q. Li, Z. Alexander, et al., 2007, Horizontal movement and strain characteristics in Tianshan and Its adjacent region with GPS deformation data, *Acta Seismologica Sinica*, 29(1): 31-37
- [9] Yang S., J. Li, Q. Wang, 2008, The deformation pattern and fault rate in the Tianshan Mountains inferred from GPS observations, *Science in China Series D: Earth Sciences*, 38(7): 872-880
- [10] Meng G., X. Shen, J. Wu et al., 2007, Present-day crustal movement in northeast China with GPS data, *J. Geodesy and Geodynamics*, 27(1): 19-23
- [11] Wang M., Z. Shen, W. Gan et al., 2008, GPS monitoring of temporal deformation of the Xianshuihe fault, *Science in China Series D: Earth Sciences*, 38(5): 575-581
- [12] Xu X., X. Wen, J. Ye et al., 2008, The Ms 8.0 Wenchuan earthquake surface ruptures and its seismogenic structure, *Seismology and Geology*, 30(3): 597-629
- [13] Working Group of the Crustal Motion Observation Network of China Project, Coseismic displacement field of the 2008 Ms 8.0 Wenchuan earthquake determined by GPS, *Science in China Series D: Earth Sciences*, 38(10):1195-1206
- [14] Xu C., Y. Liu, Y. Wen, 2009, Mw 7.9 Wenchuan earthquake slip distribution inversion from GPS measurements, *Acta Geodaetica et Cartographica Sinica*, 38(3): 195-201
- [15] Li Z., P. Zhang, S. Jin et al., 2009, Wenchuan earthquake deformation fault inversion and analysis based on GPS observations, *Acta Geodaetica et Cartographica Sinica*, 38(2): 108-119
- [16] Wen Y., 2009, Coseismic and postseismic deformation using synthetic aperture radar interferometry, PhD thesis, Wuhan University, Wuhan
- [17] Zhang G., C. Qu, X. Song et al., 2010, Slip distribution and source parameters inverted from coseismic derived by InSAR technology of Wenchuan Mw 7.9 earthquake, *Chinese J. Geophysics*, 53(2): 269-279
- [18] Wan Y., Z. Shen, M. Wang et al., 2008, Coseismic slip distribution of the 2001 Kunlun mountain pass west earthquake constrained using GPS and InSAR data, *Chinese J.*

- Geophysics, 51(4): 1074-1084
- [19] Wen Y. and C. Xu, 2009, Ms 7.9 Manyi earthquake slip distribution inversion by a sensitivity-based iterative fitting method, *Geomatics and Information Science of Wuhan University*, 34(6): 732-735
- [20] Tai K., X. Qiao, X. You, et al., 2009, Modeling InSAR coseismic deformation field caused by Gaize Ms 6.9 earthquake in 2008, *J. Geodesy and Geodynamics*, 29(S1): 1-6
- [21] Qiao X., X., You, S., Yang, et al., 2009, Study on dislocation inversion of Ms 6.6 Danmxung earthquake as constrained by InSAR measurement, *J. Geodesy and Geodynamics*, 29(6): 1-7

# Progress of Geodetic Data Processing Theory and Method in China

ZHANG Liping and YANG Yuanxi

Xi'an Research Institute of Surveying and Mapping, Xi'an 710054, China

## I. Functional model studies

Data fusion needs high accurate functional models. If there are some systematic errors which can be expressed by functional model parameter terms, then functional model may be extended. The fusion modes of the observations and derived observations with systemic errors or random model errors are discussed and the properties of the two fusion modes are analyzed (Yang and Zen, 2008). The sequential adjustment with constraints is conducted, and its characteristics are analyzed (Zen et al., 2008). After analyzing the influence of the outliers on parameters in the GPS observations, an adjustment compensation method is conducted, that is, the extra-parameters are added in the observation equation when the outliers in the GPS observations are found by means of the hypothesis testing based on the standardized residual (Zen and Zhang, 2008). The adjustment model with additional systematic error parameters has been successfully applied in large-scale GPS network data processing, which greatly weakens the systematic error and the datum error effects (Yang et al., 2009).

Some relations of the model parameters may exist, thus the functional model with constraints may be used. The generalization adjustment model is expanded to Linear Inequality Constrained Adjustment model (LICA), which defines the uniform surveying adjustment model. Under the certain condition, the paper implements the conversion of the two models (Ou and Zhu, 2009). In order to solve least squares adjustment problem with inequality constraints, one can convert the inequality constraints into the equality constraints by using aggregate function of non-linear programming, a basic augmented Lagrangean algorithm is proposed which provides the solutions identical to those obtained by the Bayesian method and/or simplex algorithm (Peng et al., 2007). With the help of active constraint concept, the linear inequality constraint adjustment can be transformed into the linear equality constraint adjustment by seeking active constraint through Kuhn-Tucker condition (Feng et al, 2007). A fictitious error equation method for solving the LICA problem is proposed (Ou and Zhu, 2007). A new algorithm for adjustment model with some nonnegative constrained parameters is suggested. In this algorithm, nonnegative constrained least-square problems are transformed to convex quadratic programming problems (Song and Zhu, 2007). Inequality constrained least-square problems can also be transformed to convex quadratic programming problems and then to the linear complementary problem (LCP) using Kuhn-Tucker conditions of quadratic programming, which consequently gives the general form of least squares estimation in adjustment model (Song et al., 2008a, 2008b). An M-estimator with inequality constraints is derived based on Bahadur linearization principle and aggregate function method (Peng et al., 2010).

## II. Stochastic model researches

Stochastic model is mainly expressed by variance components. In order to consider the astringency of variance components estimation and ensure the invariability of datum of stochastic model, the concept

of datum of stochastic model is introduced, and furthermore, the new formulae for estimating variance component of Helmert type are derived (Wang and Liu, 2007). Heteroscedastic and time correlation characteristics of the GPS observation sequence are analyzed and considered in time varying GPS data processing (Xu et al., 2008).

There are many theories and models which can control the influence of the colored state noises. A new approach is presented by polynomial-quotient which transforms the colored state noises into infinite series, and then the finite series is chosen to calculate the variance of colored state noises. The corresponding weighted fusion filter is performed (Huang et al., 2008a, 2008b). The simulation results showed that the method was not only fit for the observation noises with AR model but also for MA or ARMA models (Huang X et al., 2009). The linear filters with dynamic colored noises and observational colored noises are derived. It is proved that the Kalman filtering with dynamic white noises is the special case of Kalman filtering with dynamic colored noises (Zhao and Tao, 2008). Particle filter for colored measurement noise is presented by using polynomial-quotient for solving the problem of the colored measurement noises (Fan et al., 2009).

A method for estimating the process noises and observation noises of Kalman filter using total Hadamard variance was deduced. The prediction covariance represented by a function of the process noises and the observation covariance was constructed (Guo et al., 2010).

### **III. Outlier detecting and reliability theory**

A new Bayesian method for detecting gross errors is proposed based on the prior information of the unknown parameters, the posterior distribution of observation errors, and the variance inflation model (Gui Q et al., 2007a; 2007b; 2010; Li et al., 2007). A Bayesian method for positioning gross errors based on the posterior probability of the classification variable is put forward, and the mean shift model is constructed in order to get the Bayesian estimator for gross errors. A MCMC (Markov Chain Monte Carlo) sampling method is designed to compute the posterior probability of classification variable (Li et al., 2008). A robust Bayesian estimator for dynamic model parameter estimation with unknown contaminated factors is studied (Song et al., 2009).

In practical geodetic data processing, the outlier detection is very important. A new outlier snooping method is developed for processing the time series of satellite gravity data based on least square collocation. The main idea is to predict observable of the possible outlying point from neighboring data and to compare the prediction error with its estimated variance, and then perform outlier snooping according to a certain test statistic and a given significance level. The corresponding test statistic of t-distribution is constructed and a new statistical test of moving window is proposed (Xu and He, 2009). A method using damped least squares for spatial three-dimensional rectangular coordinate transformation is put forward, and robust estimation method for gross error detection and elimination is introduced. This method is adapted not only to large rotation angle, but also small rotation angle (Luo et al., 2007).

### **IV. Ill-conditioning diagnostics and regularization**

Different background of ill-conditioned problem should use different schemes. A new algorithm based on TIKHONOV regularization theorem is studied for short baseline GPS rapid positioning using several epochs with single frequency phase data. A new regularizer, which has explicitly physical meaning, is chosen to mitigate the ill-condition of the normal matrix (Lu et al., 2007). Two new regularizers are employed to separate systematical errors in GPS baselines. The first one is chosen by

using time series method, and the second is obtained from measurements using the auto-covariance function of the stationary stochastic process (Wang and Lu, 2007). Based on the conception of the matrix volume, the definition of the orthogonal degree of the matrices is introduced which generalizes and extends the determinant method. The orthogonal degree of the matrices is then applied to the ill-conditioning problem diagnostics (Wang et al., 2009). In practical situation, the number of observation equations may be less than that of unknown parameters, thus observation equations are rank-deficient. With ambiguity resolution, based on “select weight fitting” principle, observation equations are constrained not only through baseline components but also through systematical errors continuations of adjacent epochs. According to this method, the impact of systematical errors on GPS DD positioning accuracy can be mitigated effectively. Furthermore, the systematical errors can be achieved directly (Gao and Ou, 2009).

A class of ridge type GM estimator was proposed through combining the ridge estimator and the GM estimator. Theoretical and numerical results demonstrated that the new estimators could not only overcome the ill-conditioning but also had ability to resist the outliers in the observation space and the design space (Ma et al., 2007). In order to solve the ill-conditioned problem and outlier influences, a robust ridge and principal correlation estimation was established based on the robust M estimation theory (Fan et al., 2008). Several methods of ridge parameter determination, such as Ridge trace, general cross validation and L-curve method were formulated under the partial ridge estimation model, their performance was also analyzed (Liu et al., 2007).

## **V. Robust estimation**

Robust t-type estimation is introduced to Gauss-Markov model in geodetic adjustments which can be calculated by the EM algorithm. The scale parameter can be estimated simultaneously with the location parameters. The degree of freedom in t-distribution is a convenient tuning parameter between efficiency and robustness (Chen et al., 2008). The relation between p value and the efficiency of  $L_p$  estimation is discussed. A fast parameter estimation method of p-norm distribution is proposed (Pan X et al., 2010).

The parameter estimation for mixed integer model with the P-norm distributed observation noise is studied which employs the maximum likelihood estimation theory to derive the criterion for integer searching. Based on the fact that only real parameters can be differentiated but not the integer parameters due to their discrete property, and the least squares based integer searching criterion is just a case with normally distributed noises, the approach and iterative procedure are given for estimating p, searching integers and solving real-valued parameters (Li and Shen, 2010). A Bayesian estimator for dynamic models with contaminated distribution is also given (Song et al., 2009).

For achieving the precise kinematic positioning by the three phase differences of GPS carrier phases, a robust Kalman filtering with dynamic colored noises and observational colored noises is derived (Zhao and Tao, 2007). A robust Kalman filtering algorithm based on fuzzy control theory is put forward, combining with the fuzzy control theory. The equivalent weights are constructed by using fuzzy theory based on filtered residual deviation, which controls the influence of outlier on navigation results effectively (Li et al., 2008).

## **VI. Adaptive filtering**

Adaptive filtering is a hot issue in geodetic research areas in China. An adaptively robust filter based on Bancroft algorithm and two-stage filter in GPS navigation is developed, in order to control the

influences of the dynamic model disturbances, nonlinear problems and measurement outliers (Zhang et al., 2007). The adaptive filtering by selection of the parameter weights in the parameter estimation is applied to precise point positioning (PPP). The selecting weight fitting method is employed to determine the initial parameters and the corresponding variance-covariance components (Hao et al., 2007). An integrated GPS/INS algorithm is put forward by using the adaptive filter and improved neural network, which modifies the predicted state information from kinematic model on line. It is shown that the combined algorithm can not only improve the filter estimation accuracy, but also control the influences of measurement outliers and the disturbances of the dynamical model (Gao et al., 2007). In some cases the observations may be not enough in loosely coupled GPS/INS integrated navigation and possible faults may also exist. A neural network aided integrated navigation fault detection algorithm is put forward. The new algorithm is helpful to localize the measurement outliers when the kinematic model has significant errors, and can automatically detect and isolate the faults in the case that there are not redundant observations. The contributions of the dynamical model information and reliable measurements on the state vector estimates are balanced (Gao and Yang, 2008a). A new adaptive UKF algorithm for training neural network, by using windowing residual vectors to adaptively estimate the covariance matrices of the observational vectors and the model errors, is established (Gao et al., 2008b).

An algorithm for considering time-correlated errors in a Kalman filter was presented. The systematic errors were fitted based on observation residuals within chosen window, subsequently, the covariance matrices of the observations are modified online (Cao et al., 2010). A particle filtering algorithm named the adaptive fading extended Kalman particle filter was proposed. This method takes advantage of the adaptive fading extended Kalman filter to generate the proposal distribution function and can tune the parameter in line, which has better self adaptability and robustness (Gong et al., 2010). Combining adaptive Kalman filtering and fuzzy control theory, a fuzzy adaptive Kalman filtering is proposed based on the statistics of distribution constructed by residual deviation, which can balance the contribution of dynamics model information and observation information to the state estimates (Li and Lv, 2008). An adaptive two-stage filter based on innovation of filter was presented, the method performed well when the information of unknown random bias was incomplete (Cao and Sui, 2008).

A nonlinear adaptively robust filter is proposed and applied to satellite orbit determination, which uses nonlinear filter to improve the orbit precise, avoiding the bad influences of linearization error to orbit results. Bi-factor variance expanding model is used to adaptively adjust the covariance matrix of measurement noise, and resist the bad influence of measurement outliers to orbit results. Thirdly, an adaptive factor is used to adjust the covariance matrix of state noise, and reduce the bad influence of state model errors to orbit results (Wu and Huang, 2008). To solve the problem of real time orbit determination of LEO satellites based on GPS, the method of dynamic orbit smoothing was put forward by using adaptive Kalman filtering (AKF), which takes positioning solutions as observations (Qin and Yang, 2009).

A biased robust and adaptive filtering algorithm is proposed. Firstly, the observed values are corrected by the robust biased estimation such as robust ridge estimator, which only uses the original measurements before the filter performs. Secondly, the error effects of the dynamic model are controlled through the adaptive factor. The effects of the errors from the measurement model and dynamic model can be resisted in two steps (Gui et al., 2009).

An adaptively robust filter with multiple adaptive factors is proposed, based on the principles of

adaptive Kalman filter and bifactor robust estimation for correlated observations. The related adaptive factors for the components of the position vector and velocity vector are set up based on the discrepancy of the predicted state from the kinematic model and the estimated state from the measurements. The adaptively robust filter with multi adaptive factors is more flexible in controlling the disturbing effects of the state components compared to the adaptively robust filters with unified adaptive factor and classified adaptive factors (Yang and Cui, 2008).

A hybrid estimation strategy is proposed for evaluating the deformation parameters employing an adaptively robust filtering (Yang and Zen, 2009). An adaptive factor based on partial state discrepancy is developed and applied to tight coupled GPS/INS integrated navigation (Wu F et al., 2010). In order to improve the GPS/INS integration, the measurement noise covariance matrix is adapted based on the innovation sequence and selected weight filtering (He D et al., 2008). A new GPS/INS adaptive filtering that combines the adjustment of random errors and systematic errors is put forward. An improved BP neural network learning algorithm is set up (Gao et al., 2008).

The adaptive sequential adjustment and the adaptive robust sequential adjustment are presented based on adaptive filtering and robust estimation principle. The estimation formula of the parameters for both the adaptive sequential adjustment and the adaptive robust sequential adjustment are derived (Sui et al., 2007). To balance the covariance matrices of the signals and the observations, a new adaptive collocation estimator is thus derived in which the corresponding adaptive factor is constructed by the ratio of the variance components of the signals and the observations. A maximum likelihood estimator of the variance components is thus derived based on the collocation functional model and stochastic model. The new adaptive collocation with related adaptive factor constructed by the derived variance components is applied in a transformation between the geodetic height derived by GPS and orthometric height (Yang et al., 2009).

## **VII. Progress in other areas**

A novel model based on wavelet transform and support vector machine for dam deformation prediction is presented. Firstly, through the wavelet transform, deformation time series is decomposed into different frequency components. Then, according to the different characteristics of the decomposed components, different support vector machines are constructed to forecast the components. Finally, the predicted results of the components are reconstructed to be used as the final prediction result of deformation (Wang et al., 2008). Aiming at solving the training problem of large scale sample sets and model modifying problem of dynamic training sets, the dynamic least square support vector machine method is presented which takes full advantage of the model built by incremental algorithm. Based on the updated model, the new samples can be added gradually. The non-support vectors located in any position of the training set can be found and deleted easily. The matrix inverse algorithm is avoided, thus a high calculation efficiency can be obtained theoretically (Deng and Hua, 2008).

The total least squares (TLS) is studied (Lu et al., 2008, Qiu et al., 2010, Kong et al., 2010) which aims at controlling the error influences in both observation vector and design matrix. The iterative calculation method for TLS is proposed and the posterior precision is evaluated.

## **References**

- [1] Yang Y, Zen A. 2008. Fusion Modes of Various Geodetic Observations and Their Analysis[J]. *Geomatics and Information Science of Wuhan University*, 33(8):771-774.
- [2] Zen A, Yang Y, Ou Y. 2008. Sequential Adjustment with Constraints among Parameters[J]. *Geomatics and Information Science of Wuhan University*, 33(2):183-186.
- [3] Zen A, Zhang L. 2008. The Adjustment Compensation for the Outliers and Its Application in GPS Network Adjustment[J]. *Journal of Geomatics Science and Technology*, 25(2):90-93.
- [4] Yang Y, Tang Y, Chen C, Wang M, Zhang P, Wang X, Song L, Zhang Z. 2009. Integrated Adjustment of Chinese 2000' GPS Control Network[J]. *Survey Review*, 41, 313, 226-237.
- [5] Ou Y, Zhu J. 2009. Expanding of Classical Surveying Adjustment Model[J]. *Acta Geodaetica et Cartographica Sinica*, 38(1):12-15.
- [6] Peng J, Zhang Y, Zhang H, Liu X. 2007. The Solution of Inequality-constrained Least Squares Problem and Its Statistical Properties[J]. *Acta Geodaetica et Cartographica Sinica*, 36(1): 50-55.
- [7] Feng G, Zhu J, Chen Z, Dai W. 2007. A New Approach to Inequality Constrained Least-squares Adjustment[J]. *Acta Geodaetica et Cartographica Sinica*, 36(2): 119-123.
- [8] Ou Y, Zhu J. 2007. Fictitious Error Equation Method for Solving the LICA Problem[J]. *Bulletin of Surveying and Mapping*, (1):20-23.
- [9] Song Y, Zhu J. 2007. A New Approach for Adjustment Model with Some Nonnegative Constrained Parameters[J]. *Geomatics and Information Science of Wuhan University*, 32(10): 883-887.
- [10] Song Y, Zuo T, Zhu J. 2008a. Research on Algorithm of Adjustment Model with Linear Inequality Constrained Parameters[J]. *Acta Geodaetica et Cartographica Sinica*, 37(4): 433-437.
- [11] Song Y, Zhu J, Luo D, Zen L. 2008b. Least-Squares Estimation of Nonnegative Constrained Adjustment model[J]. *Geomatics and Information Science of Wuhan University*, 33(9): 907-909, 933.
- [12] Peng J, et al. 2010. The Mean Squares Error Matrix of Inequality Constrained M-estimated and the Conditions for Improving Solutions[J]. *Acta Geodaetica et Cartographica Sinica*, 39(2): 129-134.
- [13] Wang P, Liu C. 2007. Helmert Type for Estimating Variance Components Based on Datum of Stochastic Model[J]. *Journal of Geomatics Science and Technology*, 24(3): 213-215.
- [14] Xu R, Huang D, Zhou L, Li C. 2008. An Improved Method for GPS Stochastic Modeling[J]. *Geomatics and Information Science of Wuhan University*, 33(11): 1110-1113.
- [15] Huang X, Sui L, Fan P. 2008a. A New Approach for Colored Measurement Noises by Correcting Random Mode[J]. *Geomatics and Information Science of Wuhan University*, 33(6): 644-647.
- [16] Huang X, Sui L, Fan P, Cao Y. 2008b. An Alternative Approach for Colored State Noises by Correcting and the Random Model[J]. *Acta Geodaetica et Cartographica Sinica*, 37(3): 361-366.
- [17] Huang X, Sui L, Fan X. 2009. A New Approach for Weighted Measurement Fusion by Noises Random Model[J]. *Journal of Geomatics Science and Technology*, 26(1): 52-55.
- [18] Zhao C, Tao B. 2008. Kalman Filtering of Linear System with Colored Noise[J]. *Geomatics and Information Science of Wuhan University*, 33(2): 180-182,207.
- [19] Fan P, Sui L, Huang X. 2009. Particle Filter for Colored Measurement Noise[J]. *Journal of Geomatics Science and Technology*, 26(2): 89-92.
- [20] Guo H, Yang Y, He H, Xu T. 2010. Determination of Covariance Matrix of Kalman Filter Used for Time Prediction of Atomic Clocks of Navigation Satellites[J]. *Acta Geodaetica et Cartographica Sinica*, 39(2): 146-150.

- [21] Gui Q, Xu A, Li X, Du Y, Zhang L. 2007a. Bayesian Approach to Detection of Gross Errors Based on Posterior Distribution of Observation Error[J]. *Journal of Geomatics Science and Technology*, 24(2): 87-89,92.
- [22] Gui Q, Gong Y, Li G, Li B. 2007b. A Bayesian approach to the detection of gross errors based on posterior probability[J]. *Journal of Geodesy*, 81: 651-659.
- [23] Li B, Gong Y, Gui Q. Bayesian Approach for Detection of Gross Errors Based on Variance Inflation Model[J]. *Journal of Geomatics Science and Technology*, 2007, 24(6): 399-401,405.
- [24] Li X, Gui Q, Xu A. 2008. Bayesian Method for Detection of Gross Errors Based on Classification Variables[J]. *Acta Geodaetica et Cartographica Sinica*, 37(3): 355-360.
- [25] Song Y, Chen Y, Zen L. 2009. Bayesian Estimation for Kinematic Positioning with Contaminated Model of Measurement Noise[J]. *Geomatics and Information Science of Wuhan University*, 34(6): 736-740.
- [26] Gui Q, Li X. 2010. Bayesian Unmasking Method for Positioning Multiple Blunder[J]. *Geomatics and Information Science of Wuhan University*, 35(1):1-5.
- [27] Xu T, He K. 2009. Outlier Snooping Based on the Test Statistic of Moving Windows and Its Applications in GOCE Data Preprocessing[J]. *Acta Geodaetica et Cartographica Sinica*, 38(5): 391-396.
- [28] Zhang F, Hao J, Guo L, Ding S. 2009. Gross Error Detection and Reparation for VRS Synthetical Error Based on Unascertained Rational[J]. *Journal of Geomatics Science and Technology*, 26(6): 403-406.
- [29] Luo C, Zhang Z, Mei W, Deng Y. 2007. A Damped Least Square Robust Estimation Method for Spatial Three-Dimensional Rectangular Coordinate Transformation[J]. *Geomatics and Information Science of Wuhan University*, 32(8): 707-710.
- [30] Lu X, Wang Z, Ou J. 2007. Several-Epoch Algorithm in Short Baseline Rapid Positioning Using Single Frequency GPS Receivers[J]. *Geomatics and Information Science of Wuhan University*, 32(12): 1147-1151.
- [31] Wang Z, Lu X. 2007. Separating Systematical Errors in GPS Baselines Using Semi-parametric Model[J]. *Geomatics and Information Science of Wuhan University*, 32(4): 316-318.
- [32] Wang x, Dang Y, Xue S. 2009. A Numerical Value Index Applied to Diagnosis of ill-conditioning Problems: Orthogonal Degree of Matrices[J]. *Geomatics and Information Science of Wuhan University*, 34(2): 244-247.
- [33] Gao Y, Ou J. 2009. Selecting Weight Fitting Method for Baseline Solution with Systematical Errors Continuation[J]. *Geomatics and Information Science of Wuhan University*, 34(7): 787-789,813.
- [34] Ma C, Zhang L, Gui Q, Du Y, Han S. 2007. Ridge Type GM Estimation in Gauss-Markov Model[J]. *Journal of Geomatics Science and Technology*, 24(1): 30-32.
- [35] Fan P, Sui L, Yao H. 2008. Robust Ridge and Principal Correlation Estimation and Influence of Error[J]. *Journal of Geomatics Science and Technology*, 25(3): 216-219.
- [36] Liu Y, Li J, Liu X. 2007. Determination of the Partial Ridge Parameters[J]. *Journal of Geomatics Science and Technology*, 24(6): 413-414,418.
- [37] Chen K, Gui Q, Liu L, Liu Y. 2008. Robust t-Type Estimation and Applications in Geodetic Adjustments[J]. *Journal of Geomatics Science and Technology*, 25(1): 57-60.
- [38] Pan X, Fu Z. 2007. Parameter Adaptive Estimation of Bounded p-norm Distribution[J]. *Geomatics and Information Science of Wuhan University*, 32(4): 323-325,335.
- [39] Pan X, Cheng S, Zhao C. 2010. A Fast Parameter Estimation in p-norm Distribution[J].

- Geomatics and Information Science of Wuhan University, 35(2): 189-192.
- [40] Li B, Shen Y. 2010. Maximum Likelihood Estimation in Mixed Integer Linear Model with P-norm Distribution[J]. *Acta Geodaetica et Cartographica Sinica*, 39(2): 141-145.
- [41] Song Y, Liu Q, Zen L, Chen Y. 2009. An Algorithm for Kinematic Filtering with Contaminated Measurement Noises[J]. *Acta Geodaetica et Cartographica Sinica*, 38(2): 138-143.
- [42] Zhao C, Tao B. 2007. Robust Kalman Filtering of Linear System with Colored Noises[J]. *Geomatics and Information Science of Wuhan University*, 32(10): 880-882.
- [43] Li Q, Ge Z, Li C, Han Z. 2008. Robust Kalman Filtering Algorithm Based on Fuzzy Control[J]. *Journal of Geomatics Science and Technology*, 25(3): 209-212.
- [44] Zhang S, Yang Y, Zhang Q, Gao W. 2007. An Adaptively Robust Filter Based on Bancroft Algorithm in GPS Navigation[J]. *Geomatics and Information Science of Wuhan University*, 32(4): 309-311.
- [45] Hao J, Ou J, Guo J, Yuan Y. 2007. A New Method for Improvement of Convergence in Precise Point Positioning[J]. *Geomatics and Information Science of Wuhan University*, 32(10): 902-905.
- [46] Gao W, Yang Y, Zhang T. 2007. Neural Network Aided Adaptive Filtering for GPS/INS Integrated Navigation[J]. *Acta Geodaetica et Cartographica Sinica*, 36(1): 26-30.
- [47] Gao W, Yang Y. 2008a. Neural Network Aided GPS / INS Integrated Navigation Fault Detection Algorithms[J]. *Acta Geodaetica et Cartographica Sinica*, 37(4): 403-409.
- [48] Gao W, Yang Y, Zhang T. 2008b. An Adaptive UKF Algorithms for Improving the Generalization of Neural Network[J]. *Geomatics and Information Science of Wuhan University*, 33(5): 500-503.
- [49] Cao Y, Sui L, Wang B. 2010. Consideration of Time-Correlated Errors in a Kalman Filter Applicable to Single-Frequency GPS Precise Point Positioning[J]. *Journal of Geomatics Science and Technology*, 27(1): 23-26.
- [50] Gong Y, Gui Q, Li B, Zhou N. 2010. Application of Particle Filtering Algorithms in GPS/DR Integrated Navigation[J]. *Journal of Geomatics Science and Technology*, 27(1): 27-30.
- [51] Li Q, Lv Z. 2008. Fuzzy Adaptive Kalman Filtering Algorithm Based on the Statistics of t Distribution[J]. *Acta Geodaetica et Cartographica Sinica*, 37(4): 428-432.
- [52] Cao Y, Sui L. 2008. An Adaptive Two-Stage Kalman Filter[J]. *Journal of Geomatics Science and Technology*, 25(6): 407-409,413.
- [53] Wu J, Huang C. 2008. Nonlinear Adaptively Robust Filter for Orbit Determination[J]. *Geomatics and Information Science of Wuhan University*, 33(2):187-190.
- [54] Qin X, Yang Y. 2009. Applications of Adaptive Filtering on Real Time Orbit Determination of LEO Satellites Based on GPS[J]. *Journal of Geomatics Science and Technology*, 26(4): 238-240,244.
- [55] Gui Q, Xu A, Han S. 2009. A Stepped Robust and Adaptive Filtering and Its Applications in GPS Kinematic Navigation[J]. *Geomatics and Information Science of Wuhan University*, 34(6): 719-723.
- [56] Yang Y, Cui X. 2008. Adaptively Robust Filter With Multi Adaptive Factors[J]. *Survey Review*, 40, 309: 260-270.
- [57] Yang Y, Zen A. 2009. Adaptive Filtering for Deformation Parameters Estimation in Consideration of Geometrical Measurements and Geophysical Models[J]. *Science in China Series D: Earth Sciences*, 52(8): 1216-1222.
- [58] Wu F, Yang Y, Cui X. 2010. Application of Adaptive Factor Based on Partial State

- Discrepancy in Tight Coupled GPS /INS Integration[J]. Geomatics and Information Science of Wuhan University, 35(2): 156-159.
- [59] He D, Yuan Y, Chai Y. 2008. On Adapting Kalman Filtering for Adjusting Observation Noise Covariance in GPS/INS Integration[J]. Geomatics and Information Science of Wuhan University, 33(8): 838-841.
- [60] Gao W, Yang Y, Zhang S. 2008. GPS / INS Adaptive Filtering Considering the Influences of Kinematic Model Error[J]. Geomatics and Information Science of Wuhan University, 33(2): 191-194.
- [61] Sui L, Liu Y, Wang W. 2007. Adaptive Sequential Adjustment and Its Application[J]. Geomatics and Information Science of Wuhan University, 32(1): 51-54.
- [62] Yang Y, Zeng A, Zhang J. Adaptive Collocation with Application in Height System Transformation[J]. J Geod, 2009, 83: 403-410.
- [63] Wang X, Fan Q, Xu C, Li Z. 2008. Dam Deformation Prediction Based on Wavelet Transform and Support Vector Machine[J]. Geomatics and Information Science of Wuhan University, 33(5): 469-471, 507.
- [64] Deng X, Hua X. 2008. Learning Algorithm of Dynamic Least Square Support Vector Machine[J]. Geomatics and Information Science of Wuhan University, 33(11):1 122-1125.
- [65] Lu T, Tao B, Zhou S. 2008. Modeling and Algorithm of Linear Regression Based on Total Least Square[J]. Geomatics and Information Science of Wuhan University, 33(5): 504-507.
- [66] Qiu W, Qi Y, Tian R. 2010. An Improved Algorithm of Total Least Squares for Linear Models[J]. Geomatics and Information Science of Wuhan University, 35(6): 708-710.
- [67] Kong J, Yao Y, Wu H. 2010. Iterative Method for Total Least-Squares[J]. Geomatics and Information Science of Wuhan University, 35(6): 711-714.

## Some Activities of Astro-Geodynamics in China during 2007-2010

*HUANG Chengli, WANG Guangli, WANG Xiaoya, WU Bin, ZHOU Yonghong*

Shanghai Astronomical Observatory, Chinese Academy of Sciences, Shanghai 200030, China

**Abstract:** Some observational and research activities of astro-geodynamics by Chinese colleagues since 2007 are briefly reported, including: observations and study of the model of global and Chinese local crustal movement, the GPS applications on the meteorology and ionosphere study, the applications of VLBI on astrometry and geodesy, SLR observations and related research, the earth rotation variation and its relation with atmosphere, ocean and the interior Earth.

### I. GNSS: SITES, DATA PROCESSING AND ITS APPLICATION

#### 1. GNSS Sites Distribution

Based on 25 GPS permanent sites of the first phase, the second phase of China continental environment monitor network (CCEMN) will include 260 real time continuous GNSS sites and 2000 or so regional GNSS sites before the end of 2010. The permanent GNSS network has been finished and will be run in September 2010 under the lead of Chinese six ministries and commissions. There will be more GNSS data in the future and we wish more applications in many different fields could be obtained.

#### 2. Related GNSS Application

##### (1) Precise Orbit Determination (POD)

Beside the POD of GPS, the real time POD of COMPASS/Beidou, the Chinese national navigation system, has also be studied (Zhou et al, 2010; Chen et al., 2008). We can obtain the real time precise and predicted orbits of different satellites such as GEO/MEO/IGSO within 30 minutes by several regional GNSS sites. With addition of the number of COMPASS satellites our multi-satellite processing software will give out more precise results than our single satellite processing software which is running under single or a few satellites (Wang et al., 2009a). Also we studied POD of LEO by space-based GPS data of GRACE, CHAMP and FY-3 of China (Wang et al., 2009b).

##### (2) GPS Meteorology Application

With the addition of GNSS sites, a lot of real time GNSS observations have to be processed within short time (1 hour), and the traditional software such as GAMIT is difficult in dealing with it. Sometimes the GNSS network data is divided and processed by several computers. This method is adopted in our Yangtze River delta real time GPS data processing. Now we have developed another method based on similar PPP to get PWV and its 3-D distribution. This method can get water vapor products quickly (Huang et al., 2009; Wang et al, 2008).

We applied our results for air meteorology based on one 863 project. The whole software and

studies have been finished and we hope we will carry out these achievements in the Next Generation Air Transportation System (NextGen).

### (3) GNSS ionosphere Application

A multiple-arc method and Kriging interpolation are applied to obtain VTEC as well as DCB using ground-based GPS data. Given by the time variation characteristics of VTEC and DCB, VTEC is calculated every 30 minutes as local variables, and DCB is calculated every day as global variables. Kriging method, taking the spatial information of VTEC into account, is useful to make VTEC more precise and stable. Meanwhile, based on 3-variable spline basis function, we expand electron density into a linear combination of a set of grid points. Tomography of Ionosphere electron density is derived by MART. The results show the coherence with CHAMP occultation results. We applied these two ways to process the ground-based GPS data of Yangtze River Delta in May, 2008 when the shocking earthquake happened in Wenchuan. A simple statistic analysis reveals the response of ionosphere to the earthquake and also the abnormal signal occurred before the earthquake (Wang et al, 2010). The Ionosphere activities are also monitored and TEC prediction are done (Jin et al, 2010).

### (4) Study on geodynamical mechanisms

In SHAO groups, the rotational and orbital motions of the Earth are also studied, as well as the mass motions of the Earth's spheres, such as the atmosphere, hydrosphere, lithosphere, mantle, and core by astronomical data and space geodesy techniques. This involved in mechanism studies of the Earth's rotation variation and their interactions between the motions of the various spheres.

## **II. SLR: SYSTEM CONSTRUCTION, OBSERVATION, DATA PROCESSING, AND ITS APPLICATION**

### *1. SLR system update and reconstruction*

Under the project of China continental environment monitor network, 5 SLR sites (Beijing, Shanghai, Changchun, Wuhan, Kunming) and 2 mobile SLR sites are required to update or reconstruct their systems. It includes the establishment of daylight ranging observation system, KHz laser ranging and control system, meteorological parameter recorder system and so on. Some SLR sites have finished the update and reconstruction and they can already do KHz and daylight ranging observation, while the left will be finished before the end of 2010. We hope these updates will be helpful to SLR applications (Wang et al. 2009c).

In 2005, National Astron. Obs. of China (NAOC) moved a SLR system to the National Univ. of San Juan of Argentina (NUSJ), a cooperative 60-cm SLR station (ID 7406) of China and Argentina was installed at San Juan Observatory. It began to observe in the beginning of 2006. Thanks to the serious work and elaborate maintenance for the instrument by the technologists of both sides as well as the good weather in San Juan. This station became very quickly one of the most productive stations of the ILRS network, a most welcome improvement to the network geometry and performance, especially for the coverage of the southern hemisphere. The daytime tracking function and a co-located GPS station are going to be realized.

### *2. SLR data Processing*

As ILRS Associate Analysis Center, SHAO provides weekly analysis report about range biases,

time biases and also provide some precise orbit determination for COMPASS/Beidou by SLR data and microwave signals. SHAO has finished preparing for the SLR data auto-processing including choosing satellite (any satellite with SLR data is ok), downloading data, preparing for files, running program and outputting results. The weekly SINEX SLR solutions and related productions will be provided to ILRS by our multi-satellite SLR data processing software. (Wang et al. 2009c). This work is also applied in China Continental Environment monitor network.

### 3. Related SLR Researches

#### (1) Precise Orbit Determination Based on SLR Observation

Beside the POD of Lageos1-2 satellites, the POD of COMPASS is also done in SHAO. The residual RMS for Lageos1-2 is about 1cm or so. But residual RMS for COMPASS is about 1-6 cm due to the lack of observation and unreasonable site distribution. Occasionally the residual RMS can get to more than 15 cm due to the severe lack of SLR data (Wang et al. 2009d).

#### (2) Determination of EOP by SLR

The attempt to derive daily EOP from SLR data is still in progress in SHAO, by loose constrains and combining SLR EOP with VLBI, DORIS and GNSS.

#### (3) Geocenter Motion Estimations

By SLR data processing we can get the geocenter motion. And also we can get the geocenter coordinate by SLR solution combination. The comparison is in progress.

#### (4) Determination of low order gravitational field and its temporal variations

The data is still processing and the results are also compared in progress.

### 4. Laser Time Transfer (LTT) experiments

The LTT payload onboard the Chinese experimental navigation satellite COMPASS-M1 with an orbital altitude of 21500 km was launched on April 13, 2007. The payload included dual-SPAD-detector, dual-timer based on TDC device, DSP, power supply and a LRA. The time transfer experiment at the Changchun SLR station has been performed between ground and satellite since August 2007. The experiment has shown that the time and relative frequency differences between the ground hydrogen maser and the China-made space rubidium clocks have been obtained with the time precision of about 300ps for single measurement and the uncertainty of frequency difference measurement of about  $3 \times 10^{-14}$  in 2000 seconds. After 17 months orbital flight, the LTT payload has kept its good performance (Yang et al. 2009).

Two new LTT payloads were designed for the next Compass missions. They were in orbit by mid-2009 and the beginning of 2010 respectively. Some upgrading of the new LTT payloads:

- 1) Add gating circuit in the payload for reducing the effect of the dead time of SPAD. It is of importance when the noises are strong.
- 2) Reducing the FOV and adopting two FOV for two detectors respectively: one is bigger for nighttime experiment; another is smaller for daylight experiment.
- 3) 20 Hz onboard timing data will be downloaded instead of 1 Hz before. During last mission (Compass-M1), only 1Hz timing data were downloaded in spite of 20Hz laser firing at the ground

station, so a lot of useful data were lost.

4) Narrowing the bandwidth of the interferometric filter from 8.8nm to 4nm due to smaller FOV for IGSO orbit.

### III. ASTROMETRIC AND GEODETIC VLBI ACTIVITIES IN CHINA

#### 1. VLBI role in Crustal Motion Observation Network of China (CMONOC)

CMONOC is a project employing multi-space geodetic observation technologies such as GPS, SLR, VLBI etc to observe the crustal motion of China, starting from early in 2008, and lasting about two years. Its main goals are the construction of observation network systems and data acquisition and data processing mechanism

Three VLBI stations are joined to CMONOC: Sheshan in Shanghai, Nanshan in Xinjiang and Kunming in Yunnan Province. They are closely to complete to recast for satisfying the CMONOC.

The VLBI data analysis software dedicated to CMONOC VLBI routine data processing is finished coding and in debug and examination.

#### 2. VLBI Observations

Sehsan25 and Urumqi VLBI stations participated in APSG VLBI experiments two times a year. APSG is the abbreviation of Asia-Pacific Space Geodynamics Project, and VLBI has began operation in APSG since 1997, including six stations located around Asian-Pacific area in Japan, Australia, US and China.

These two VLBI stations joined in IVS EOP network and routinely operate weekly as well.

As CMONOC VLBI stations, Seshan25, Urumqi and Kunming have carried three 24-hour VLBI experiments. And since 2007 in the name of Chinese lunar mission CE-1, four VLBI experiments have been carried to obtain high precision station coordinates, these experiments also including Miyun VLBI station, although it is not joined CMONOC.

#### 3. Research works

Zhang et al. (2008) compare the tropospheric zenith delays derived from VLBI and GPS data at VLBA stations collocated with GPS antennas. Both the systematic biases and standard deviations are at the level of sub-centimeter. Based on this agreement, the authors suggest a new method of tropospheric correction in phase-referencing using combined VLBI and GPS data.

In order to evaluate the real accuracy of the geocentric coordinate velocities determined with GPS, VLBI and SLR under the ITRF200, RongMin et al. (2009) compare the geocentric coordinate velocities obtained with the three techniques co-located on the same site. After that, we can obtain the transformation parameter and analyze mean square error of differences between the geocentric coordinates two by two, which, reflecting the real accuracy of VLBI, GPS and SLR geocentric coordinate velocities, is within 1 mm/a. It is shown that the real accuracy of the geocentric coordinate velocities with VLBI and GPS are better than that with SLR.

Guo et al. (2010) present the first successful CVN (Chinese VLBI Network) phase-referencing observation of the pulsar B0329+54 on October 16, 2008 in S band. A new background source, J0347+5557, 2.5 degree away from the pulsar was employed as a position reference, which is

closer to the pulsar and better for the ‘nodding’ mode than that used in previous observations. The position by fitting image of the pulsar relative to the calibrator is accurately determined at the level of tens of  $\mu\text{as}$ , which is comparable with the present differential VLBI astrometric accuracy, proving that CVN will be a potential powerful tool for astrometry and astrophysics.

Li et al. (2010) have carried local tie measurements between Seshan25 VLBI station and near around GPS and SLR stations.

Wei et al. (2010) carried research work on application of VLBI technique to earthquake prediction.

#### **IV. STUDY OF THE VARIATION OF EARTH ROTATION AND TERRESTRIAL REFERENCE FRAME**

##### *1. Atmospheric, oceanic and else contributions to the Earth’s variable rotation*

Zhou et al. (2008) investigated the individual tropospheric and stratospheric wind contributions to the Earth’s variable rotation during the period 2000-2005 to further the understanding of the role of wind in exciting polar motion and the variation of the Earth’s rotational rate. Instead of the previous empirical approach, which simply assumed the tropopause as an equal-pressure level, Zhou et al. (2008) employed a tropopause from the NCEP/NCAR reanalyses, that is space- and time-dependent. For the axial component, the tropospheric and stratospheric wind effects are essentially additive. For the equatorial components, however, a significant cancellation is found between the tropospheric and stratospheric wind terms based on the NCEP/NCAR reanalysis model. (Zhou et al., 2008)

The time-variable characteristics exist in 50-day fluctuation of LOD change. Frequency and amplitude of the oscillation change with time. We also find the good consistence exists in LOD change and the axial AAM. The oscillation of the axial AAM can explain most parts of variances of the LOD during 1976–2006. Excitation contribution from the axial OAM is less. The unexplained part of the 50-day oscillation variance in LOD is mainly from some other excitation sources, such as upper atmospheric winds, hydrological processes etc. (Ma et al, 2008)

The continental water cycling model is calculated, and its contribution to the annual variation of PM is confirmed (<20%) (Zhong et al, 2008)

The excitation of annual polar wobble by global oceans is also studied. By comparing effective OAM functions estimated from assimilated models SODA to the non-atmospheric hydrologic residual, it is found that, for the seasonal fluctuation, the SODA assimilated effective OAM functions agree better with the non-atmospheric hydrologic residual, than those estimated from the previous assimilated model SODA beta7, also for the annual variations. It has also been found that annual effective OAM vectors for SODA and ECCO in each latitude band are much closer along the Greenwich meridian, than along the 90E meridian, (Zhong & Yan, 2008)

The Indian summer monsoon rainfall (ISMR) plays an important role in the climate system of South Asia. The Scargle periodogram and wavelet transform methods is used to study the periodicity of ISMR changes between 1871 and 2004. It is shown that complicated ISMR variations have periodicities with remarkable time-variable characteristics and that solar activity affects the ISMR variations to some extent. (Ma et al., 2007)

##### *2. Application of mathematical methods in the study of earth rotation*

Real-time rapid prediction of variations of the Earth's rotational rate is of great scientific and practical importance. However, due to the complicated time-variable characteristics of variations of the Earth's rotational rate, it's usually difficult to obtain satisfactory predictions by conventional linear time series analysis methods. Wang et al. (2008) employs the non-linear artificial neural networks (ANN) to predict the LOD variations. The topology of the ANN model is determined by minimizing the root mean square errors (RMSE) of the predictions. Considering the close relationships between the LOD variations and the atmospheric circulation movement, the operational prediction series of the axial AAM is incorporated into the ANN model as an additional input. The results show that the LOD prediction is significantly improved after introducing the operational prediction series of AAM into the ANN model. (Wang et al., 2008)

The concept of normal Morlet wavelet transform (NMWT) is developed and applied to the study of the Earth's polar motion (PM), and finds that the ocean always offsets the atmospheric effects on Earth's annual PM and that the observed Chandler wobble has only one instantaneous frequency all the time (Liu et al, 2007).

### *3. Study of the construction of mm-level terrestrial reference frame*

A time series of geocenter motion measured with SLR on LAGEOS1/2 is estimated and then analyzed with the wavelet transformation and the least squares method, respectively. The secular and periodic variations of geocenter motion are detected. The long-term movement indicates that the crustal figure is changing, the north hemisphere and 180-degree hemisphere are shrinking, and the south hemisphere and 0-degree hemisphere are swelling. The seasonal variations are the main components which may be caused from the mass distribution of Earth fluid layer, e.g. ocean, atmosphere and continental water. There are many other periodic or quasi-periodic variations. There are long periodic variations through 2 to 5 years. Many periods gradually change, which indicates that there exist non-regular fluxes for the environment and mass of the whole Earth system. (Guo et al., 2009)

The ITRF2005 was analyzed and found that it does not satisfy the need of monitoring mm-level geodynamic change. In construction of mm-level TRF, there are 2 key problems: 1) non-linear characteristic of crust movement: Its vertical annual motion in GPS data and geophysical modeling can be better than 2 mm, and its phase better than 30 degree; and 2) geocenter movement: Its annual motion is about 1-1.5 mm. In order to monitor them, it is suggested to use space technology (GPS, VLBI, SLR and GRACE) and related geophysical factors (atmosphere, snow, soil moisture, etc.) should be modeled carefully. (Zhu et al., 2008)

## **V. STUDIES OF PHYSICS OF THE EARTH INTERIOR**

The coupling between the earth nutation and the electro-magnetic field near the core-mantle-boundary (CMB) is studied. Nutation amplitudes are computed in a displacement field approach that incorporates the influence of a prescribed magnetic field inside the Earth's core. The magnetic field influence is directly introduced into the motion equation and in the boundary conditions used in precise nutation theory, and a new strategy to compute nutations is established. By using well-accepted electro-magnetic parameters near CMB, The results show that the free core nutation period decreases by 0.38 day, and that the out-of-phase (in-phase) amplitudes of the retrograde 18.6yr and the retrograde annual nutation increase (decrease) by 20 and 39 micro-arc-second respectively. Comparisons of these results with previous studies are made, and

discussions are also presented on the contribution of Coriolis force and the prescribed magnetic field itself on the coupling constants. (Huang et al., 2008).

A new integrated formula to obtain the equilibrium figures of the earth interiors to third-order accuracy is developed, in which both the direct and indirect contribution of the anti-symmetric crust layer are included, i.e., all the non-zero order and odd degree terms are included. Using this new potential theory and replacing the homogenous outermost crust and oceanic layers in PREM with various real surface layers data, the global dynamic flattening (H) is obtained and it's shown that the 1% difference between HPREM that is calculated from the traditional potential theory and PREM model and Hobs that is derived from very precise precession observation can be removed by 2/3 (Liu & Huang, 2008).

Galerkin method is applied to compute the eigenfuncions and eigenperiods of some of the Earth spheroidal and toroidal modes. The boundary conditions are treated using a Tau method. We show that for a realistic Earth model the difference between the computed and observed periods is less than 1.4%. It shows that the Galerkin method may be an effective tool for the studies of the Earth's normal modes. (Zhang & Huang, 2008)

Using the gravity data by Beijing-Tangshan gravimetry network during 1987~1998 (46 repeated campaigns), the plumb-line variation (PLVs) near Tangshan is calculated and compared with 38 earthquakes ( $M \geq 4$ ) happened near Tangshan in the same periods, it is found that they are well related to each other. (Li & Li, 2008)

## VI. MISCELLANEOUS

Asia-Pacific Space Geodesy Program (APSG) hosted by both Shanghai Astronomical Observatory and Wuhan Institution of Geophysics and Geodesy, Chinese Academy of Sciences, has pursued several observational campaigns and much research studies focusing on the Asia-Pacific area since 1995, and related workshops have been held once a year.

## References

- [1] Chen Liu-Cheng, Hu Xiao-Gong, Han Chun-hao, et al., 2008, Research on Almanac Parameters Fitting Algorithm for Navigation Satellites, *Acta Astronomica Sinica*, 49(3):288-296.
- [2] Guo Jinyun, Chang Xiaotao, Han Yanben, Sun Jialon, 2009, Periodic Geocenter Motion Measured with SLR in 1993-2006, *Acta Geodaetica et Cartographica Sinica*, 38(4): 311-317
- [3] Guo Li, Zheng Xingwu, Zhang Bo, et al., 2010, New determination of the position of the pulsar B0329+54 with Chinese VLBI network. *Science China Physics, Mechanics & Astronomy*, 53(8): 1559-1
- [4] Han Yanben, Hu Hui, 2007, Application of Astronomic Time-latitude Residuals in Earthquake Prediction, *Earth, Moon, and Planets*, 100: 125-135
- [5] Han Yanben, Liu Weidong, E. Actis, et al., 2008, Successful operation of a cooperative SLR station of China and Argentina in San Juan, *Chinese Science Bulletin*, 53(16): 2417-2420
- [6] Huang C.L., Dehant V., Liao X.H. et al., 2008, On the coupling between magnetic field and nutation in a numerical integration approach, 11th SEDI Symposium, July 26-31, 2008, Kunming, China

- [7] Huang Shan-Qi, Jie-Xian Wang, Xiao-Ya Wang et al., 2009, Application of LAMBDA Method to the Calculation of Slant Path Wet Vapor Content of GPS Signals, *Chinese Astronomy and Astrophysics*, 33(4):421-430.
- [8] Jin S G, Y W Zhu and E Afraimovich, 2010, Co-seismic ionospheric and deformation signals on the 2008 Mw 7.9 Wenchuan earthquake from GPS observations, *Int. J. Remote Sens.*, 31.
- [9] Li Jinling, Qiao Shubo, Liu Li, 2010, the application of coordinate transformation in to data analysis of site survey at Sheshan 25m radio telescope, *Science of Surveying and Mapping*, Vol.35, No.2
- [10] Li Z.X. and Li H., 2008, The relationship between the plumbline variation near Tangshan and the earthquakes happened nearby during 1987-1998, *Science in China (Series D:Earth Sciences)*, 38(4): 432-438.
- [11] Liu L., H. Hsu, and E. W. Grafarend, 2007, Normal Morlet wavelet transform and its application to the Earth's polar motion, *J. Geophys. Res.*, 112, B08401, doi:10.1029/2006JB004895.
- [12] Liu Y., Huang C.L., 2008, The direct contribution of the surface layers to the Earth's dynamical flattening, *Proc. IAU Symp.* 248, 403-404
- [13] Ma Lihua, Han Yanben, and Yin Zhiqiang, 2007, The possible influence of solar activity on Indian summer monsoon rainfall, *Applied Geophysics*, 4(3): 231-237
- [14] Ma Li-hua, 2007, Variation of Earth's rotation rate on seasonal and quasi-biennial time scales, *The Observatory*, 127(1200): 364-365
- [15] Rong Min, Sun Fuping, Zhou Wei and Jia Xiaolin, 2009, Accuracy Test of GPS, VLBI and SLR Geocentric Coordinate Velocities Under ITRF2005. *Journal of Geodesy and Geodynamics*. 29(Supp): 37-40
- [16] Wang Qijie, Liao Dechun, Zhou Yonghong. 2008, Real-time rapid prediction of variations of earth's rotational rate. *Chinese Science Bulletin*, 53(7): 969-973
- [17] Wang Qijie, Liao Dechun, Zhou Yonghong, Liao Xinhao, 2008, Importance of Atmospheric Angular Momentum Function in Non-linear Prediction of Length of Day Variation. *ACTA Astr. Sinica*, 49(1): 93-100 (in Chinese)
- [18] Wang Xiaoya, Hu Xiaogong, HuangYong, 2009a, The project analysis of POD for regional navigation system., *Satellite navigation Precise Orbit Determination and Time Transfer Conference*, Xian, China, 8 July 2009.
- [19] Wang Xiaoya, Hu Xiaogong, HuangYong, 2009b, GPS application in and precision analysis on LEO orbit determination, *The Seventh Chinese Space Sciences Conference*, Dalian, China, 27 August 2009.
- [20] Wang Xiaoya, Yang Jian, Hu Xiaogong, 2008, GPS 4D water vapor tomography based on history Radiosonde data, *APSG 2008*.
- [21] Wang Xiaoya and Xing Nan, 2010, Tomography of Ionosphere electron density and its abnormality analysis during Wenchuan earthquake, *EGU General Assembly 2010*, Vol.12, EGU2010-1123-2, Vienna, Austria, 2 May 2010.
- [22] Wang Xiaoya, Yuanlan Zhu, WeiJing Qu, et al., 2009c, A simple introduction of SLR data auto-processing and results analysis in Shanghai Astronomical Observatory, *2009 ILRS Analysis Workshop*, Vienna, Austria, 18, April, 2009.
- [23] Wang Xiaoya, Bin Wu, Xiaogong Hu, et al., 2009d, Impact of SLR Tracking on

- COMPASS/Beidou, International Technical Laser Workshop on SLR Tracking of GNSS Constellations”, Metsovo, Greece, 13, Sep, 2009.
- [24] Wei Erhu, Zhou Peilai, Chen Xiaohui, Li Guan, 2010. On Application Of VLBI Technique to Earthquake Prediction. *Journal of Geomatics* Feb., 34 (1), pp1-3
- [25] Zhang Bo, Zheng Xing-Wu, Li Jin-Ling and Xu Ye, 2008, An Approach of Tropospheric Correction for VLBI Phase-Referencing using GPS Data *Chin. J. Astron. Astrophys.* 8(1): 127–132
- [26] Zhang M., Seyed-Mahmoud B., Huang C.L., 2008, Preliminary result of the Earth's free oscillations by Galerkin method, *Proc. IAU Symp.* 248, 409-410
- [27] Zhong Min, Yan Haoming, 2008, Excitation of Annual Polar Wobble by Global Oceans, *Chinese Astronomy and Astrophysics*, 32: 91-99
- [28] Zhou YH, Chen JL, Salstein DA, 2008, Tropospheric and stratospheric wind contributions to Earth's variable rotation from NCEP/NCAR reanalyses (2000–2005), *Geophysical Journal International*, 174: 453-463
- [29] Zhou Jianhua, Chen Liu-cheng, Hu Xiao-gong, et al., 2010, The precise orbit determination of GEO navigation satellite with multi-types observation, *Science in China (Series G: Physics, Mechanics & Astronomy)*, 40: 520~527。
- [30] Zhu Wen-Yao, Xiong Fu-Wen, Song Shu-li, 2008, Notes and Commentary on the ITRF2005, *Progress in Astronomy*, 26(1): 1-14

## Geoid Determination in Coastal Region

ZHANG Chuanyin<sup>1</sup>, GUO Chunxi<sup>2</sup> and ZHANG Liming<sup>1</sup>

1 Chinese Academic of Surveying and Mapping, Beijing, 100039, China

2 Geodetic Data Processing Center of State Bureau of Surveying and Mapping, Xi'an 710054, China

Geoid or Quasi-geoid is the datum of Elevation System, and its grid numerical model can be considered as a reference frame of elevation determination. Presently, the main method to determine the (quasi) geoid is based on Stokes or Molodensky theory. In fact, this theory implied a basic condition—that is the datum of all gravity data must be consistent. Theoretically, the gravity datum in small land area can be considered as consistent, since we often measure the surface gravity values based on gravity base net of a country or region. But in coastal region including both land and ocean parts, the gravity data present diversity characteristics. The gravity datum of various data is inconsistent because of different acquiring methods, such as continental gravity data, satellite altimetry data, shipborne gravimetric data and so on. In coastal region especially in the transition from land to ocean, the satellite altimetry data precision is low and the shipborne gravity measurement is impracticability, so there will be a ribbon region of data blank, which greatly influenced the determine precision of the (quasi) geoid. Therefore, it is very important to research and discuss the method of determining the (quasi) geoid in coastal region. Meanwhile, how to use the existing high precision topographic data to fill the data blank section has also been a problem.

According to the special conditions of the determination of (quasi) geoid in coastal region, with the research progress and author's thinking, this paper mainly discusses the following issues:

- (1) Satellite altimetry data processing in shallow water area and inversion of high precision gravity data;
- (2) Precision processing of topographic data in gravity field calculation;
- (3) Multisource gravity data fusion and unifying datum issue;
- (4) Determination of (quasi) geoid in coastal region.

### I. Satellite altimetry in shallow water area and its inversion of gravity field

Since the offshore coastline is more irregular and many islands distributed, a altimetry satellite orbit arc segment on the sea surface usually separated into several parts by the land or islands (Huang, 2005). Meanwhile because of the complicated ocean dynamics phenomenon, influence of land reflection and error of altimeter observation, these factors are unfavorable to offshore altimetry. Therefore we have to careful study the processing method of offshore satellite altimetry data.

Presently, the general method of deducing sea area gravity anomaly data by using the satellite altimetry data is: firstly calculate the vertical deflection of the cross point, then use the Vening-Meinesz formula to calculate the gravity anomaly. Therefore, how to acquire the high

precision and high resolution vertical deflection has been the key issue of the establishment of sea area gravity anomaly model. Sandwell (1992) proposed using the position and time information from altimetry record, solving vertical deflection in crossing point. Such method is rigorous theoretically, but it gets the sea level gradient indirectly based on altimetry satellite operating speed, so the altimetry vertical deflection will be affected. Hwang (1998) suggested obtaining along-track vertical deflection directly by using position information, calculating the average vertical deflection. Such methods of solution pass the time information only use position information to get the along-track vertical deflection, but it easily appear ill-posed problems when adjustment. Deng, Bao and Zhang (2008) combined T/P data, T/P new track data, ERS2 data, GFO data, Geosat GM data and ERS-1/168 data, using position information of altimetry satellite recording point to calculate the directional derivative of along track geoid immediately, and derive the vertical deflection at the cross point, then calculate a gravity anomaly model of China seas and vicinity at the resolution of  $2' \times 2'$  by using Vening-Meinesz formula. Such method of solution has following advantages: on one hand, use position information of altimetry satellite recording point to calculate the along track vertical deflection immediately, whose precision is higher than Sandwell's position and time information indirectly derived method; on the other hand, derive the vertical deflection component at the cross point, which can effectively overcome the ill-posed problem equation in Hwang's method. Presently, the precision of gravity anomaly inversion with coastal region satellite altimetry data can reach 6.0 mgal.

## II. Precise processing of topographic data

Up to now, most of the gravity topographic processing formulas are based on plane approximate derivation, which already couldn't meet the requirements. Therefore, through rigorous theoretical derivation, the author obtained precise topographic formula and its fast algorithm formula with the spherical approximation (Zhang chuanyin, 2009).

### 1. Topographic effect of disturbing potential

With spherical approximation, the topographic effect of disturbing potential can be expressed as

$$T^t = T^B + T^R = 4\pi G \tilde{\rho} \frac{R^2 H}{r} \left( 1 + \frac{H}{R} + \frac{H^2}{3R^2} \right) + T^R \quad (1)$$

Where

G: gravitational constant

H: elevation

r: geocentric distance of the calculating point

The topographic equivalent density is

$$\tilde{\rho}' = \frac{1}{H'} \int_R^{R+H'} \rho'(\lambda', \phi', r') dr' \quad (2)$$

$(r', \lambda', \phi')$  is spherical coordinate of flowing point,  $H'$  is terrain elevation of flowing point.

According to the definition, considered only the surface density  $\rho$ , the local topographical correction of disturbing potential can be expressed as

$$T^R = G \int_{\lambda'} \int_{\phi'} \rho \int_{R+H}^{R+H'} L^{-1}(r, \psi, r') r'^2 dr' \cos \phi' d\phi' d\lambda' \quad (3)$$

Where  $(r, \lambda, \phi)$  is spherical coordinate of calculating point,  $L^{-1}$  is reciprocal of space distance L from flowing point to calculating point.)

And,

$$L(r, \psi, r') = \sqrt{r^2 + r'^2 - 2rr' \cos \psi}, \quad \cos \psi = \cos \phi \cos \phi' + \sin \phi \sin \phi' \cos(\lambda - \lambda')$$

$$\int L^{-1}(r, \psi, r') r'^2 dr' = \frac{1}{2}(r' + 3rt)L + \frac{r^2}{2}(3t^2 - 1) \ln|r' - rt + L| + C \quad (4)$$

Where,  $t = \cos \psi$ , C is integral constant.

### 2. Topographic correction of disturbing gravity

With spherical approximation, the topographic correction of disturbing gravity can be expressed as

$$\delta g^t = \delta g^B + \delta g^R = 4\pi G \tilde{\rho} \frac{R^2 H}{r^2} \left( 1 + \frac{H}{R} + \frac{H^2}{3R^2} \right) + \delta g^R \quad (5)$$

According to the definition, the local topographic correction of disturbing gravity can be expressed as

$$\delta g^R = G \int_{\lambda'} \int_{\phi'} \rho \int_{R+H}^{R+H'} \frac{\partial L^{-1}(r, \psi, r')}{\partial r} r'^2 dr' \cos \phi' d\phi' d\lambda' \quad (6)$$

Where

$$\int \frac{\partial L^{-1}(r, \psi, r')}{\partial r} r'^2 dr' = \frac{(r'^2 + 3r^2)t + rr'(1 - 6t^2)}{L} + r(3t^2 - 1) \ln|r' - rt + L| + C \quad (7)$$

### 3. Fast algorithm of local topographic effect (or correction)

#### (1) Fast algorithm of local topographic effect of disturbing potential

Let  $\mathcal{G} = \frac{1}{2}(r' + 3rt)L + \frac{r^2}{2}(3t^2 - 1) \ln|r' - rt + L|$ , then

$$\frac{\partial \mathcal{G}}{\partial r'} = \frac{r'^2}{L}, \quad \frac{\partial^2 \mathcal{G}}{\partial r'^2} = \frac{2r'}{L} - \frac{r'^3 - rr'^2 t}{L^3}, \quad \frac{\partial^3 \mathcal{G}}{\partial r'^3} = \frac{2}{L} - \frac{5r'^2 - 4rr't}{L^3} + \frac{3r'^2(r' - rt)^2}{L^5} \quad (8)$$

Where  $r$  is geocentric distance of ground surface point which beneath calculating point,  $r' = r + h'$ , expand  $\mathcal{G}$  by Taylor series at about  $r' = r$ , neglect  $O(\Delta h^4)$  and then substituted into formula (3):

$$T^R = G \int_{\sigma} \rho \left( \frac{r^2 \Delta h}{L_0} + \frac{r \Delta h^2}{L_0} - \frac{r^3 - rr'^2 t}{2L_0^3} \Delta h^2 + \frac{\Delta h^3}{3L_0} - \frac{5r^2 - 4rr't}{6L_0^3} \Delta h^3 + \frac{r^2 (r - rt)^2}{2L_0^5} \Delta h^3 \right) d\sigma \quad (9)$$

Where  $\Delta h = H' - H$  is the difference of elevation between flowing point and the ground surface beneath the calculating point.

$$\Delta h^2 = H'^2 - 2H'H + H^2, \Delta h^3 = H'^3 - 3H'^2H + 3H'H^2 - H^3, L_0 = \sqrt{r^2 + r'^2 - 2rr'} \quad (10)$$

Substituted formula (10) into formula (9), define  $r'$  as the average surface geocentric distance,  $r$  as average calculating point geocentric distance, expand formula (9), then we can perform fast algorithm by using FFT method.

(2) Fast algorithm of local topographical correction of disturbing gravity

$$\begin{aligned} \text{Let } \Theta &= \frac{r'(r+r't)+3rt(r-2r't)}{L} + r(3t^2-1)\ln|r'-rt+L|, \text{ then} \\ \frac{\partial \Theta}{\partial r'} &= \frac{r'^3t-rr'^2}{L^3}, \quad \frac{\partial^2 \Theta}{\partial r'^2} = \frac{3r'^2t-2rr'}{L^3} + 3r'^2 \frac{(r-r't)(r'-rt)}{L^5} \\ \frac{\partial^3 \Theta}{\partial r'^3} &= \frac{6r't-2r}{L^3} + 3r' \frac{2(r'-rt)(3r't-2r)+rr'+r'^2t}{L^5} - 15r'^2 \frac{(r'-rt)^2(r-r't)}{L^7} \end{aligned} \quad (11)$$

Expand  $\Theta$  by Taylor series at about  $r' = r$ , neglect  $O(\Delta h^4)$  and then substituted into formula

(6):

$$\delta g^R = -G \int_{\sigma} \rho' \left( \begin{aligned} &\frac{r-r}{L_0^3} r'^2 \Delta h + \frac{3r-2r}{2L_0^3} r' \Delta h^2 + 3 \frac{(r-r')(r-rt)}{2L_0^5} r'^2 \Delta h^2 + \frac{3r-r}{3L_0^3} \Delta h^3 \\ &+ r \frac{2(r-rt)(3r-2r)+rr'+r'^2t}{2L_0^5} \Delta h^3 - 5r'^2 \frac{(r-rt)^2(r-r')}{2L_0^7} \Delta h^3 \end{aligned} \right) d\sigma \quad (12)$$

Where  $r'$  and  $r$  is constant, expand formula (9), then we can perform fast algorithm by using FFT method.

#### 4. Singular integral of local topographical effect (or correction)

(1) Singular value of local topographic effect of disturbing potential

When the calculating point and flowing point have same position,  $T^R$  is singular integral:

$$T^R|_0 = \frac{1}{6} G \rho^0 A_0 \sqrt{\frac{A_0}{\pi}} (h_{xx} + h_{yy}) \quad (13)$$

Where  $h_{xx}$ 、 $h_{yy}$  is second order partial derivative of the topography beneath calculating point,

$\rho^0$  is the topographic density and  $A_0$  is grid area.

(2) Singular value of local topographic correction of disturbing gravity

When the calculating point and flowing point have same position,  $\delta g^R$  is singular integral:

$$\delta g|_0 = \frac{G \rho_0}{2} \sqrt{\pi A_0} (h_x^2 + h_y^2) \quad (14)$$

Where  $h_x$ 、 $h_y$  is first order partial derivative of the topography beneath calculating point (that is topographic gradient on the north and east).

In formula (3) and (6), replace surface density  $\rho$  by  $\rho - \varepsilon$  ( $\varepsilon$  is seawater density), and replace the integral interval of  $r$  by  $[R - h, R]$  ( $h$  is the water depth), then formula (3) and (6) will be respectively transformed into the sea local topographical correction formula of the extraterrestrial space disturbing potential and disturbing gravity.

In order to meet the requirement of high precision computation of local gravity, Chinese Academy of Surveying and Mapping has developed a high precision computing platform (PALGrav1.0), which realized precise calculation of affect of any extraterrestrial space height and various type of field unit topography, including discrete field unit topography and fast FFT calculation. PALGrav1.0 can solve the problems of the earth surface disturbing gravity, vertical deflection, topographical correction of gravity gradient, and other complicated topographic effect of airborne gravity, satellite gravity as well as inversion of sea area satellite altimetry gravity.

### III. Multisource gravity data fusion and unifying datum scheme in coastal region

There are various types of gravity data in coastal region, which could not be applied in geoid calculating directly since they have inconsistent datum, therefore, we have to fuse multisource data and unify the datum for application. Up to now, there are fewer researches on multisource gravity data fusion problem. In order to improve the calculation accuracy of geoid, the author do some research on multisource data fusion and some significant conclusions are obtained.

We believe that the gravity data fusion should not only concern fixed weight of different data source on the error, but also considering the distribution density of data source, promote the control effect of high precision data source in the process of gravity fusion, avoid the low precision source effect. When the high density data source has low precision, the weight should be decreased further on the basis of error analysis. The multisource gravity data fusion scheme in coastal region is as shown in Figure 1. Take the fusion of altimetry gravity and shipborne gravimetric data as an example, the concrete steps are as follow: 1) Perform difference of satellite altimetry gravity anomaly. That is to form a differential equation for each grid point, use shipborne gravity anomaly as boundary condition to constitute a boundary-value problem of two-dimensional differential equation, then the boundary-value problem can be converted into a linear least squares adjustment problem by discretization; 2) Analyze the error between altimetry gravity anomaly and shipborne gravity anomaly and determine weight, to solve the linear least squares problem and obtain the adjusted value of gravity anomaly in computational domain, thus realizing the fusion of altimetry gravity anomaly and shipborne gravity anomaly in computational domain. According to the fusional gravity precision and resolution, the gravimetric geoid can be estimated by the following empirical formula:

$$\sigma_N(\text{cm}) = 0.4v\sigma_{\Delta g}(\text{mGal})$$

$\sigma_{\Delta g}$  : precision of grid gravity (units: cm).

$v$  : resolution of gravity (units: minute).

Practice shows that if the distribution density of shipborne gravity anomaly is higher than the minimum wavelength of sea surface topography in the same region, then the fusion can eliminate most of the effects on altimetry gravity anomaly which caused by sea surface terrain error. When

the shipborne gravity anomaly is sparse, then the effect of sea surface nonlinear terrain error will affect the fusional gravity anomaly as residual error, since the linear least squares adjustment method can only eliminate the effects by systematic errors of altimetry gravity anomaly and linear errors.

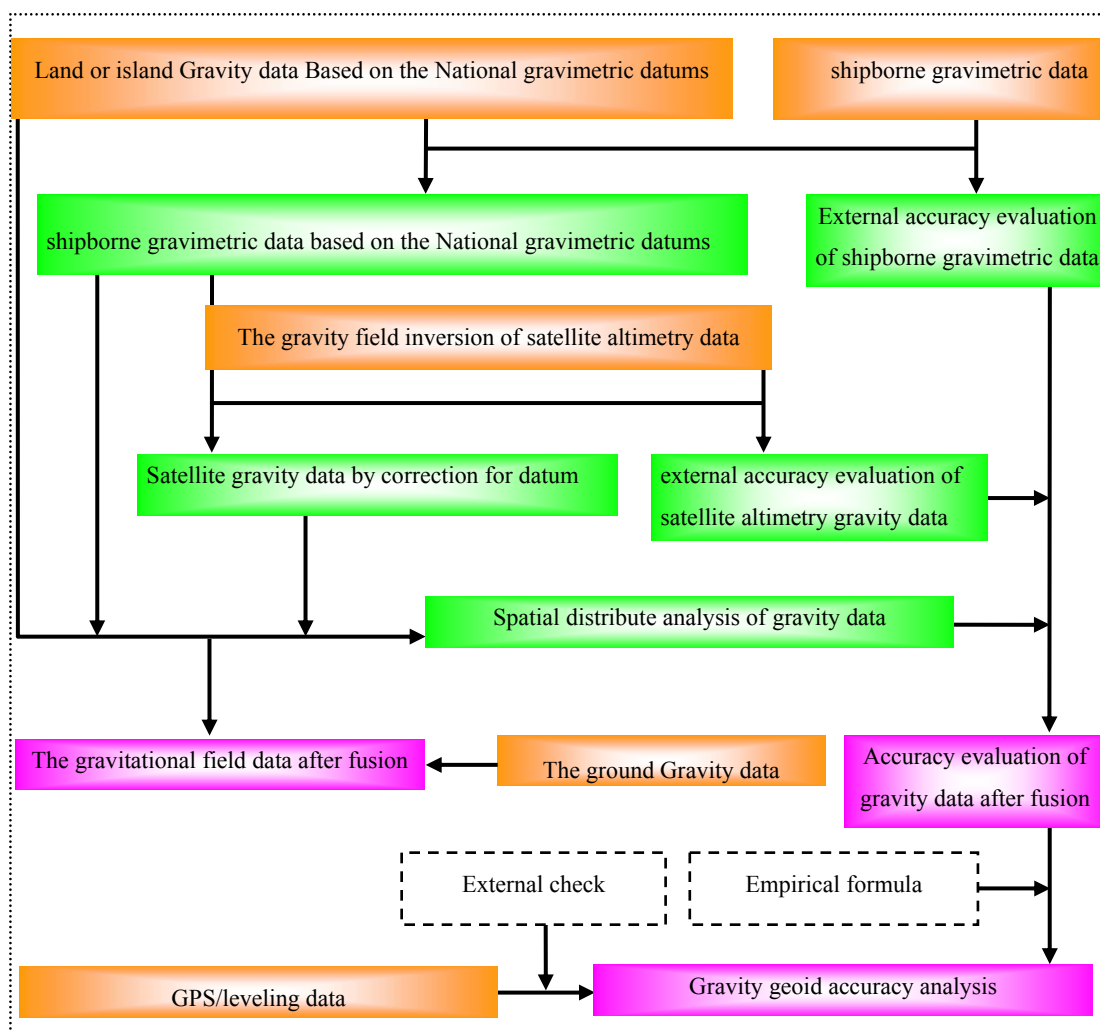


Figure 1: The multisource gravity data fusion and precision evaluation scheme

#### IV. Discussion on the calculation method of geoid determination in coastal region

In the traditional concept, the geoid calculated by using land gravity data is called as land gravity geoid and the geoid using oceanic data is called as oceanic geoid. Theoretically such two types of geoid should be consistent as long as the datum is unified; therefore, the two types should also be seamless spliced in the land-sea joint region that is to say there isn't any splicing difference. Actually this kind of ideal condition does not exist since the two adjacent geoids are different types of data and independently determined by respective principle and method. Even ignoring the possible systematic error and only considering the observation error between the two types of geoid, it's still inevitable to produce splicing difference. However, the land-sea splicing issue must be concerned on the determination of geoid in coastal region.

Presently, there are two types of usual method for the land-sea geoid determination: One is respectively calculate the continental geoid and oceanic geoid then splice them by mathematical

fitting method, such method does not have physical meaning; The other is called expanding method (Chen Junyong, 2003; Li Jiancheng, 2003) which combine the continental measured gravity anomaly data and inversion gravity anomaly data to form unified grid data of gravity anomaly. Then we solve the gravity (quasi) geoid including the ocean, according to Stokes formula by using the unified grid data. Pay attention that such (quasi) geoid is mostly determined by continental gravity data, the addition of altimetry gravity anomaly can be considered as finite extension of land gravity data along its land-sea boundary to the ocean, then fitting the continental part of the gravity geoid by using high precision GPS leveling data, in the meantime, the oceanic gravity geoid can be corrected by using fitting function.

A splicing method similar to geometry has been put forward by Zeng Chuanjun, etc. (2008), which is extrapolate the two kinds of geoid respectively to form overlapping band of land-sea boundary region, and then perform polynomial fitting of the difference between two types of geoid within superposed band, then the oceanic altimetry geoid systematic error can be corrected by such fitting. The advantage of such method is approximately reflects the possible systematic error between the two geoids and also corrected it to some extent; what's more, when the calculation of the two types of geoid was respectively combined the shipborne gravity data, then the splicing effect will be much better. What need to be improved are as follows: One is the extrapolation error may be large; The other is: When the overlapping range is small (in contrast with the whole ocean area), the fitted systematic error parameter is not that accurate, so there may be large correction error to the ocean area far from the overlapping range.

Theoretically the expending method shows more physical meaning, but the disadvantage is it has not considered the inconsistency of vertical datum in land-sea gravity anomaly, therefore that will introduce a systematic error in the calculation of integral land-sea geoid. So we can improve it on the basis of expending method. Generally, the oceanic gravity anomaly is believed to be with global characteristics and the continental gravity anomaly is localized. So first we need to determine the potential difference or vertical datum deviation according to Bursa method by using GPS leveling data and gravity model, and then correct the continental gravity anomaly. Since it has been with global characteristics, it will be more perfect theoretically when substituted into Stokes formula as a whole. Meanwhile, with the accumulation of GNSS data, the disturbing gravity data can be used, so the splicing method by using disturbing gravity data may become more important (Li Fei, 2005; Zhang Liming, 2009).

## Reference

- [1] Chen Junyong, Li Jiancheng, Chao Dingbo, et al. Geoid Determination on CHINA Sea and its Merge with the Geoid in CHINA Mainland[J]. Chinese Journal of Geophysics, 2003, 46 (1)
- [2] Deng kailiang, Bao Jingyang, Zhang Chuanyin, et al. Determination of Vertical Deflection over China Sea by Combination of Multi-satellite Altimeter Data [J]. Hydrographic Surveying and Charting.2008, 28 (3)
- [3] Deng kailiang, Bao Jingyang, Liu Yanchun, Zhang Chuanyin, etc. Determination of gravity anomalies over China sea by combination of multi-satellite altimeter data [J]. Science of Surveying and Mapping. 2009, 34 (1)

- [4] Hwang C. Inverse Vening-Meinesz Formula and Deflection Geoid Formula: Applications to the Prediction of gravity and geoid over the South China Sea [ J ]. Journal of Geodesy, 1998, (72)
- [5] Huang Motao, Zhai Guojun, etc. Marine Gravity Field Measurement and its Application [M]. Beijing: Surveying and Mapping Press, 2005
- [6] Li Fei, Yue Jianli, Zhang Liming. Determination of Geoid by GPS/Gravity Data. Chinese J. Geophys. 2005, 48(2)
- [7] Li Jiancheng, NING Jinshen, CHEN Junyong, LUO Zhicai. Problem of Piecing Together Between China Mainland-Geoid and Altimetry-Derived Geoid in China Sea Area [J]. Geomatics and Information Science of Wuhan University, 2003, 28(5)
- [8] Li Jiancheng, Chen Junyong, Ning Jinsheng, Chao Dingbo. Earth gravity field approximation theory and China 2000 geoid determination [M]. Wuhan: Wuhan University Press, 2003
- [9] Sandwell D T. Antarctic Marine Gravity Field from High density Satellite Altimetry [J]. Geophy J Int. 1992, 109 (2)
- [10] Zeng Chuanjun, Yao Yibin, Gao Bo. On merging of CHINA Continent-Marine geoid [J].Journal of Geomatics Oct . 2008, 33 (5)
- [11] Zhang Chuanyin, Chao Dingbo, Ding Jian, Zhang Liming. Precision Topographical Effects for any Kind of Field Quantities for any Altitude [J]. ACTA Seismologica Sinica. 2009, 38(1)
- [12] Zhang Liming, Li Fei, Chen Wu, Zhang Chuanyin. Height datum unification between Shenzhen and Hong Kong using the solution of the linearized fixed-gravimetric boundary value problem [J]. Journal of Geodesy. 2009, 83(5)